Facile Synthesis of ZnO-CuO,ZnO-Co_3O_4,CuO-Co_3O_4 and ZnO-CuO-Co_3O_4 Nanocomposite: Characterization and Photocatalytic Activity Study on Organic Dye

A Dissertation In Partial Fulfillment of the Requirements for the Degree of Master of Science (Mixed Mode) in Analytical and inorganic Chemistry

Submitted by

Farjana Akter

Examination Roll: 22014002

Registration No: 22014002

Session: 2019-20 (M.Sc.)

Department of Chemistry

Comilla University

October, 2024

Abstract

Photocatalytic degradation of dyes using semiconductor nanomaterials activated by sunlight has been the subject of extensive research due to its low cost, eco-friendly operation and absence of secondary pollutants. In this study, three binary nanocomposites ZnO/CuO (1:1), ZnO/Co_3O_4 (1:1), CuO/Co_3O_4 (1:1) and a new ternary metal oxide nanocomposite ZnO/CuO/Co_3O_4 (1:1:1) was prepared aiming the enhancement of photocatalytic performance to degrade Methylene Blue (MB) dye. The prepared samples were subjected to characterization via Fourier-transform infrared spectroscopy, field emission scanning electron microscopy, energy-dispersive Xray, X-ray diffraction, UV-vis spectroscopy. The XRD analysis disclosed that the average crystal size of ZnO/CuO, ZnO/Co_3O_4, CuO/Co_3O_4, ZnO/CuO/Co_3O_4 were 23.14nm, 18.15nm, 9.10nm and 23.57nm respectively. The degradation of methylene blue was investigated under different conditions at room temperature by analyzing and fitting the absorbance peaks of MB during degradation. The composites ZnO/CuO, ZnO/Co_3O_4 and CuO/Co_3O_4 nanocomposite show degradation rate of 97.82%, 88.34% and 93.14% at 180 minutes with rate of reaction 0.00707min^{-1}, 0.01477min^{-1} and 0.01117min^{-1}. Notably, the ternary nanocomposite (ZnO/CuO/Co_3O_4) demonstrated exceptional degradation capabilities for MB dye with 98.44% degradation rate at 120min. The reaction follow a pseudo first order kinetics with a rate of reaction 0.06667 min^{-1}. The composite show remarkable efficiency and stability with six reusability cycle. The narrow bandgap of the synthesised nanocomposites and the combined action of the three components may be responsible for this better photocatalytic activity. This finding implies that the creation of composite broadens the solar spectrum response range and decreases the recombination of photo-generated electron/hole pairs, leading to a notable increase in photocatalytic efficiency.

Contents

List of Figures

List of Tables

List of abbreviation

MB	Methylene Blue
NP	Nanoparticles
UV	Ultra-Violet
FTIR	Fourier transform infrared
XRD	X-ray Diffraction
FESEM	Field emission scanning electron microscopy

Chapter One – Introduction

1.Background:

Water contamination resulting from inappropriate handling of textile industry waste is a genuine global issue, with varying effects and ramifications contingent upon a nations socioeconomic circumstances. The discharge of industrial dye into water sources by factories has been associated with a range of health concerns, such as cancer, redness, skin irritation and allergic reaction [1].Wastewater is treated and purified using nanoparticles because of their high reactivity, large surface area, functionalization, and efficacy [2], [3], [4] . Conventional water treatment techniques include coagulation, flocculation, membrane filtration, precipitation, biodegradation,and oxidation are insufficient for treating wastewater [5], [6], [7]. The great effectiveness of metal oxide containing nanocomposites in sustainable development features, their photocatalytic breakdown and lack of secondary contamination during water treatment, make them an important study area at the moment [2], [8]. CuO nanoparticles have exceptional photocatalytic qualities, such as a high surface area and an appropriate bandgap energy, which allow for the production of reactive oxygen species (ROS) when exposed to visible light. By oxidation processes these ROS can effectively break down a variety of organic dyes, eliminating hazardous contaminants from wastewater [9] CuO is low band gap (1.2eV) p-type semiconductor that finds utility as a high temperature superconductor in gas sensing, photocatalysis, photovoltaics, magnetic storage, and battery technology [10]. Because of its advantageous optical and electrical characteristics, Zinc Oxide (ZnO) is a wide band gap (3.37eV) n-type semiconductor with a wide range of applications in photovoltaics, including as a transparent conducting oxide electrode, gas sensing, photocatalysis, UV protection, pharmaceuticals and more [11]. It is commonly recognized that the photocatalytic activity of low-dimensional Zinc Oxide structures, such as one dimensional structures, is increased due to their broad surfaces, effective carrier migration, and short charge carrier migration paths [5], [12], [13]. In other words, the carefully controlled composition and the properly defined shape of different exposed crystal faces that is polar and non-polar faces with variable energies on the surface can be used to identify the properties and potential applications of low- dimensional Zinc

Oxide nanocrystal [14] With a direct bandgap of 1.48eV to 2.19eV, great mechanical strength, and chemical stability at high temperatures, Co3O4 is a spinal structure of p-type semiconductor. Presence of Co3+ ions allow Co3O4 nanoparticles to exhibit high conductivity. Wide-bandgap semiconductors can also be activated by cobalt species to cause visible-light water oxidation [15] .

Application and research on mixed metal oxides are growing in the fields of engineering, chemistry, physics and materials science. In a variety of technological applications, materials with unique physical and chemical properties that result from the combination of two or more metals in an oxide matrix can perform significantly better [16]. The performance of a nanostructured system can be significantly enhanced by the interactions between its constituent materials. Microscopic charge transfer, longer charge carrier lifetimes, and improved charge separation efficiency are all facilitated by the close contact surfaces of composited materials with complementary band potentials Click or tap here to enter text.

ZnO has some drawbacks such as larger band gap .Prior to the commercialization of ZnO-NPs as photocatalysts, its properties must be improved because the recombination rate of light generated electron hole (LGEH) pairs is quite high. Combination with other metal oxide to form composite can improve the properties to inhibit LGEH[19]Similarly. Doping or making composite also improve the properties of CuO and Co_3O_4. The present work details the synthesis of three binary and a ternary nanocomposite comprising ZnO, CuO and Co_3O_4 using co-precipitation method. They were characterized by using UV -Vis spectroscopy, Fourier transform infrared spectroscopy (FTIR), X-rat diffraction (XRD), scanning electron microscope (SEM) and EDX (Energy dispersive X-ray spectroscopy). This study aims to introduce a new multiphase mixed metal oxide nanocomposite that may have variety of possible application specially photocatalysis of dye.

1.2. Rational of the study

Methylene Blue is a common dye used in various industries and act as a pollutant when release in water. Photocatalytic degradation using nanocomposite offers a promising method to break down these dyes into harmless components. Metal oxide nanoparticles can be good choice for this as they have shown rapid expansion in treating wastewater. Metal-metal and metal-oxygen-metal

interactions in mixed metal oxides can lead to novel structural and electronic properties not found in the single oxide which can remove organic pollutant by photocatalytic degradation. Two metals can behave as 'isolated units' that bring their intrinsic properties to the system, or could possess properties modified by metal-metal or metal-oxygen-metal interaction. ZnO, CuO and Co_3O_4 are good photocatalyst reported in various work. Combination of this three photocatalyst can increase the efficiency of each of them.

1.3. Statement of the problem:

Water is an important source of survivals and plays a significant role in developing industry and economy on earth. Rapid industrial expansion caused the release of several harmful mineral and biological pollutanta (dense material,dyes etc.)in water. Less than 1 ppm of dye can still be seen and has toxicologically hazardous effects. The presence of organic dyes inhibits photosynthesis and contribute to various significant health problems for human populace. To tackle this issues, it is crucial to treat wastewater produce by the sectors before discharging it.

1.4. Objectives:

- To synthesize ZnO/CuO, ZnO/Co_3O_4, CuO/Co_3O_4 and ZnO/CuO/Co_3O_4 nanocomposite using co-precipitation method.
- To characterize synthesized nanocomposites by UV-Vis, FT-IR, XRD, FE-SEM and EDX.
- To study the photocatalytic activity of the composites and the effect of Initial dye concentration, amount of catalyst dosage and irradiation time on the photocatalytic degradation of MB dye.

Chapter two: Literature review

Vijaya Kumari et al., reported on the synthesis of heterogeneous ZnO/CuO hierarchical nanostructures for photocatalytic degradation of organic pollutant. They outlined that the heterostructure has better photo degradation capability than the single one. The structure has improved optical response, change in morphology (bitter gourd or mulberry like) and have effective photoinduced charge carriers [20]

Vasi Uddin Siddiqui et al., explained the optimization of ZnO/CuO nanophotocatalyst for Dye Degradation by Visible light irradiation. Their synthesized composite had higher surface area than single ZnO and CuO nanoparticle($83.13 m^2.g^{-1}$). It showed 98% of degradation efficiency for BPB and RhB dye**.** Again it has high regression R^2 value and first ordr kinetics [21]

Pradip Sable et al., synthesized ZnO/CuO nanocomposite via co-precipitation method and studied the effect on structural morphological and optical properties of pure and ZnO , CuO and ZnO/CuO nanocomposite. XRD analysis exhibited that pure ZnO, CuO and ZnO/CuO nanocomposite has a nanometer size with an average of 15.19nm. The FE-SEM and EDX analysis revealed that ZnO has hexagonal structure and CuO has a monoclinic structure [22]

M. Nami et al., fabricated ZnO/CuO coating nanocomposite by simple anodic oxidation of alpha brass. ZnO/CuO shows flower and patches like heterostructure. After 30min of photocatalytic performance after 30min the anodized brass showed 54% and 49% degradation of MB and phenol. The composite showed highest efficiency after 300min [23].

Javed Shokraiyan et al., synthesized ZnO nanorod, CuO microspheres and ZnO/CuO nanocomposite by template-free precipitation method. They found that under LED light irradiation

ZnO/CuO has higher photocatalytic activity than ZnO and CuO in the degradation of MB and 4-nitrophenol (98 and 97%) respectively [24]

A B Migdadi et al., reported hydrothermal synthesis of ZnO/CuO nanocomposite and its kinetic degradation study of MB. Band gap of ZnO reduced from 3.36 to 3.1 eV.Pure ZnO showed photocatalytic efficiency of 74.5% and the composite of ZnO and 10% CuO showed a high rate of efficiency around 97.15% in 90min .

Nargol Jalali et al., showed the effect of pH on the change in morphology of ZnO/CuO and its photocatalytic activity. The synthesis was done by chemical bath precipitation. The reported that with the change of pH the morphology of nanocomposite also changes [25]

Susmita Das et al., synthesized and characterized ZnO/CuO nanocomposite by electrochemical method. Band gap energy obtained is 3.4eV. They showed that ZnO exhibited higher reflectance than ZnO/CuO nanocomposite. ZnO/CuO showed higher electrochemical activity than bare ZnO nanoparticle [26]

N. Kumaresan et al., showed ZnO/CuO along with rGO ternary nanocomposite can be used as a potential materials for energy and environmental remediation. The reported that the ternary composite has band gap value of 2.8eV which is less than single ZnO. The flowerlike structure showed enhanced photocatalytic activity. The ternary nanocomposite show 99% and 93% of degradation efficiency respectively against RhB dye and 4-Chlorophenol for 20min under visible light irradiation [27]

Aklilu Guale Bekru et al., synthesized ZnO/CuO nanocomposite from *Verbascum sinaiticum* and examined photodegradation of MB and reduction of 4-Nitrophenol. 20% CuO/ZnO compared to ZnO and CuO demonstrated improved photocatalytic activity against MB dye with a $0.017min^{-1}$ rate and reduction of 4-Nitrophenol at $0.237min^{-1}$ rate. The enhancement is due to the synergy between ZnO/CuO and reduced electron hole recombination rate [28]

Ambreen Ashar et al., reported the capability of ZnO/CuO for tha removal of heavy metal from water. The showed ZnO/CuO nanocomposite has high harvesting power of solar radiation due to low band gap energy 2.9eV. They grafted ZnO/CuO onpolyester fabric through SILAR method. In acidic condition the composite removed 97% of Cr(VI) after four hours. It has 11 batches reusability under sunlight [29]

Irum Shaheen et al., reported use of foliar fuel in the synthesis of ZnO/Co_3O_4 and investigated its electrochemical behaviour for supercapacitors. The size of their synthesized nanocomposite was 20nm and specific capacitance of 165Fg^{-1} calculated by CV. Based on charge discharge results, the phyto-functionalized nanocomposite demonstrated an energy density of 4.1 W h kg^{-1} and a power density of 7.5 kW kg^{-1} [30]

Halah T. Mohammed et al., showed that ZnO/Co_3O_4 p-n heterojunction is a good photocatalyst to remove antibiotics from wastewater which was synthesized by co-precipitation method. FE-SEM showed the average particle size is 68.52nm. The used the composite against the antibiotics azithromycin and ciprofloxacin. The removal of ciprofloxacin and azithromycin was 84.5% and 71.7% respectively in 80min under visible light [12].

Yuanjun Liu et al., reported that Co_3O_4/ZnO has excellent gas-sensing properties and have real application. The composite were synthesized using an easy wet-chemistry route and characterized using XRD, FE-SEM, HRTEM and EDX. The nanocomposite exhibit enhanced gas-sensing performance such as high stability and high sensing response. The integration of Co_3O_4 with ZnO increase the sensing ability of Co_3O_4/ZnO [13].

Eshetu M. Abebe et al., examined the influence of temperature on ZnO/Co3O4 nanocomposite for high energy storage supercapacitors. The composite was synthesized by a two-step chemical bath deposition method followed by calcination which produce ZnO nanosheet grown on Ni and then flat nanosheets were developed and formed porous film. The conductivity of Co3O4 increases due to the presence of ZnO nanotube. The product has high specific capacitance of 940 F g^{-1} . [14].

D. Bekermann et al., synthesie Co3O4/ZnO p0n heterojunction nanocomposite using Plasma Synthesis for gas sensing application. The successful creation of pure and high-area nanocomposites with a targeted overdispersion of Co3O4 particles on ZnO and an intimate contact between the two oxides was demonstrated by structural, morphological, and compositional investigations. Furthermore, the chosen synthesis approach offers exciting new avenues for the design of p/n composite nanoarchitectures for a variety of uses, such as ferromagnets in spintronic devices, photoinduced pollutant degradation, and heterogeneous catalysis. In this direction, efforts are presently being made [15].

Ramesh Kumar et al., synthesize spindle like Co3O4 nanocomposite Scaffold for Hydrazine Sensing and degradation of RhB dye. 98% degradation of the dye was ovserved in 50min. They

studied the sensing using Co3O4/ZnO nanocomposite modified gold electrode for hydrazine. Due to improved surface area and charge separation efficiency the composite showed good sensing abilities and photodegradation efficiency [16].

Irum Shaheen et al., reported green synthesis of ZnO-Co3O4 nanocomposite and its electrochemical behaviour. The used E. cognata for the synthesis which was obtained by sol-gel method. The particle size of the composite was 20nm which was investigated as an electrode material for supercapacitor. As a result, cyclic voltammetry demonstrated that the nanofeatures and phyto-organic functional groups offered plenty of active sites for charge storage nanwith a specific capacitance of 165 F g^{-1} [17].

Beshir A. Hussein et al., made a sensitive non-enzymatic electrochemical glucose sensor based on a ZnO/Co_3O_4/rGO nanocomposite using hydrothermal method. The composite exhibited excellent electrochemical performance with higher photocatalytic activity and low working potential. The ZnO/Co_3O_4/rGO glassy carbon electrode (GCE) modified electrochemical glucose sensor showed a fast reaction time (about 3 s), low detection limit (0.043 μM), high sensitivity (1551.38 μA mM^{-1} cm^{-2}), and wide linear range (0.015–10 mM) when glucose measurement was performed under ideal conditions. In addition, the ZnO/Co_3O_4/rGO/GCE electrochemical sensor's practical application is highly suitable for the detection of glucose in real samples for use in medical diagnostics and the food industry. The obtained results were found to be in good agreement with data obtained from hospital spectrophotometric methods as well as glucose label values [37]

M Rashad et al., fabricated p-p type nanocomposite of NiO/Co_3O_4 and CuO/Co_3O_4 with different contents by using direct precipitation method. The average crystalline size of mixed and pure nanoparticles has been computed. It is possible to produce substitution alloys because the ionic radius of $Co2^+$ is noticeably less than that of $Ni2^+$ and $Cu2^+$ [38]

Desalegn Tesfa Tefera et al., showed green synthesis, characterization and antioxidant and antibacterial activities of CuO, Co_3O_4 and CuO-Co_3O_4. UV-Vis analysis revealed the band gap are 3.22eV, 3.36eV and 3.66eV for CuO, Co_3O_4 and CuO-Co_3O_4 nanosystem. CuO have monoclinic crystal structure with crystallite size of 11.59nm, Co_3O_4 has cubic structure with 12.25nm and CuO-Co_3O_4 has average crystallite size 9.53nm. When compared to CuO NPs and Co3O4 NPs, the CuO-Co3O4 nano combination shown more inhibitory effects against the chosen bacterial strains [39]

Chapter Three- Materials and Methods

3.1 Chemicals

Analytic-grade reagents of Cobalt dichloride hexahydrate extrapure AR,99%($CoCl_2.6H_2O$) purchased from Merk, Germany and Zinc Nitrate Hexahydrate ($Zn(NO_3)_2.6H_2O$) Cupric Nitrate Trihydrate ($Cu(NO_3)_2.3H_2O$), Sodium Hydroxide (NaOH), Methylene Blue Dye, purchased from Sigma Aldrich company were employed.

3.2. Reaction Scheme:

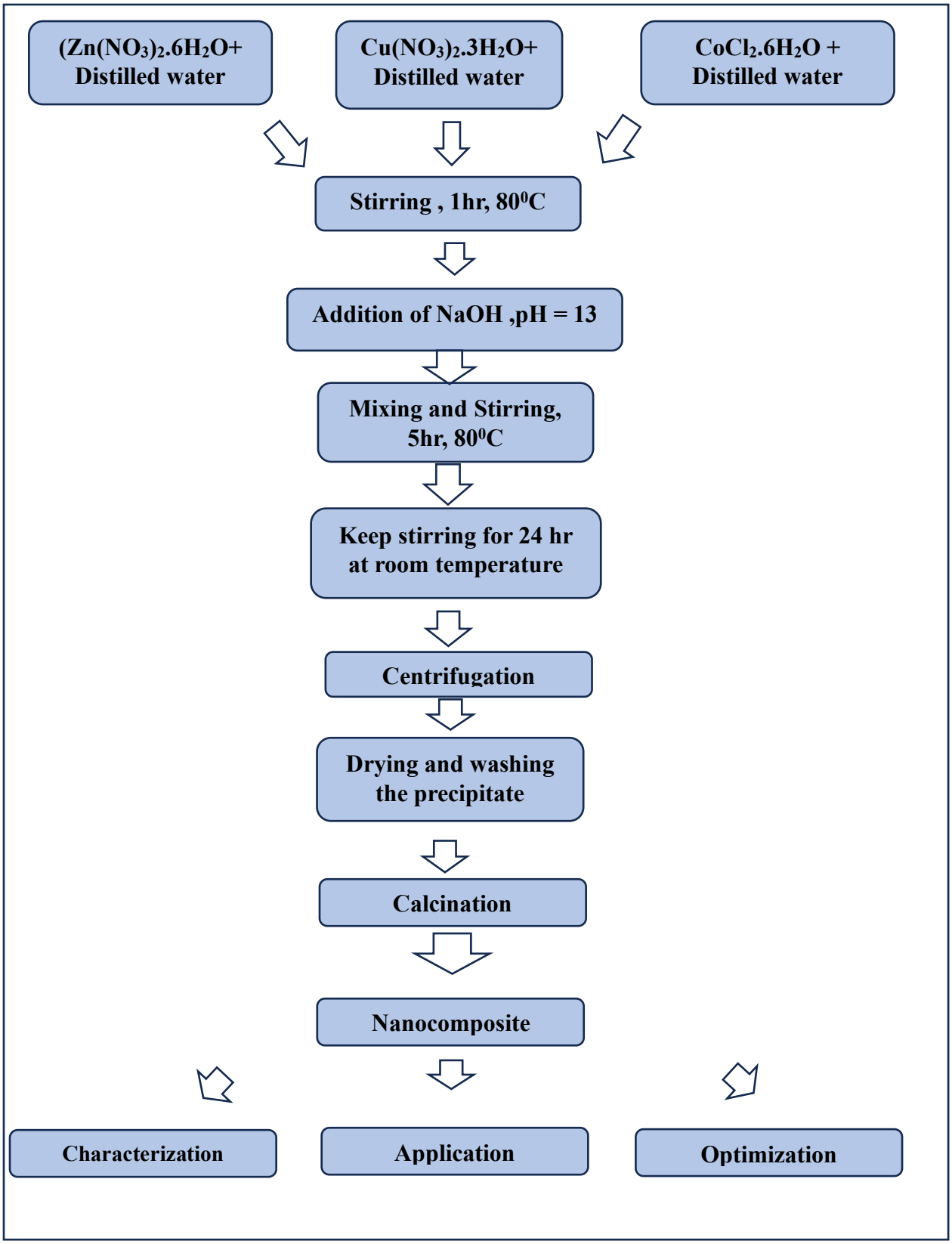

3.3.Synthesis of nanocomposite:

3.3.1. Synthesis of ZnO/CuO nanocomposite :

ZnO/CuO nanocomposite can be synthesize using sol-gel method [40] Co-precipitation method [41], perfume spray pyrolysis method [42] Bras anodization process [23], Chemical bath precipitation [25]Electrochemical method [26]In our study, ZnO/CuO was synthesized by following co-precipitation method. At first, 0.2416gm of $Cu(NO_3)_2.3H_2O$ was dissolved in 100ml of distilled water and 0.3gm $Zn(NO_3)_2.6H_2O$ was dissolved in 100ml of distilled water in two separate beakers. In a hot plate the solutions were stirred for 1hr in 80^0C. After completely dissolving the salts 1M NaOH solution was added dropwise in both solution until the pH become 13. After adding NaOH the solution started to produce precipitate. The solution containing Zinc salt turns from colourless to white and solution containing Copper salt give sky blue precipitate. The solutions then mixed in a beaker and kept stirring for 24 hour at room temperature. The solution with precipitate was centrifuged at 4000rpm for 30min. The precipitate obtained was dried and washed with distilled water. Then the product was calcined at 3500C for 2hr in Muffle Furnace. The final product was collected and it was powder with black color.

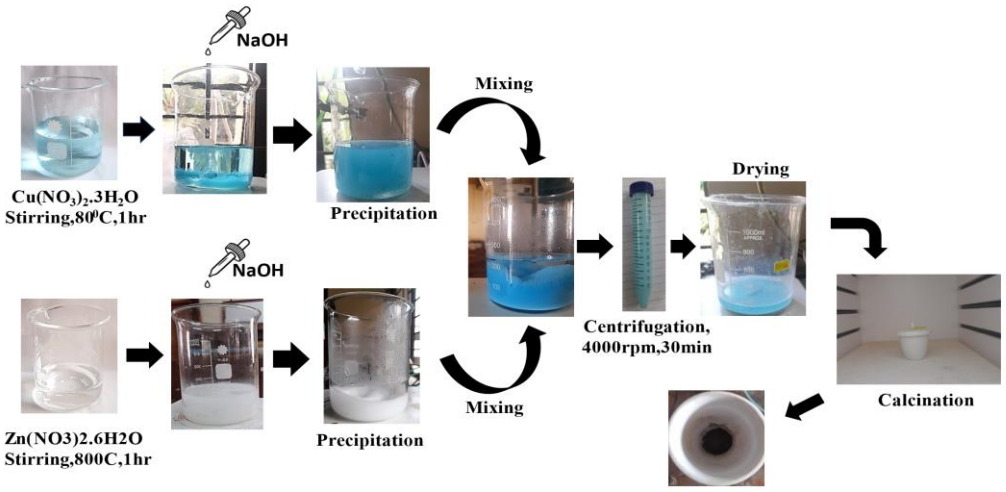

Figure 1: Synthesis of ZnO/CuO nanocomposite

3.3.2. Synthesis of ZnO/Co_3O_4 nanocomposite :

Wet-chemical route for the synthesis of ZnO/Co3O4 nanocomposite was reported in [32]In our study, 0.24gm of $CoCl_2.6H_2O$ and 0.3gm $Zn(NO_3)_2.6H_2O$ were dissolved in 100ml of distilled water in two separate beakers. In a hot plate the solutions were stirred for 1hr in 80^0C. After completely dissolving the salts 1M NaOH solution was added dropwise in both solution until the pH become 13. After adding NaOH the solution started to produce precipitate. The solution containing inc salt turns to white and solution containing Copper salt give sky blue precipitate. The solutions then mixed in a beaker and kept stirring for 24 hour at room temperature. The solution with precipitate was centrifuged at 4000rpm for 30min. The precipitate obtained was dried and washed with distilled water. Then the product was calcined at 350^0C for 2hr in Muffle Furnace. The final product was collected and it was powder with black color.

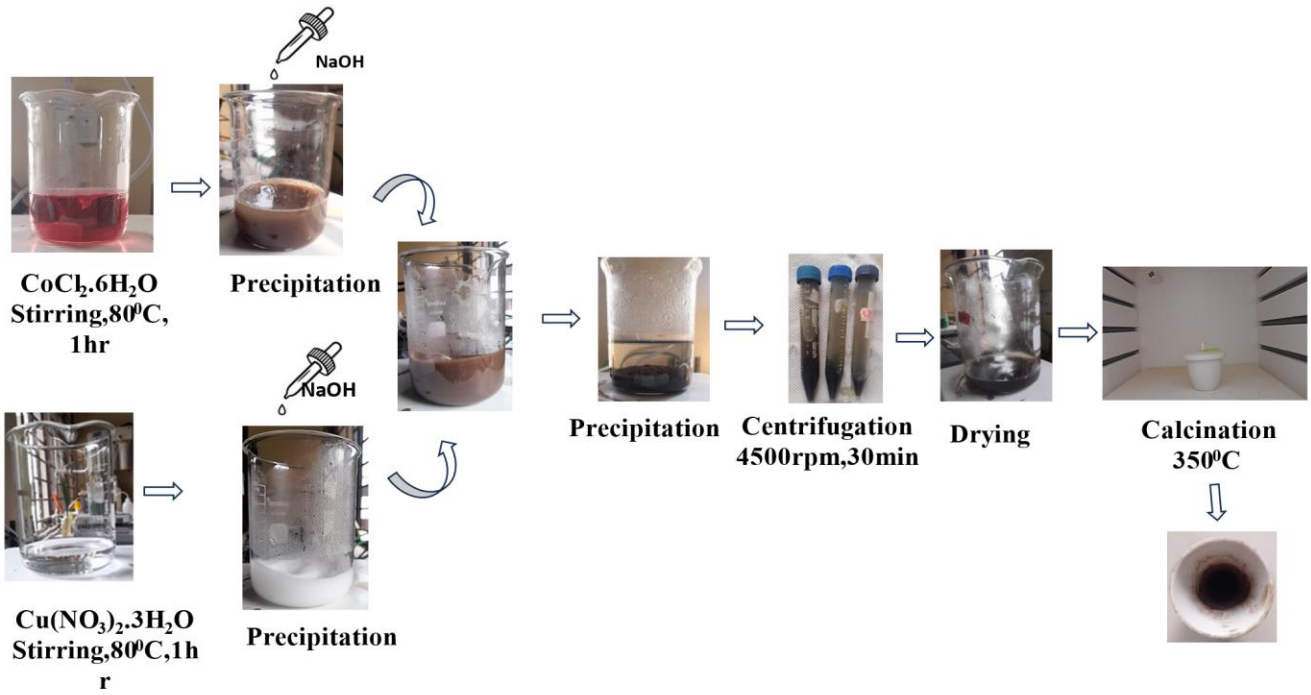

Figure 2: Synthesis of ZnO/Co_3O_4 nanocomposite

3.3.3. Synthesis of CuO/Co_3O_4 nanocomposite:

0.24gm of $CoCl_2.6H_2O$ and 0.2416gm of $Cu(NO_3)_2.3H_2O$ were dissolved in 100ml of distilled water in two separate beakers. In a hot plate the solutions were stirred for 1hr in 80^0C. After completely dissolving the salts 1M NaOH solution was added dropwise in both solution until the pH become 13. After adding NaOH the solution started to produce precipitate. The solution containing inc salt turns to white and solution containing Copper salt give sky blue precipitate. The solutions then mixed in a beaker and kept stirring for 24 hour at room temperature. The solution with precipitate was centrifuged at 4000rpm for 30min. The precipitate obtained was dried and washed with distilled water. Then the product was calcined at 350^0C for 2hr in Muffle Furnace. The final product was collected and it was powder with black color.

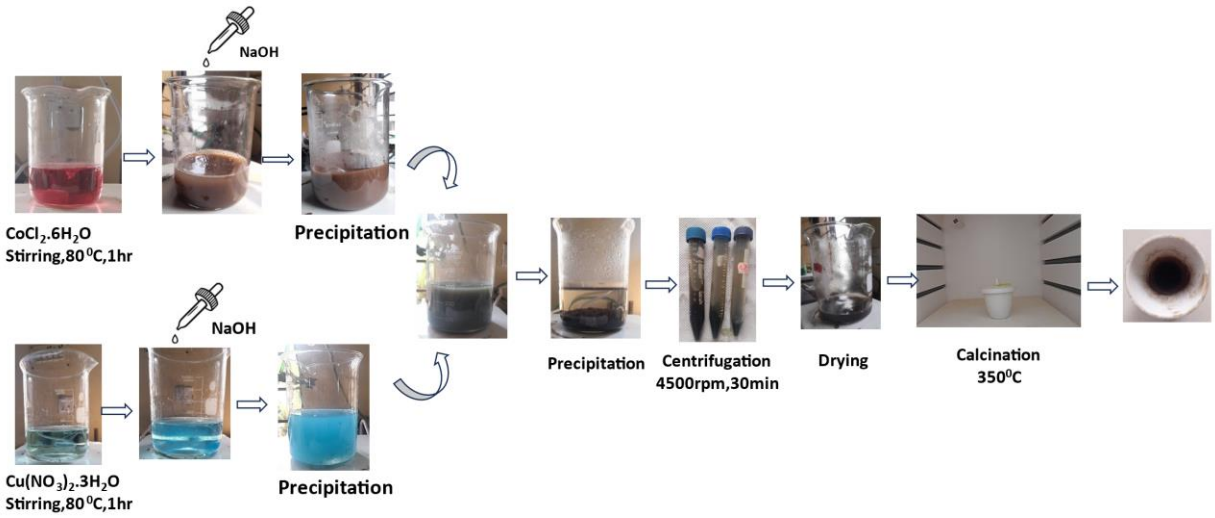

Figure 3 : Synthesis of CuO/Co3O4 nanocomposite

3.3.4. Synthesis of ZnO/CuO/Co_3O_4 nanocomposite:

0.3gm Zn(NO3)2.6H2O, 0.24gm of $CoCl_2.6H_2O$ and 0.2416gm of $Cu(NO_3)_2.3H_2O$ were dissolved in 100ml of distilled water in two separate beakers. In a hot plate the solutions were stirred for 1hr in 80^0C. After completely dissolving the salts 1M NaOH solution was added dropwise in both solution until the pH become 13. After adding NaOH the solution started to produce precipitate. The solution containing inc salt turns to white and solution containing Copper salt give sky blue precipitate. The solutions then mixed in a beaker and kept stirring for 24 hour at room temperature. The solution with precipitate was centrifuged at 4000rpm for 30min. The precipitate obtained was dried and washed with distilled water. Then the product was calcined at 350^0C for 2hr in Muffle Furnace. The final product was collected and it was powder with black color.

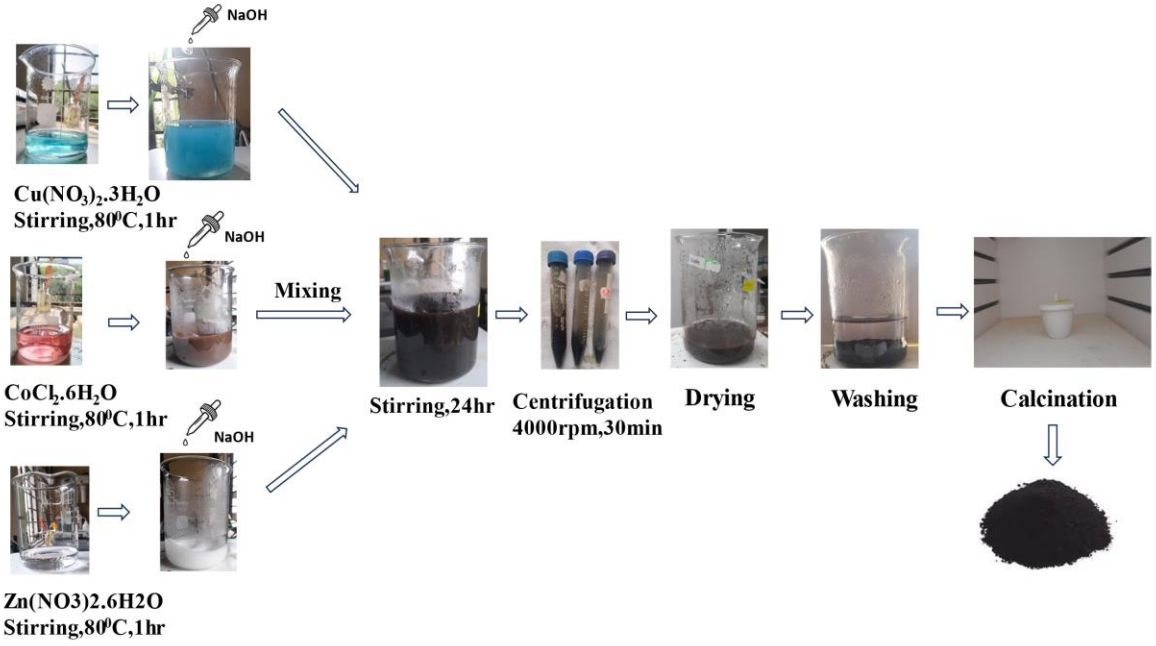

Figure 4 : Synthesis of ZnO/CuO/Co3O4 nanocomposite

3.4. Characterization

- **UV:** A freshly prepared solution of cobalt oxide dispersed in water was prepared for UV-Visible spectrometric analysis. The optical spectral analysis of these colloids was performed using 1 cm quartz cuvettes and using Drawell DU-8800D UV/VIS double beam spectrophotometer at scanning range 200-800 nm wavelength.

- **IR:** 1-2 mg of the final product Cobalt Oxide was grinded in the special mortar and pestle (both made of agate) until it is shiny. Then around 80 mg of anhydrous KBr was added and mixed quickly with the sample (since KBr will absorb moisture from the air, therefore always keep the lid of bottle of KBr tightly sealed since it quickly absorbs moisture). The contents (~30-40 mg) of the ground mixture were added to the press and left the sample under pressure for 30 seconds before carefully removing one of the bolts. A successfully formed pellet is almost translucent. IR spectrum was obtained by carefully placing the KBr press in the holder of the sample chamber of the IR. IR facility provided by Leather Engineering Institute, Dhaka.

- **XRD:** The samples were analyzed for their particle size and by powder X-ray diffraction (PXRD). For the PXRD dried samples from muffle furnace were grounded in a mortar with a pestle then taken in the sample holder. The XRD facility provided by the BCSIR (Bangladesh Council of Scientific and Industrial Research), Dhaka. The X-ray source consisted of unfiltered Cu Kβ radiation ($\lambda = 1.5418$ Å). Spectra were recorded with 2 theta (2θ) values ranging from 10 to 80 degrees in steps of 0.01 degree.

-

- **FE-SEM and EDX:** FE-SEM and Energy dispersive X-ray spectroscopy were taken by Scanning Electron Microscope in different multiplication to know the morphology of the product. This was done in the BCSIR (Bangladesh Council of Scientific and Industrial Research), Dhaka.

3.5 Photocatalytic activity test

The breakdown of methylene blue is frequently used as an example to illustrate how well photocatalysts work in wastewater treatment processes. Methylene blue (MB) is a kind dye molecule that is frequently used to characterise semiconductors by photocatalytic degradation [43]**.** In the present work, the nanocomposite was used as a catalyst to degrade MB dye in presence of sunlight at room temperature (25°C). The photocatalytic activity was done in between 11.00am-3.00pm in day time. The MB dye degradation experiment was done by using a series of catalyst dosage (2mg-6mg) and using different initial dye concentration ($5mgL^{-1}$-$20mgL^{-1}$) for 120min. The nanocomposite of specific weight was added to 100ml of MB dye solution and the mixture were vigourously stirred for 20min to achieve an adsorption-desorption equilibrium. The pH of the solution was 6.68. During the experiment optimization of the various parameters catalyst dosage, initial dye concentration , reaction time were done.

6 After each 20minute of time interval under sunlight, 5ml of aliqiot were taken off from the solution for monitoring the photodegradation of the dye. It was then centrifuged for 5minute and the resultant clear solution was employed for examining using UV-Visible Spectrophotometer at λ_{max} =665nm noted for MB. The percent dye degradation efficiency of the catalyst expressed by the following equation

Degradation efficiency (%) = $\frac{C0-Ct}{C0} \times 100$

To calculate the kinetic measurements, the formula used is ln $(\frac{Ct}{C0})$ = Kt ; where, K is the rate of reaction. C_0 is the initial concentration of dye and C_t is the dye concentration at time t.

Reusability test: Checking the reusability of photocatalyst is crucial for the evaluation of efficiency of photocatalyst. After the degradation process the photocatalysts used were collected and used for the reusability test under the same condition as previously done. At first the photocatalyst were collected from the dye solution. Then washed by ethanol and distilled water and dried in the oven at 80^0C. The dried product were used for the reusability test.

Chapter Four- Result and discussion

4.1. Uv-Visible Spectroscopy Analysis:

4.1.1.UV-Visible spectrum of ZnO/CuO:

ZnO exhibits distinct n-type semiconductor characteristics, characterized by direct bandgap of 3.24eV[44] . CuO function as a p type semiconductor with a band gap 1.4eV[45]. The amalgamation of p-CuO and n-ZnO in heterojunction strategically laverages the intrinsic advantages of p-n heterojunction [46] .The integration of ZnO and CuO in ZnO/CuO nanocomposite mitigates the rate of electron-hole pair recombination. As a result, this process make it easier for charge carriers to separate effectively, which make the nanocomposite a material that responds well to visible light [47]**.** The room temperature UV-Visible spectrum for ZnO/CuO nanocomposite is shown in the Fig.4.1. This characterization was done by using UV-vis spectrophotometer. The absorption curve for the synthesized ZnO/CuO nanocomposite is obtained at 296nm. Pure ZnO shows strong absorbance in between 300nm to 400nm whereas pue CuO shows absorbance in between 300 to 800nm [48].The UV-Vis absorption spectra of the synthesized ZnO/CuO nanocomposite shows a shift from 300nm which confirms that there is higher amount of ZnO in the composite.

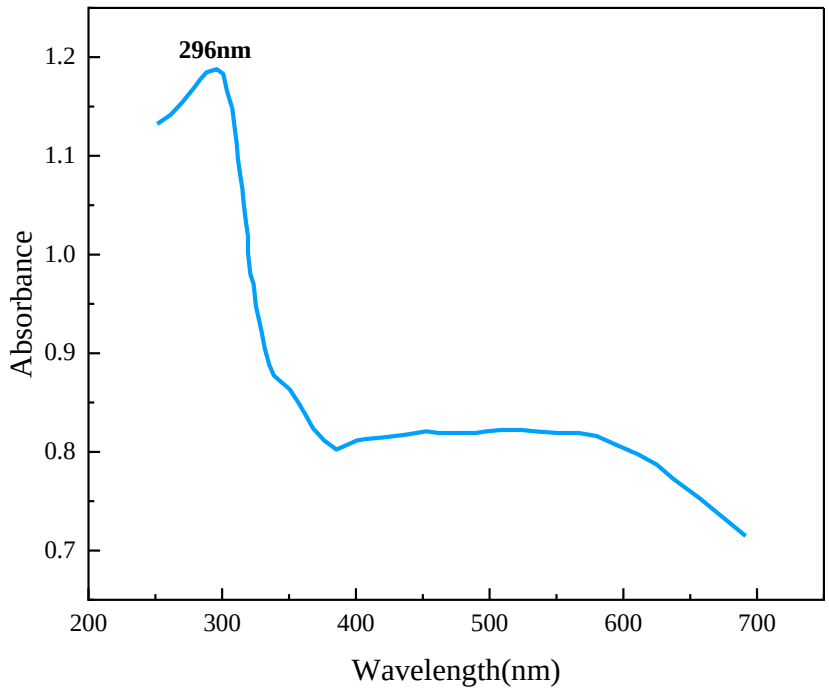

Figure 5 : UV-Visible spectrum of ZnO/CuO nanocomposite

4.1.2.UV-Visible spectrum of ZnO/Co_3O_4 nanocomposite:

The formation of the nanocomposite results in a broad absorption spectrum. This phenomenon significantly influences optical parameters, including the complex refractive index and absorption

co-efficient, thereby enhancing the nanocomposites properties. The binary nanocomposite ZnO/Co_3O_4 shows two broad peaks at 377nm and 546nm. The multiple peaks are attributed due to the possibilities of O^{2-} to Co^{2+} and O^{2-} to Co^{3+} charge transfer process in Co_3O_4. The obtained result is in accordance with the literature [49]

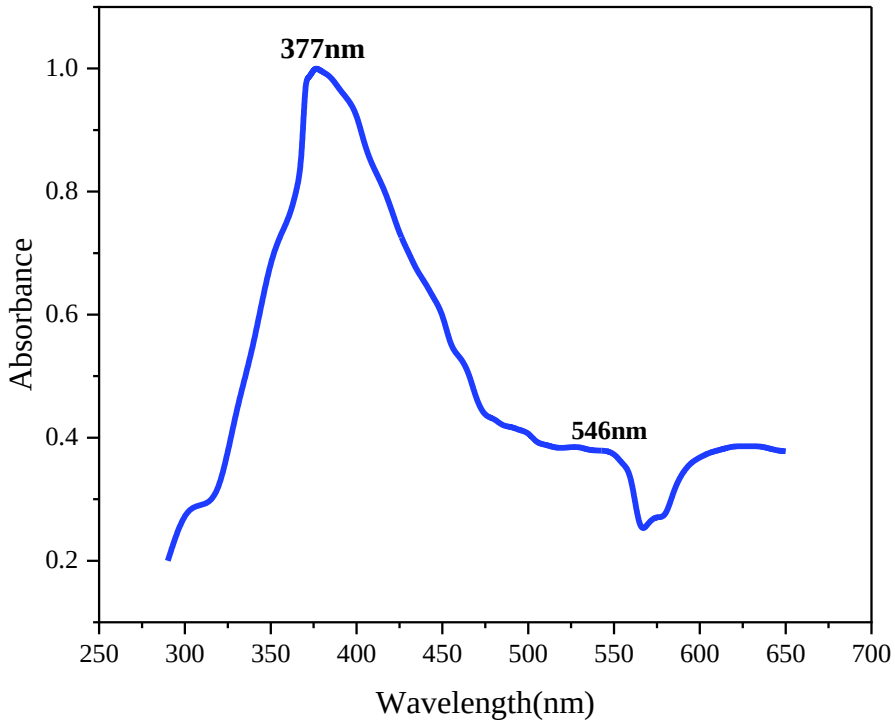

Figure 6 : UV-Visible spectrum of ZnO/Co3O4

4.1.3.UV-Visible spectrum of CuO/Co_3O_4 nanocomposite:

UV-Vis absorption spectra of CuO/Co_3O_4 binary nanocomposite is shown in the Fig. The composite shows a peak at 265nm which is in accaordance with the literature [50]. The absorbtion band at 265nm confirm the formation of CuO nanoparticles [51]

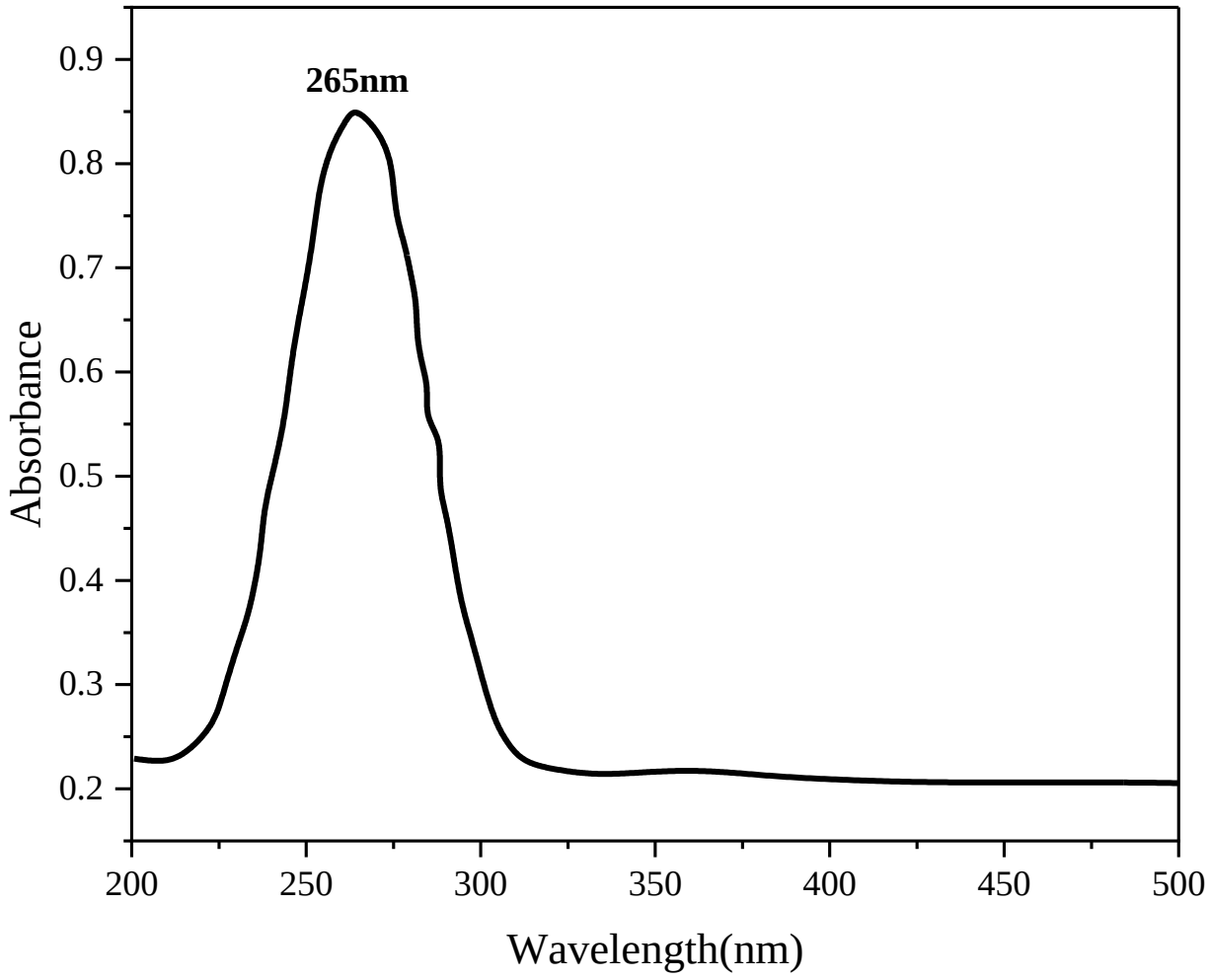

Figure 7 : UV-Visible spectrum of CuO/Co3O4

4.1.3.UV-Visible spectrum of ZnO/CuO/Co_3O_4:

The ternary nanocomposite in our study was synthesized in (1:1:1) ratio using co-precipitation method. Fig. shows three peaks for ternary nanocomposite at 330nm, 390nm and 443nm.

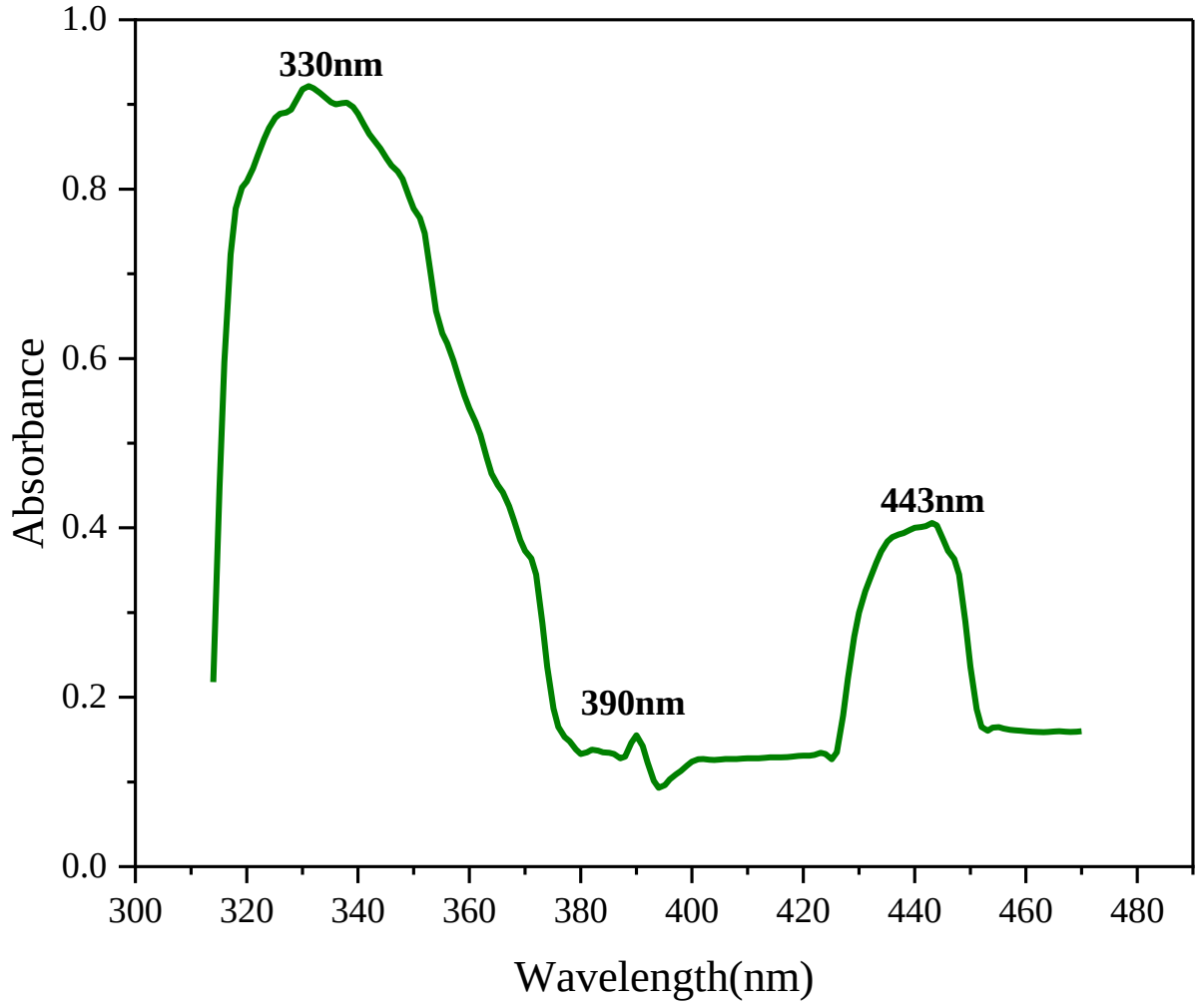

Figure 8 : UV-Visible spectrum of ZnO/CuO/Co3O4

4.2.Band gap energy:

With the UV-Vis absorption spectrophotometer being utilized to analyze how much light the nanocomposites are capable of absorbing, the initial absorption which confirms with the electron excitation from valance band to conduction band was adopted to deduce the optical band gap value of manufactured nanocomposites. The band gap of the nanocomposites were obtained by plotting $(\alpha h\upsilon)2$ as a function of energy ($h\upsilon$). Extrapolating the linear portion of the curve to absorption axis gives the band gap energies of the synthesized nanocomposite obtained. The relationship between absorption co-efficient (α) and energy($h\upsilon$) was given by Tauc Equation,

$$\alpha h\upsilon = K (h\upsilon - Eg)^n$$

Where,

E_g = band gap energy

α = absorption co-efficient

K = proportionality constant

$h\upsilon$ = energy of the incident photon

n = ½ for indirect band gap, 2 for direct band gap

h = Plancks constant

4.2.1 Band gap of ZnO/CuO nanocomposite:

In a nanostructure aspect, the electronic states become completely discrete , as per atoms and molecules. But in the case of electronic population between pair of discrete states , controlling the transitions weather it is allowed or not leads to the red shift [42]. Fig. shows the band gap energy plot of ZnO/CuO nanocomposite. Tauc plots were employed to asscertain the band gap of the ZnO/CuO nanocomposite. The average band gap value at 2.37eV using UV-Vis spectra for the entitled nanocomposite has describe a red shift.

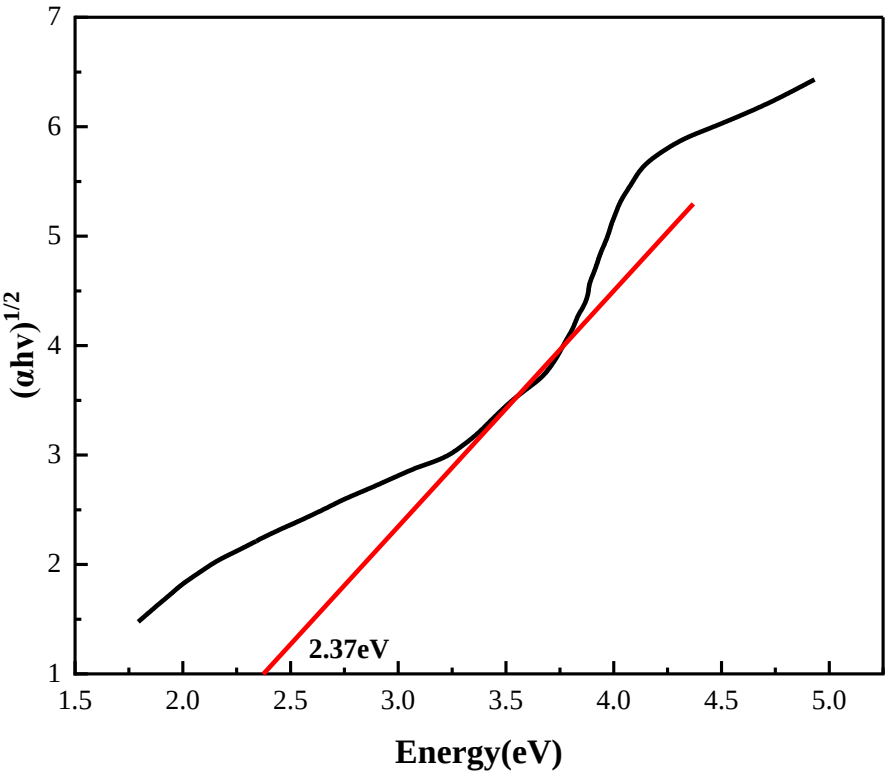

Figure 9 : Band gap of ZnO/CuO nanocomposite

4.2.2.Band gap of ZnO/Co_3O_4 nanocomposite:

The existance of two metal oxide nanoparticle in one composite affects the final band gap of the binary nanocomposite. Fig. shows plots of $(\alpha h\upsilon)^{1/2}$ versus photon energy of ZnO/Co_3O_4 nanocomposite. There are two regions in optical absorption. The first one (2.14eV) is related to Co_3O_4 and second one (2.34eV) is related to ZnO [52]

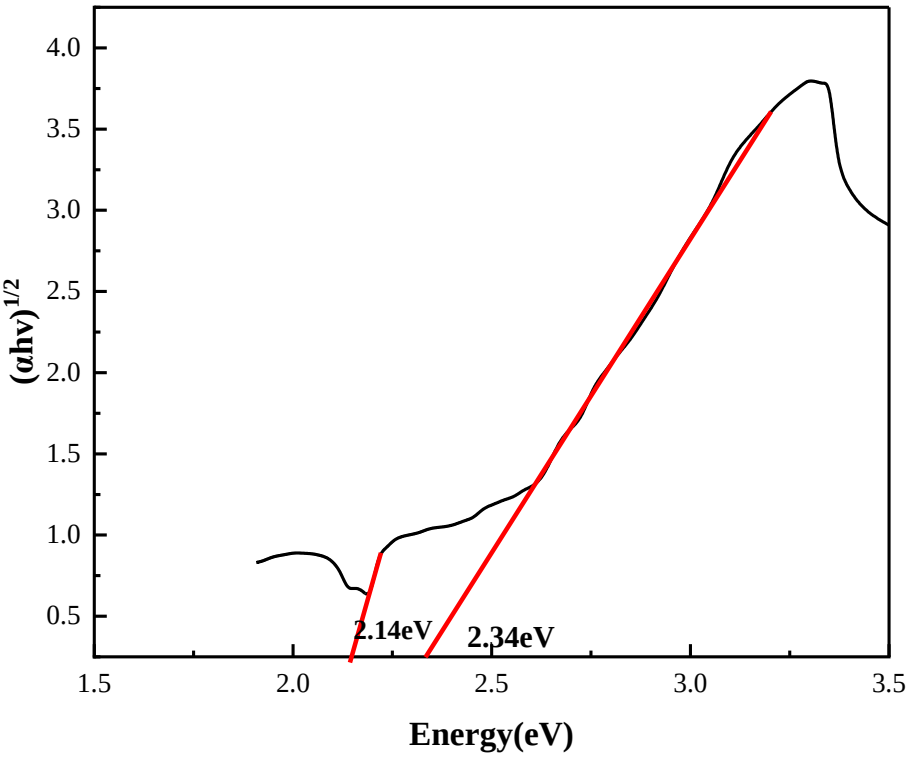

Figure 10 : Band gap of ZnO/Co3O4 nanocomposite

4.2.3.Band gap of CuO/Co_3O_4 nanocomposite:

Co_3O_4 nanoparticle exhibit two band gap energies 1.46eV and 2.0eV [53]Fig: shows band gap energy of CuO/Co_3O_4 nanocomposite . The band gap energy of synthesized nanocomposite is 3.78eV. The resultant nanocomposite have larger band gap compared to their monometallic equivalent. This suggests that substantial quantum confinement, which causes the conduction and valence bands' energy levels to move apart and results in a blue shift in the transition energy as particle size decreases, was present in the composite NPs [54]

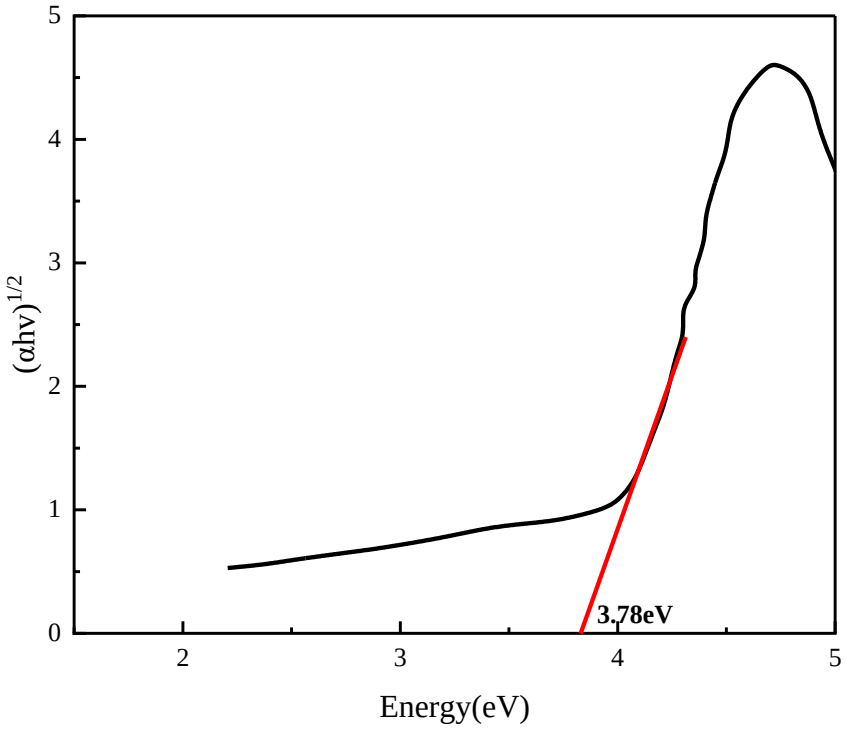

Figure 11 : Band gap of CuO/Co3O4 nanocomposite

4.2.4.Band gap of (ZnO/CuO/Co_3O_4) nanocomposite:

When a semiconductor absorbs photons of energy larger than the gap of semiconductor , an electron is transferred from the valance band to the conduction band there occurs an abrupt increase in the absorbency of material to the wavelength corresponding to the band gap energy [53].The synthesied ternary nanocomposite shows band gap of 2.2 eV at low intensity absorption and 3.19 eV at high intensity absorption.

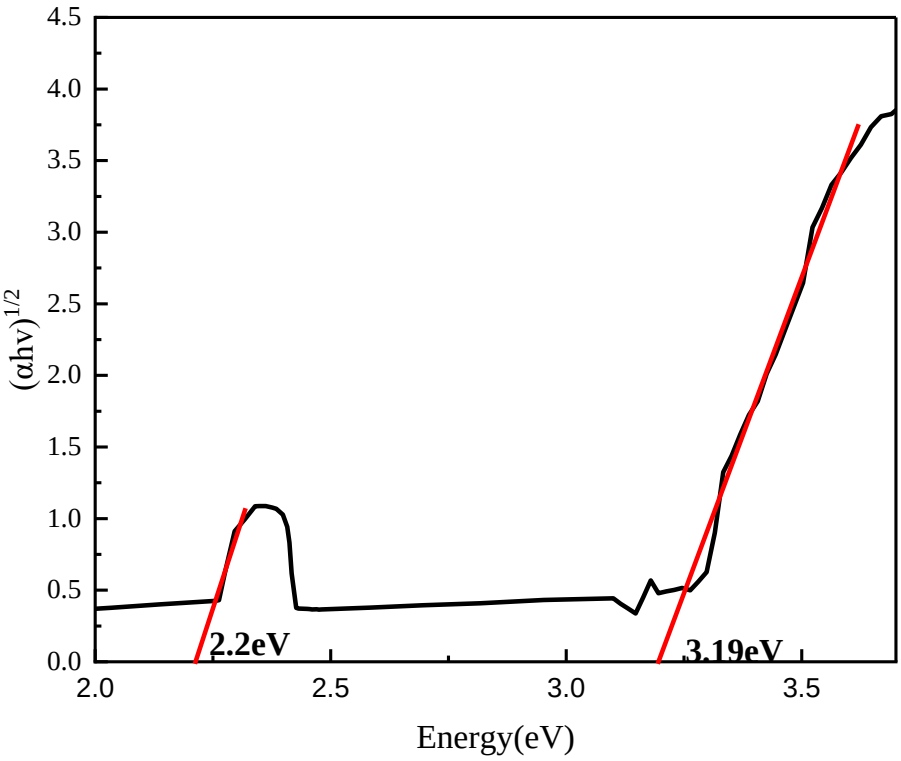

Figure 12 : Band gap of ZnO/CuO/Co3O4 nanocomposite

4.3. Fourier transform infrared spectroscopy:

FT-IR spectroscopy was also used to identify the functional group of the synthesized nanocomposites ZnO/CuO, ZnO/Co_3O_4, CuO/Co_3O_4 and ZnO/CuO/Co_3O_4. The resultant spectra are depicted at a scanning rate of 4000cm^{-1} to 500cm^{-1}.

Table 1 : Reference FTIR Data

Nanoparticle	Frequency	Vibrational Mode	Reference
ZnO	446cm^{-1}, 576cm^{-1}	Zn-O	[56]
	3472cm^{-1}	O-H stretching	
	1613cm^{-1}	H-O-H bending	
ZnO	782, 688, and 548 cm-1	Zn-O	[57]
CuO	601,508 and 487	Cu(II)-O	[55]
	601cm-1	Cu-O bond formation	

Co3O4	~570 and ~668cm-1	Co(III)-O and Co(II)Co(III)-O	[58]
Co3O4	574 cm-1 and 666 cm-1	Co-O	[59]
ZnO-CuO	494,512,530,532cm^{-1}	Zn-O	[11]
	429,476,612,583,653cm^{-1}	Cu-O	
	3000-3500 cm^{-1}	O-H stretching	
ZnO/Co3O4	662 and 563 cm^{-1}	Co^{2+}-O, Co^{3+}-O	[33]
	411 cm^{-1}	Zn-O	

4.3.1. FTIR spectra of ZnO/CuO nanocomposite:

The spectra of ZnO/CuO nanocomposite showed peak at~ 678cm^{-1} with low intensity which corresponds to Cu-O stretching and ~ 835cm-1 is for Zn-O which is due to the combination of CuO with ZnO. The band observed at ~1369 cm^{-1} could be assigned to the stretching of NO^{3-} group resulted from the precursors used in synthesis. The broad band in the range of ~3200-3500cm-1 corresponds to O-H bond stretching which might be owing to the surface-adsorbed molecules of water. The results are in accordance with literature [60]

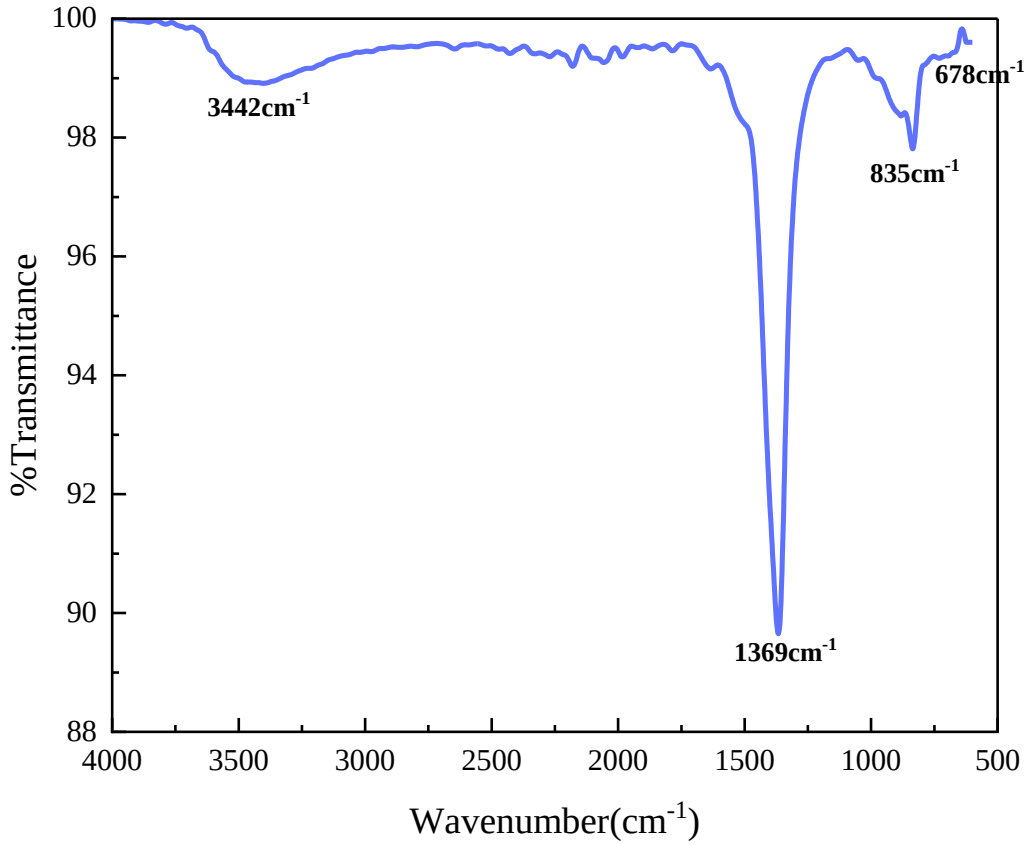

Figure 13 : Fourier transform infrared spectra of ZnO/CuO nanocomposite

Table 2: Infrared vibration of ZnO/CuO nanocomposite

Wavenumber(cm^{-1})	**Bond**
678cm^{-1}	Cu-O stretching
835cm^{-1}	Zn-O stretching
1369cm^{-1}	NO^{3-}
3442cm-1	O-H vibration

4.3.2. FTIR spectra of ZnO/Co_3O_4 nanocomposite:

Fig. shows the FTIR spectra of ZnO/Co3O4 nanocomposite. The broad band ata 3432cm-1 and 1616cm-1 could be attributed to O-H stretching and bending. The band at 654cm^{-1} is due to the bridging vibration of O-Co-O and it is in good agreement with the literature values [61]

Table 3 : Infrared vibration of ZnO/Co_3O_4 nanocomposite

Wavenumber(cm^{-1})	**Bond**
654cm^{-1}	O-Co-O
862cm^{-1}	Zn-O
1616cm^{-1}	O-H Bending
3432cm^{-1}	O-H stretching

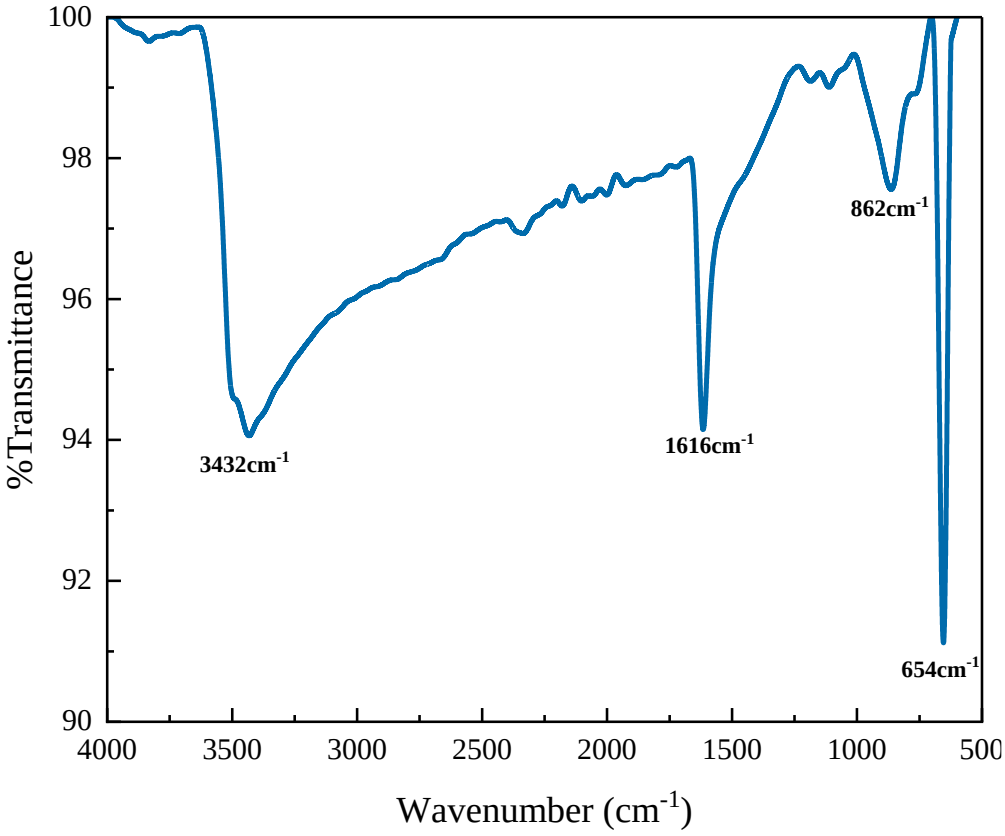

Figure 14 : FTIR spectra of ZnO/Co3O4 nanocomposite

4.3.3. FTIR spectra of Co_3O_4/CuO nanocomposite:

The FTIR spectra of Co3O4/CuO binary nanocomposite synthesized by co-preciptation method shows peaks at 645cm-1,828cm^{-1},1346cm^{-1},3407cm^{-1} respectively. The Broad peak at ~3000-3500cm-1 is for O-H stretching. The band at 654cm-1 represent Co-O stretching. The band observed at 1346cm-1 is may be due to NO3- group as we used nitrate salts while the synthesis procedure.

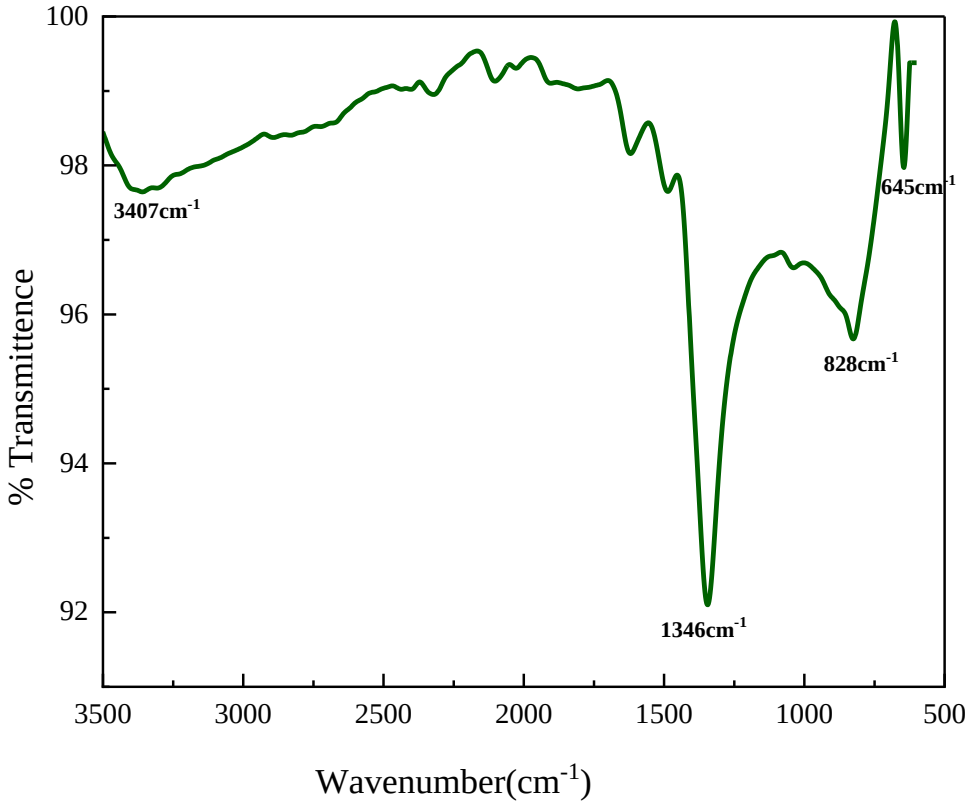

Figure 15 : : FTIR spectra of Co3O4/CuO nanocomposite

Table 4 : Infraredvibration of CuO/Co_3O_4 nanocomposite

Wavenumber(cm^{-1})	Bond
645cm^{-1}	Co-O
828cm^{-1}	Cu-O
1346cm-1	NO^{-3}
3407cm^{-1}	O-H

4.3.4. FTIR spectra of ZnO/CuO/Co_3O_4 nanocomposite:

The frequency of the bands may change their position due to the presence of three Metal oxide nanoparticle in one heterojunction. The broad peak at ~3000-3500cm^{-1} in the Fig. is for O-H stretching and band at 1634cm^{-1} is for O-H bending.

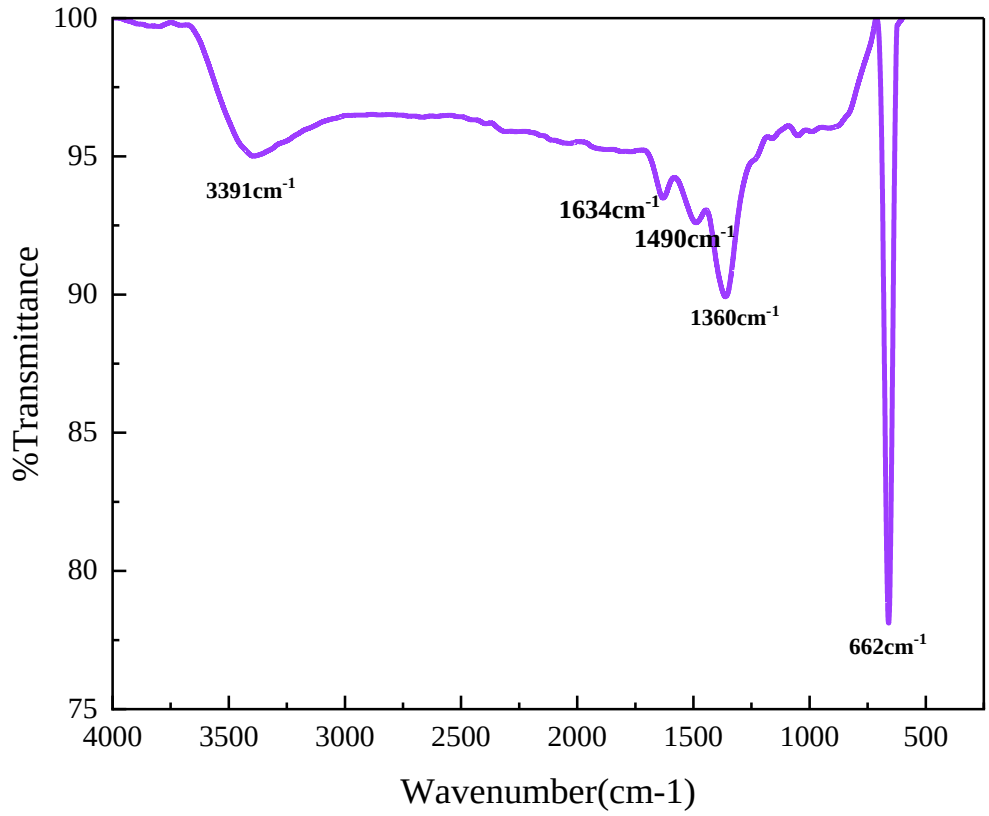

Figure 16 : FTIR spectra of ZnO/CuO/Co3O4 nanocomposite

Table 5: Infrared vibration of ZnO/CuO/Co_3O_4 nanocomposite

Wavenumber(cm^{-1})	Bond
662cm^{-1}	Co(II)-O stretching
869cm^{-1}	Zn-O
1634cm^{-1}	O-H bending
3391cm^{-1}	O-H stretching

4.4. X-ray diffraction spectra analysis:

XRD is an analytical tool used to distinguish crystalline phase and cell dimensions of nanoparticles. Along with this the detection of average size of particles is possible by using Debye-Scherrer equation**.** The crystallinity and crystal phase of the obtained powder products were probed by an X-ray diffraction (XRD) instrument with Cu Kβ radiation. The average particle size were determined Using Debye-Scherer formula :

$$D = k\lambda/\beta cos\theta$$

Where, D = Particle size

β = full width at half maximum of diffraction angle in radian (FWHM)

θ = The scattering angle

λ = The X-ray wavelength of radiation with 1.54 Å

k = 0.9

The lattice parameter (ao) determined according to the relation $a_o = d_{hkl} (h^2+k^2+l^2)^{1/2}$

Table 6 : Reference XRD data of ZnO,CuO,Co3O4

Nanoparticle	**2θ**		**Structure**	**References**
ZnO	31.768º, 34.422º, 36.253º, 47.539º, 56.594º, 62.858º, 66.374º, 67.947º, 69.085º, 72.568º, 76.959º, 81.387º and 89.613º with miller indices (100), (002), (101), (102), (110), (103), (200), (112), (201), (004), (202), (104), and (203)		Wurtzite	[56]
Co3O4	(111), (220), (311), (222), (400), (422), (511) and (440) at 2θ angle of 18.9, 31.14, 36.68, 38.51, 44.68, 55.75, 59.31 and 65.10 i		Cubic spinal	[59]
ZnO/CuO	ZnO	31.79, 34.45, 36.26, 47.58, 56.6, 62.88, 66.4, 67.98, and 69.11 were	Hexagonal	[28]

		indexed as (100), (002), (101), (102), (110), (103), (200), (112), and (201)		
	CuO	32.48, 35.62, 38.78, 48.94, 53.5, 58.29, 61.7, 65.9, 66.4, 68.08, and 72.46 indexed as (110), (11-1), (111), (20-2), (020), (202), (11-3), (022), (31-1), (220), and (311)	Monoclinic	
ZnO/Co_3O_4	ZnO	34.67, 47.61, 56.72, 62.75, and 68.17° - (002), (102), (110), (103), and (112)	Hexagonal	[33]
	Co_3O_4	19.07, 31.32, 36.84, 59.36, and 65.24°- (111), (220), (311), (511), and (440)	Cubic	

4.4.1.X-ray diffraction spectra of ZnO/CuO:

The diffraction peaks located at 2θ = 31.84°, 34.50°, 36.34°, 47.59°, 56.73°, 62.93°, 69.13°, 77.03° represented hexagonal wurtzite structure of ZnO (JCPDS card no – 00-036-1451) which are matched with miller plane (1 0 0), (0 0 2), (1 0 1), (1 0 2), (1 1 0), (1 0 3), (1 1 2) and (2 0 1) respectively. The additional diffraction peaks appeared in composites located at 2θ = 32.42°, 35.57°, 38.83°, 47.59°, 55.67°, 66.35°, 68.03° are indexed to monoclinic CuO (JCPDS card No. 01-080-1268) and assigned to miller plane (1 1 0), (-1 1 1), (1 1 1), (-2 0 2), (2 0 2), (-1 1 3), (-3 1 1) and (2 2 0) respectively [41], [62] .From the XRD pattern, it is confirmed that ZnO/CuO nanocomposite showed a well crystalline nature with no impurity peaks. Further, there is no secondary phase observed which confirms the pure phase. The average crystallite size of ZnO/CuO nanocomposite was found to be 35nm.

Table 7 : Peak position and average crystal size of ZnO/CuO nanocomposite

Peak Position	Intensity	FWHM	Crystallite size D (nm)	Average size (nm)
27.99796	370.8	0.1474	58.02674	23.14
29.15786	989.4	0.257	33.35563	

31.83751	4775.2	0.4322	19.96233	
32.42053	1516.6	0.4178	20.68298	
33.51251	313.8	0.2113	41.00361	
33.93747	1202.2	0.2773	31.28927	
34.49765	3677.2	0.3607	24.08866	
35.56789	4233.1	0.621	14.03117	
36.33996	7491.5	0.4822	18.10904	
38.83093	3341.9	0.7932	11.09088	
40.06471	308.6	0.408	21.6487	
44.72044	170.9	0.5182	17.31453	
47.58773	1003.3	0.6835	13.26783	
48.82111	736	0.8644	10.54126	
51.48373	177.6	0.3757	24.51703	
53.39085	214.3	0.7029	13.21254	
55.66632	209.6	0.8172	11.48146	
56.7287	2494.8	0.5547	16.99922	
58.28411	312	0.9938	9.55913	
61.62226	553.1	1.0322	9.3597	
62.93042	1430.6	0.653	14.89637	
66.34751	695.7	0.8436	11.75099	
68.03174	1807.9	0.6739	14.85471	
69.13022	693.5	0.7608	13.24429	
72.70927	267.7	0.6559	15.70838	
75.08799	251.8	0.7362	14.21522	
77.02914	128.5	0.3827	27.71202	

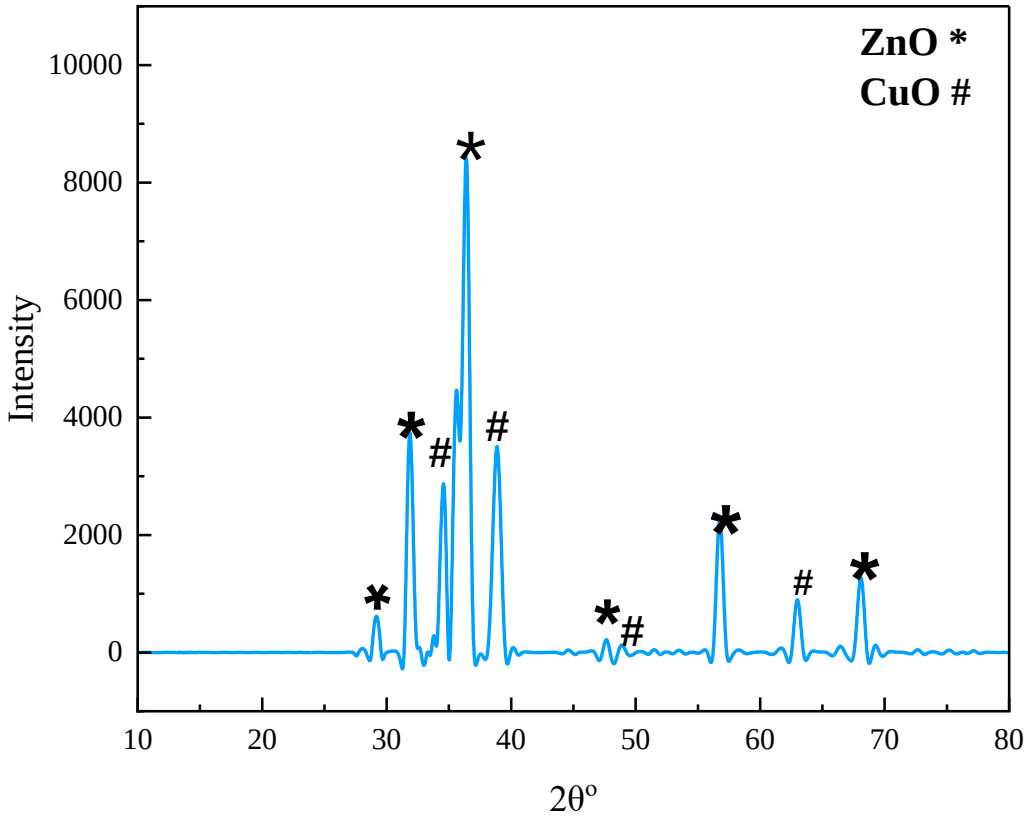

Figure 17 : XRD of ZnO/CuO

4.4.2.X-ray diffraction spectra of CuO/Co_3O_4:

The diffraction peaks of CuO at 32.54, 35.54, 38.88°,48.69°, 63.72°, 70.38° corresponds to the the planes (1 1 0), (0 0 2), (1 1 1), (-2 0 0), (-1 1 3) and (3 1 0) according to JCPDS No. 05-0661 [63] The peaks at 2θ = 19.14, 31.14,36.74,44.9,58.68,94.98 indexed to the planes (1 1 1), (2 0 2), (1 3 1), (0 4 0), (1 5 1) and (4 0 4) confirming the formation of cubic phase of Co_3O_4. All peaks confirm the presence of CuO and Co3O4 which demonstrated the formation of CuO and Co3O4 without impurities and all the peaks of the final products are either for CuO or Co3O4 NPs. Thus the same crystal phase in the binary composite.

Table 8 : Peak position and average crystal size of CuO/Co3O4 nanocomposite

Peak Position	**Intensity**	**FWHM**	**Crystallite size D (nm)**	**Average size (nm)**
19.14	213	0.7527	10.23	

31.14	5254	2.61	3.3	9.1
32.54	1516.6	0.4178	9.6	
35.54	4233.1	0.621	14.03	
36.74	6895	2.29	3.8	
38.88	1965	0.67	13.1	
44.9	4159	3.1	2.9	
48.69	736	0.8644	10.54	
58.68	1084	1.37	6.9	
63.72	1430.6	0.653	14.89	
64.98	1401	1.20	8.2	
65.10	695.7	0.8436	11.75	

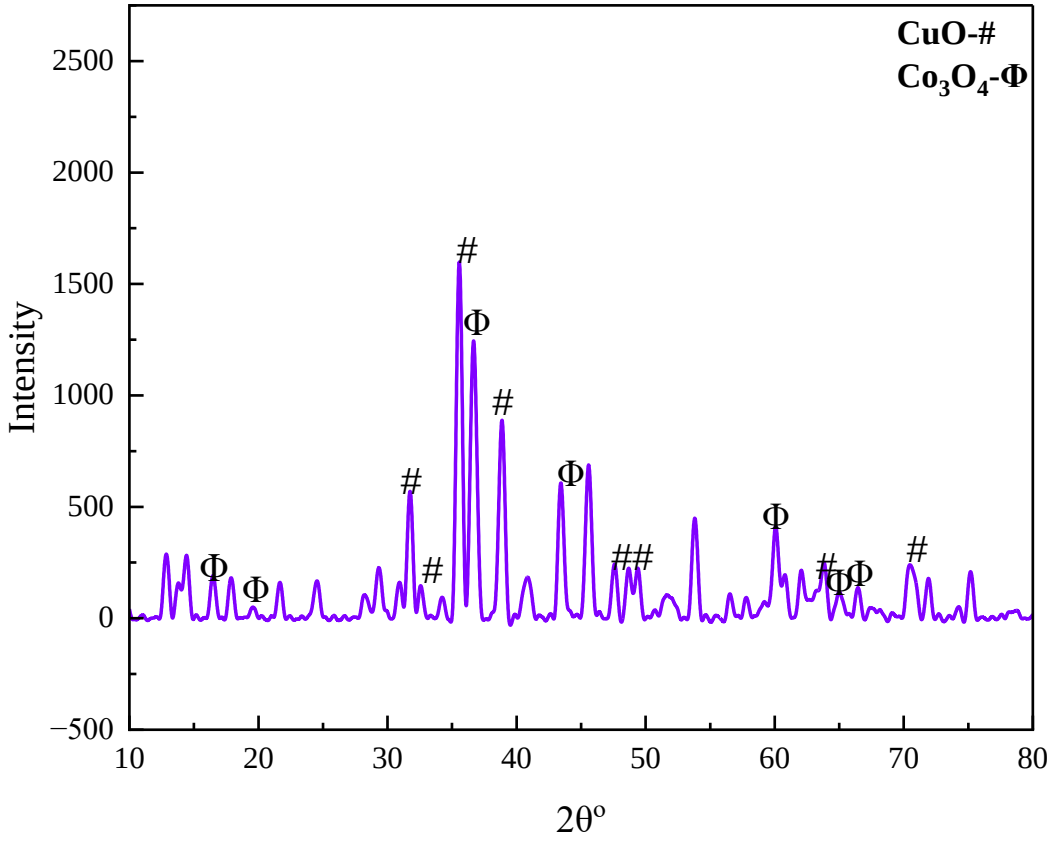

Figure 18 : XRD of CuO/Co3O4

4.4.3.X-ray diffraction spectra of ZnO/Co_3O_4:

The X-ray diffractogram shows Co_3O_4 at 2θ = 18.73°, 36.50°, 45.08°, 56.73°, 59.16°, 65.19° corresponding to the (1 1 1), (3 1 1), (4 0 0), (4 2 2), (5 1 1) and (4 4 0) hkl planes respectively. The characteristic peaks of ZnO at 2θ = 31.59°, 34.5°, 36.28°, 47.81°, 56.73°, 63.09°, 68.09°, 69.61° and 77.32° correspond to the (1 0 0), (0 0 2), (1 0 1), (1 0 2), (1 1 0), (1 0 3), (1 1 2), (2 0 1) and (2 0 2) lattice reflection planes, respectively. Therefore, the final product is composite of two metal oxides ZnO and Co3O4 and no additionl phase can be observed. Additionally, Debye-Scherrer formula was used to determine the crystallite size of ZnO/Co3O4 nanocomposite based on the full width half maximum of the peaks. The average particle size of the composite was 18.15nm.

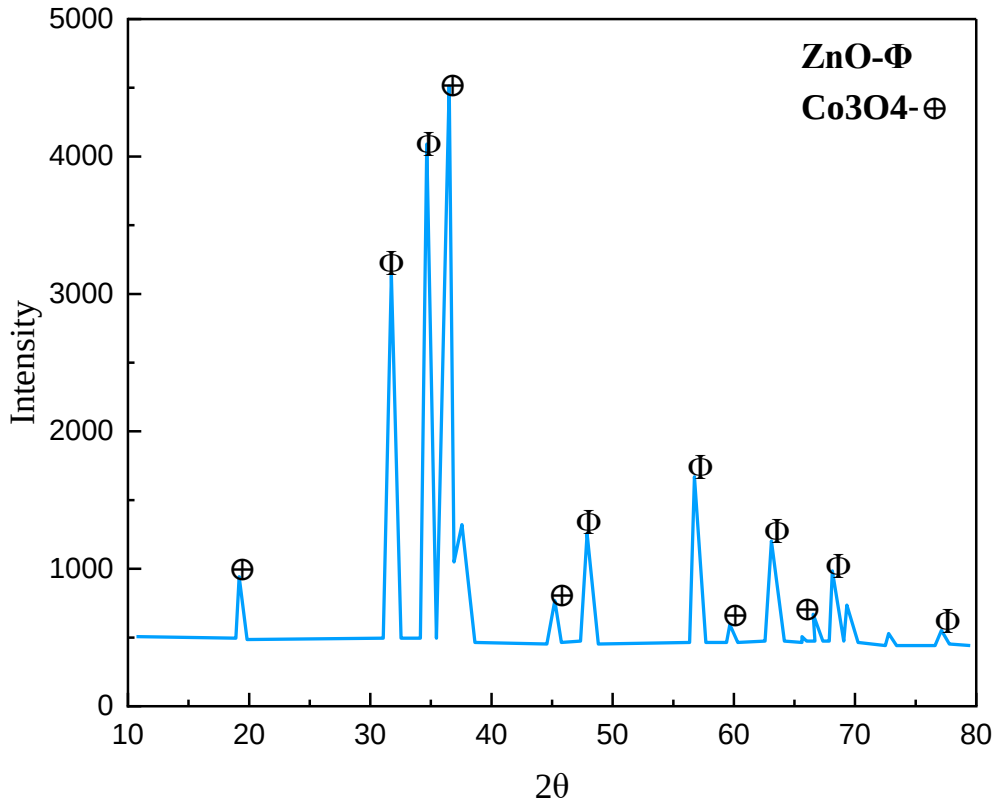

Figure 19 : XRD of ZnO/Co3O4 nanocomposite

Table 9 : Peak position and average crystal size of ZnO/Co3O4 nanocomposite

Peak Position	Intensity	FWHM	Crystallite Size D (nm)	Average size (nm)
18.73	855.97057	0.7527	20.2623	18.145
31.59	3136.6723	0.5275	16.6108	
34.48	3995.4725	0.3199	20.2909	
36.50	4318.0532	0.4533	19.2693	
45.08	707.41369	0.3128	21.2637	
47.81	1191.2846	0.5127	16.1680	
56.73	1594.5104	0.5594	16.8520	
59.16	560.2716	0.1370	19.1129	
63.09	1097.9060	0.6812	14.2811	
65.67	466.8930	0.1200	21.2801	
66.68	547.5382	0.4802	20.6594	
68.09	936.6157	0.6536	15.3176	
69.61	533.3899	0.6598	15.2752	
72.79	440.0113	0.4376	23.7375	
77.32	466.899	0.8187	12.9649	

4.4.4.X-ray diffraction spectra of ZnO/CuO/Co_3O_4:

The X-ray diffractogram spectra of ZnO/CuO/Co3O4 nanocomposite showed noticeable diffraction pattern at 2θ = 31.708°, 34.41°, 35.419°, 36.343°, 38.75°, 44.64°, 56.66°, 59°, 62.83°, 64.86°, 67.97°, 74.99°. The apparent diffraction peaks at 2θ=31.708, 34.41,36.343,56.66, 62.83, 67.97 were indexed to the lattice planes (1 0 0), (0 0 2), (1 0 1), (1 0 2), (1 1 0), (1 0 3) and (1 1 2) of hexagonal ZnO crystals (JCPDS card No. 00-36-1451) and the peaks at 2θ=44.64, 59, 64.86 were indexed to (4 0 0), (5 1 1) and (4 4 0) planes of cubic Co3O4 (JCPDS card No. 00-43-1003).

In addition, the peaks at 2θ= 35.41, 38.75 could be assigned to the planes (0 0 2), (1 1 1) of monoclinic CuO crystal (JCPDS card No. 45-0937)

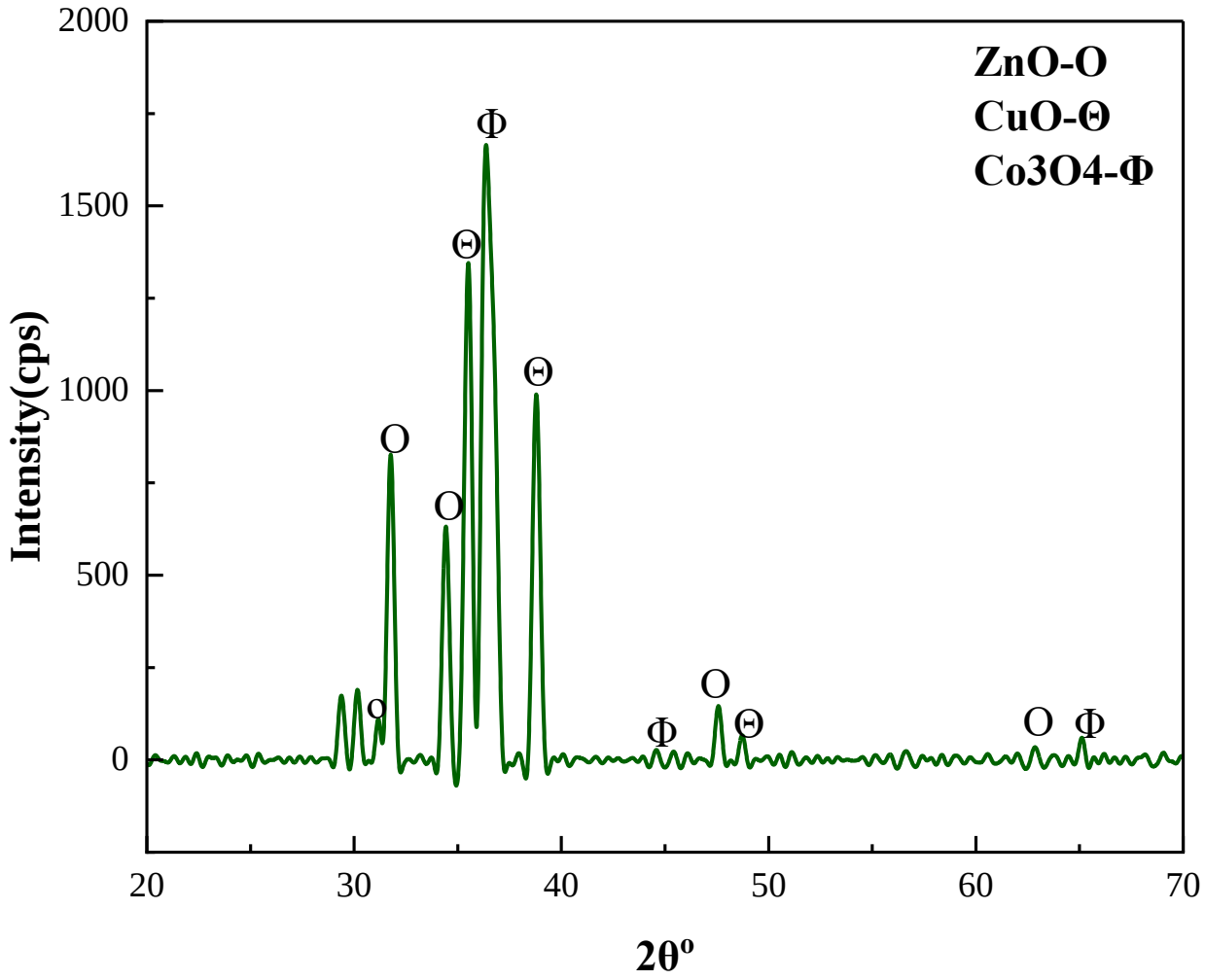

Figure 20 :: XRD of ZnO/CuO/Co_3O_4 nanocomposite

Table 10 : Peak position and average crystal size of ZnO/CuO/Co_3O_4 nanocompositeTable: Crystallite size of ZnO/CuO/Co_3O_4

Peak Position	Intensity	FWHM	Crystallite SizeD(nm)	Average Size(nm)
31.708	1536.635	0.23	36.8	23.57nm
34.41	2390.839	0.26	33.2	
35.419	2243.012	0.39	22.4	
36.343	3455.804	0.80	10.9	
38.75	2968.238	0.40	22.1	
44.64	1451.837	0.49	18.2	
56.66	1350.788	0.40	23.4	
59.00	1526.673	1.03	9.3	
62.83	1582.705	0.29	33.1	
64.86	1746.168	0.94	10.5	
67.97	1426.455	0.51	19.9	
74.99	1221.06	0.24	43.0	

Table 11 :The Average particle size

Composite	The average particle size (nm)
ZnO/CuO	23.14nm
ZnO/Co3O4	9.1nm
CuO/Co3O4	18.145nm
ZnO/CuO/Co3O4	23.57nm

4.5.SEM: Scanning Electron Microscope Analysis

SEM images were collected to study the morphology of the synthesized nanocomposites**.**

4.5.1. Scanning electron microscope (ZnO/CuO):

The synthesised ZnO–CuO nanocomposite powder surface's clarified morphology was investigated using high intensity electron scanning**.** The typical FESEM image in the Figure shows that ZnO/CuO composed of flowerlike microstructure and some leaflike nanopatches growing on 3D microstructure. It can be predicted that the ZnO/CuO nanocomposite synthesize by co-precipitation method is composed of 3D flowerlike ZnO microstructure modified by leaflike CuO

nanopatches. The FESEM images of synthesized ZnO/CuO nanocomposite resembles the SEM images of ZnO/CuO in literature [64]

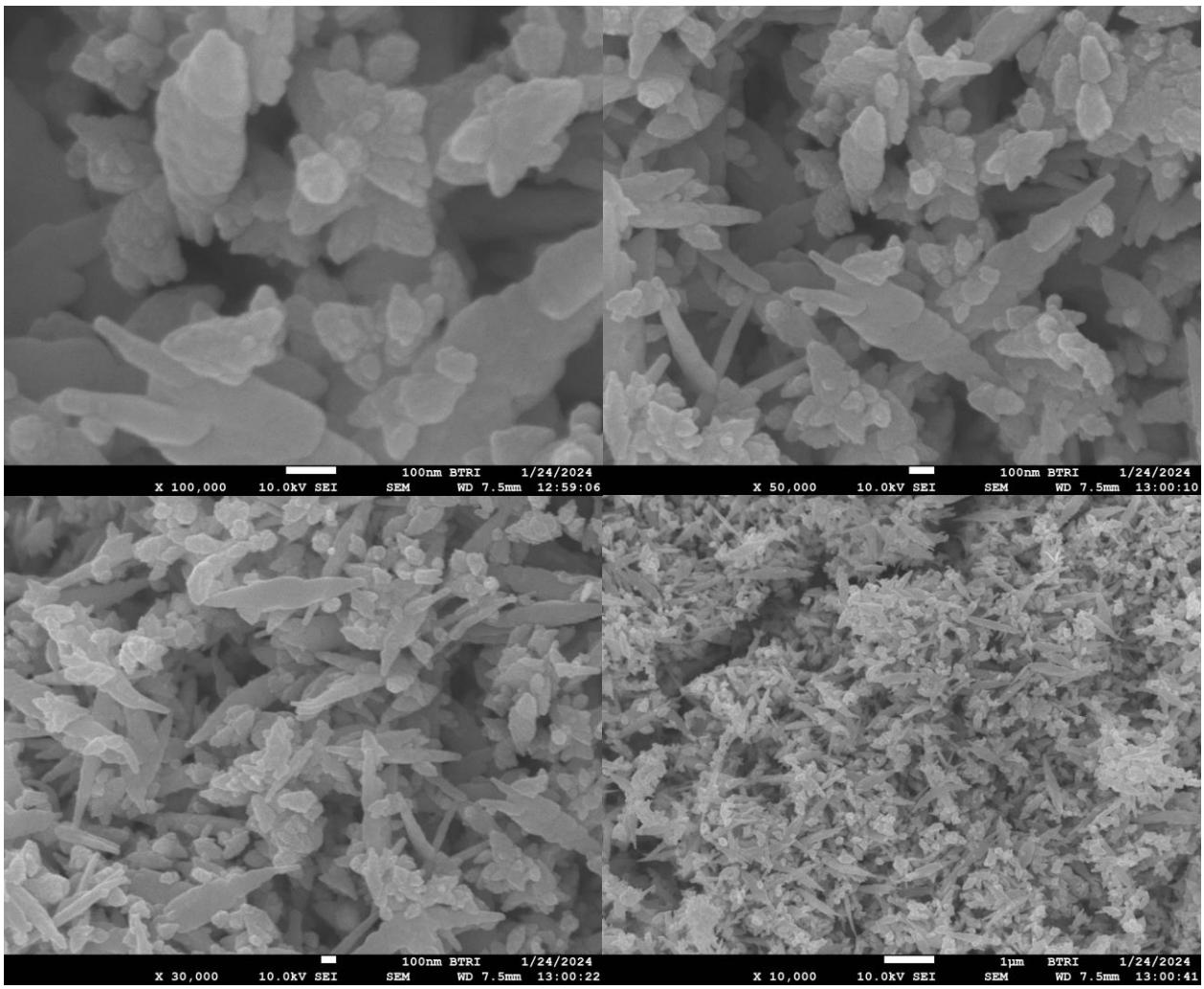

Figure 21 : FESEM images of ZnO/CuO

4.5.2. Scanning electron microscope(ZnO/Co_3O_4):

Figures show the FE-SEM images of ZnO/Co_3O_4 nanoparticles at different magnification, which clearly exhibit the nanoparticles like morphology indicate well uniform particles with narrow size distribution lies in the range of 15-20 nm. The images of ZnO/Co_3O_4 nanocomposite show that its particles are arranged in a uniform porous structure. The uniformity of the particles distribution can be observed in the Fig. also show the presence of spherical shaped particles superimposed in the porous structure.

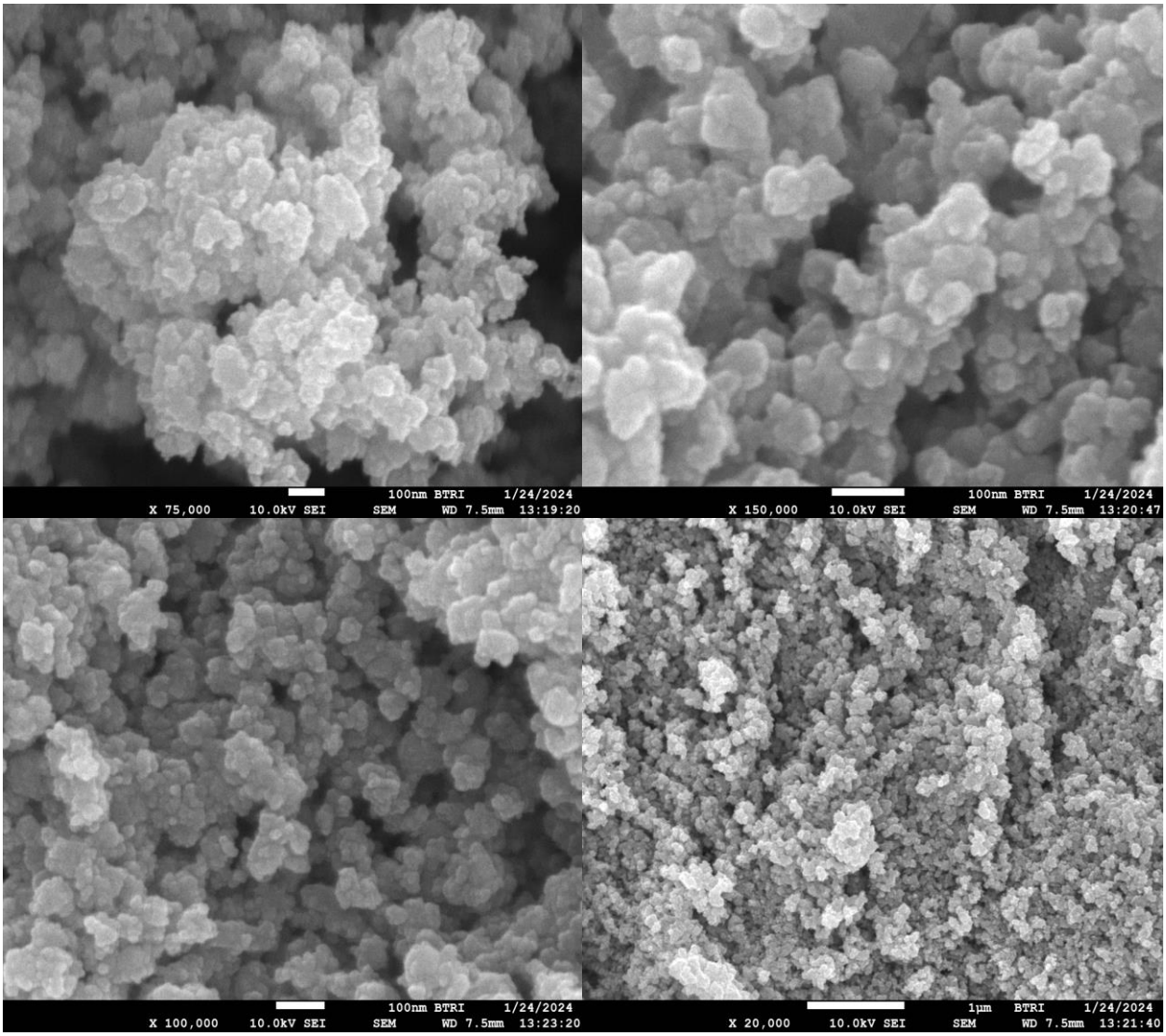

Figure 22 : FESEM images of ZnO/Co3O4

4.5.3.Scanning electron microscope(CuO/Co_3O_4):

Fig. shows the FESEM images of CuO/Co_3O_4 nanocomposite. As the active substances are forming hydrogen connections with the molecules surrounding them, the component seems to be agglomerated to some extent [65]. The SEM picture identified the form and size inhomogeneity of the CuO/Co_3O_4 composite NPs. The CuO/Co_3O_4 composite NPs exhibit both spherical and irregular geometries, with varying particle sizes, as the micrographs demonstrate.

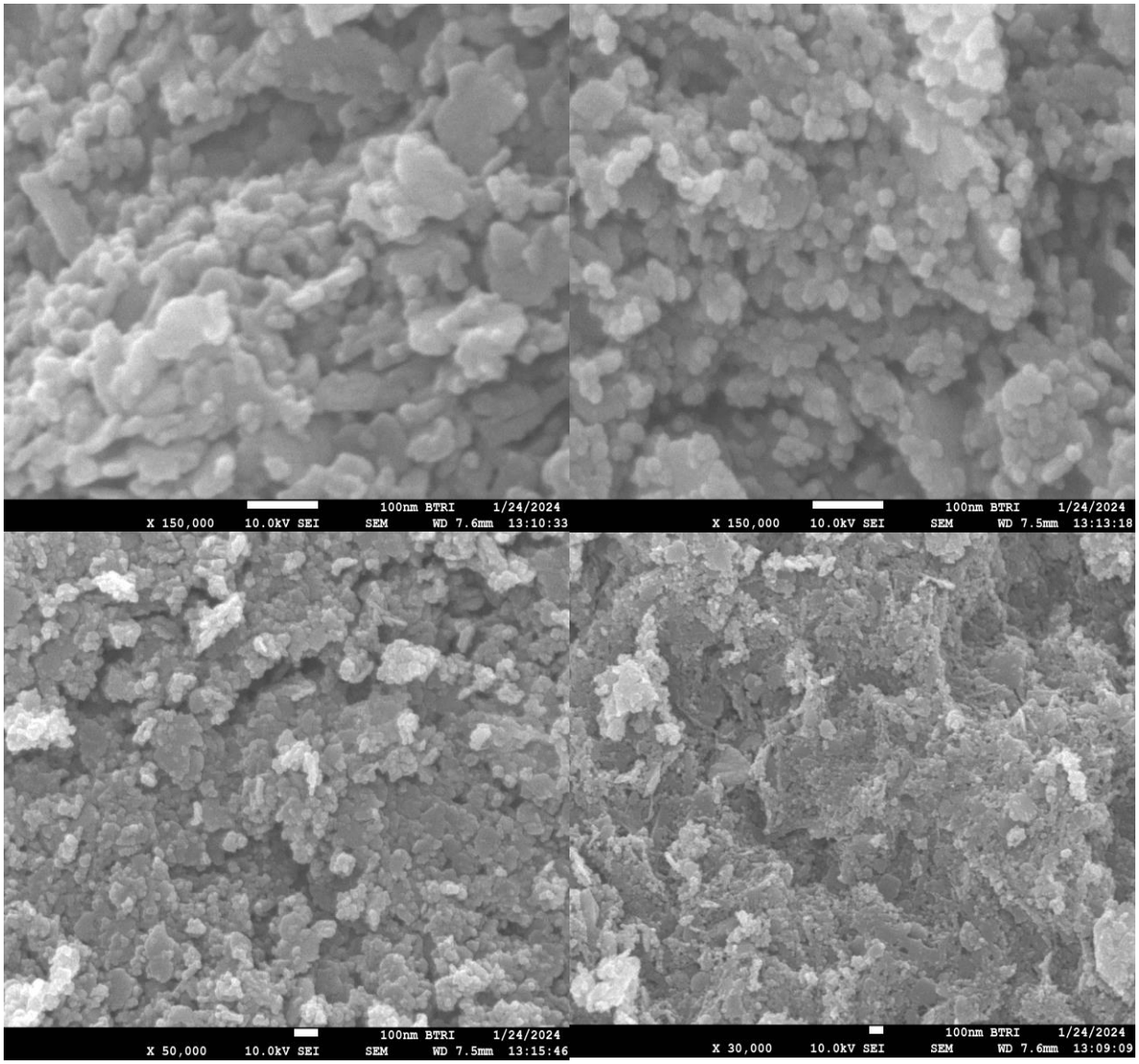

Figure 23 : FESEM images of CuO/Co_3O_4

5.5.Scanning electron microscope($ZnO/CuO/Co_3O_4$):

Figure shows the SEM images of the synthesized ternary nanocomposite indicating its microstructure. The figures shows combination of different types of structures. The leaflike nanopatches in between the spherical shapes indicates the presence of ZnO and CuO. The spherical particles are Co_3O_4 nanoparticles.

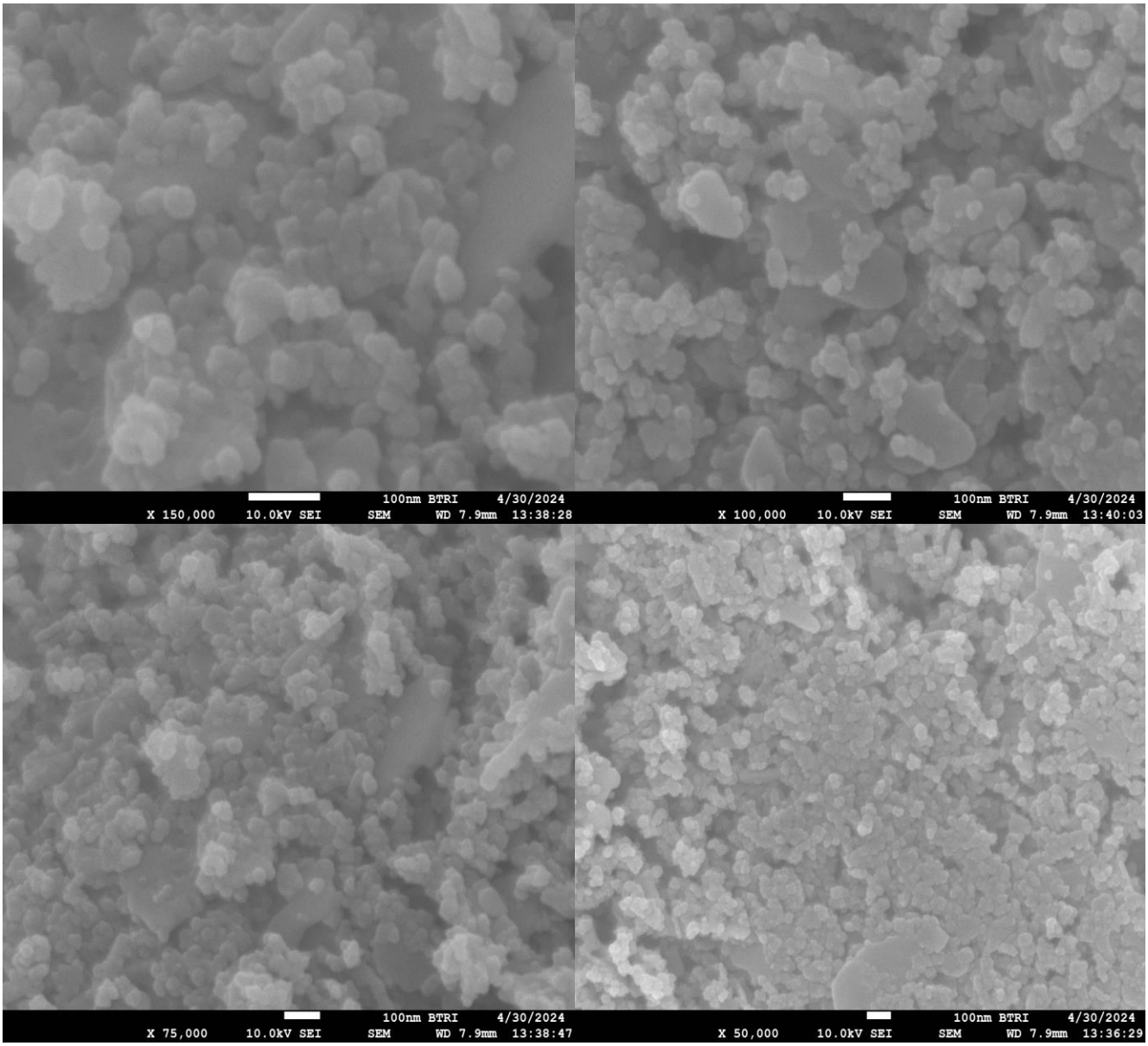

Figure 24 : FESEM images of $ZnO/CuO/Co_3O_4$

EDX is an analytical technique used for elemental analysis of chemical characterization of sample. This technique is based on the generation of characteristic X-rays in atoms of the specimen by

incident beam electrons. The EDX microanalysis provides semi-qualitative and semi-quantitative information about elemental composition.

4.6.1. Energy Dispersive X-ray spectroscopy (ZnO/CuO):

Molecular formula Compositional properties of ZnO/CuO nanocomposite have been characterized by Energy disperse X-ray spectroscopic technique. The EDX analysis of ZnO/CuO nanocomposite showed that it contain 16.93% Oxygen(O), 45.04% Zinc(Zn) and 38.3% Copper (Cu) by weight percentage.

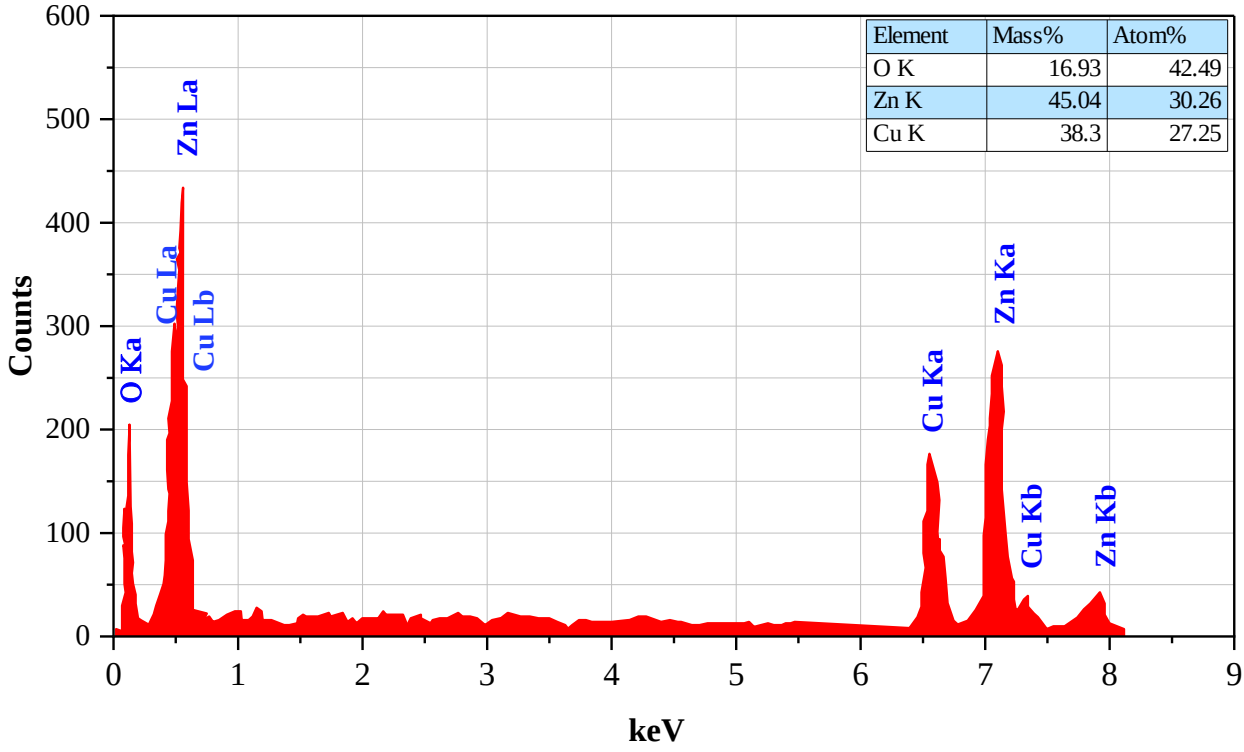

Figure 25 : EDX of ZnO/CuO

4.6.2. Energy Dispersive X-ray spectroscopy (ZnO/Co_3O_4):

EDX studies were carried out in order to confirm the presence of elements in the ZnO/Co_3O_4 nanocomposite. The EDX spectrum shown in the Fig. confirms the presence of Zinc(Zn),Cobalt(Co) and Oxygen(O). The mass percentage of Zinc(Zn), Cobalt(Co) and Oxygen

are 42.04%,39.1% and 18.86% respectively. The extra peaks in the spectrum are may be due to impurities as we used NaOH while preparing the nanocomposite.

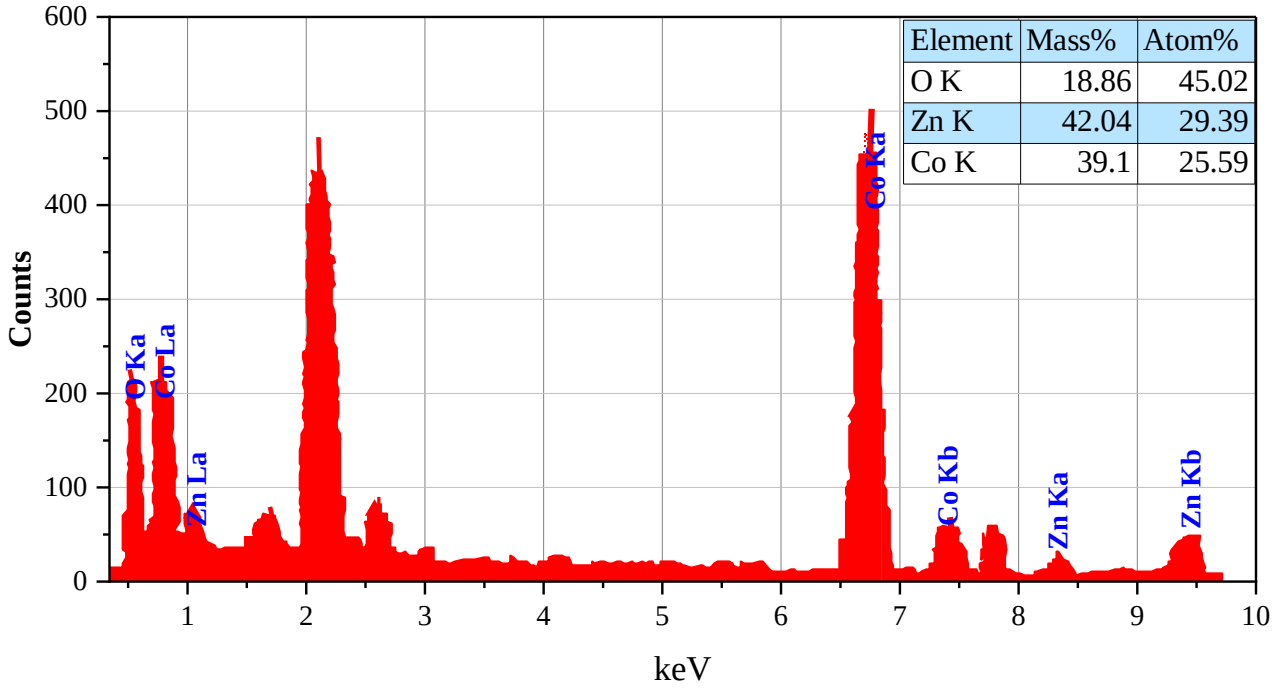

Figure 26 : EDX of ZnO/Co_3O_4

4.6.3. Energy Dispersive X-ray spectroscopy (CuO/Co_3O_4):

Molecular formula compositional properties of CuO/Co_3O_4 nanocomposite have been characterized by Energy dispersive X-ray spectroscopic technique. The EDX analysis showed 18.04%,41.18% and 40.78% of mass percentage for Oxygen (O), Cobalt (Co) and Copper (Cu)

respectively. The atomic percentage are 45.69%, 28.31% and 26% for Oxygen (O), Cobalt (Co) and Copper (Cu).The total perentage is 100% which confirms that there is no impurities in this nanocomposite. The compositional data from the EDX analysis agree well with theoretically calculated values, indicating a good compositional homogeneity across the nanoparticles.

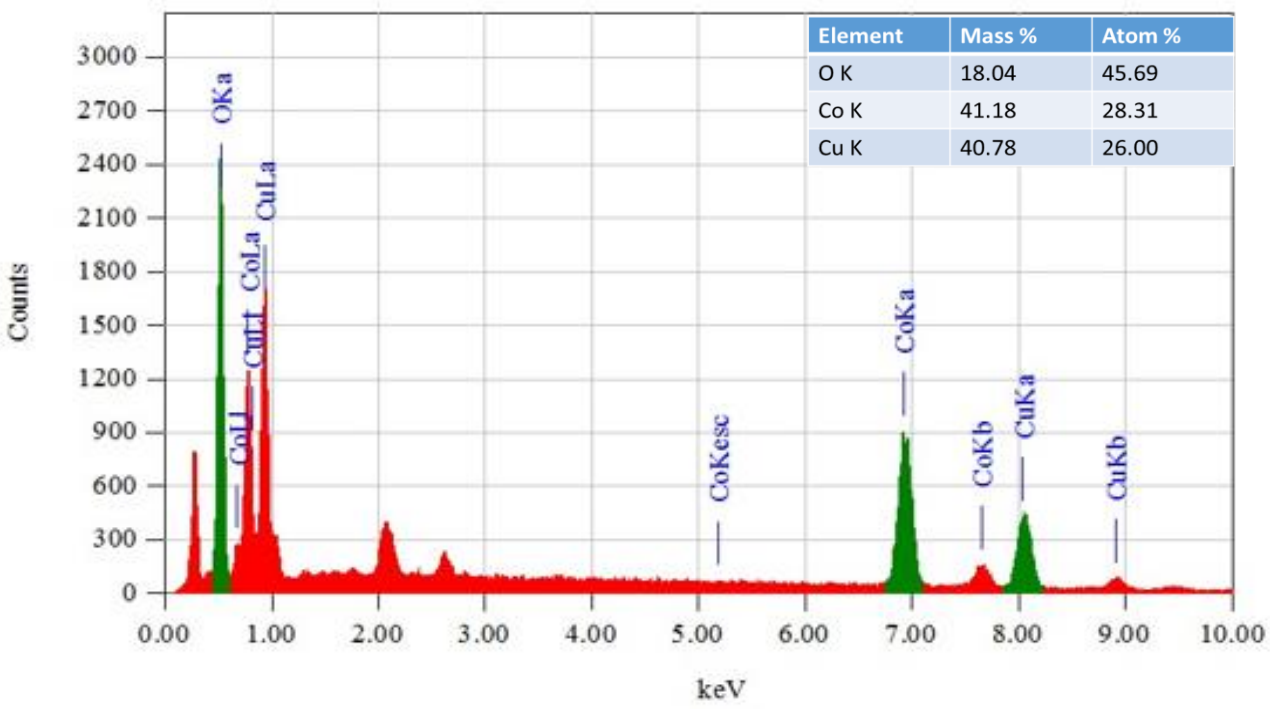

Figure 27 : EDX of CuO/Co_3O_4

4.6.4. Energy Dispersive X-ray spectroscopy ($ZnO/CuO/Co_3O_4$):

Energy dispersive X-ray spectroscopy of ZnO/CuO/Co3O4 nanocomposite showed that the product contain 17.93% of Oxygen (O), 29.72% of Cobalt (Co), 29.11% of Copper and 23.24% of Zinc by mass percentage. The atomic percentage of Oxygen. Cobalt, Copper and Zinc are 45.95%, 20.68%, 18.79%, 14.58% respectively.

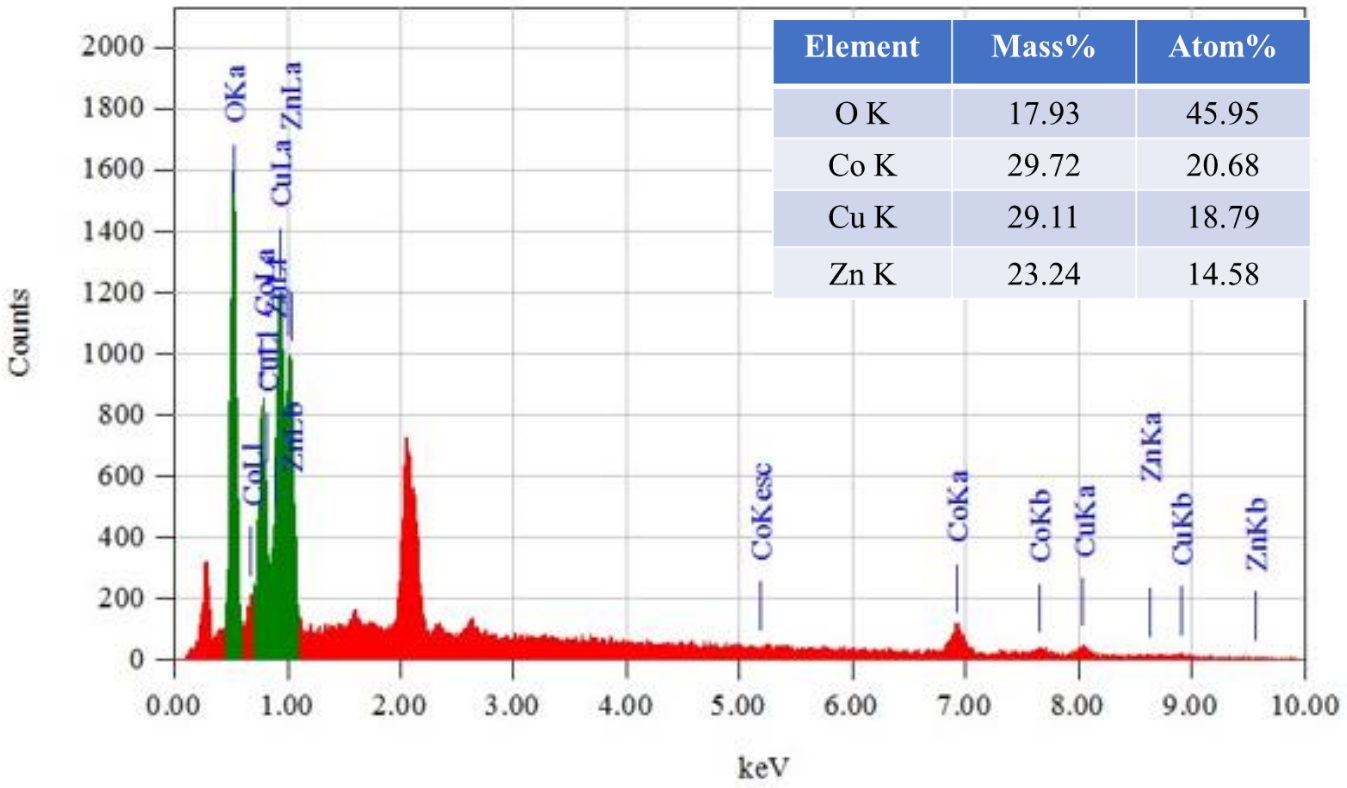

Figure 28 : EDX of ZnO/CuO/Co_3O_4

4.7. Photocatalytic degradation study of Methylene Blue Dye

The natural solar light compelled photocatalytic activity of the synthesized nanoparticles were evaluated with Methylene Blue Dye as demonstrative pollutant. This experiment was done in presence of sunlight. Blank study was first monitored. After studying the blank dye solution degradation a suitable amount of the synthesized nanocomposites were mixed with the MB dye solution to their effectiveness towards the degradation of the dye. The sample was first agitated for 20minutes in dark to attain saturation equilibrium[66]. After that, the solution was irradiated to sunlight. 20min later 5 ml of the solution was taken and centrifuged for 5min. Absorbance was taken by using a UV-Vis spectrophotometer. The λ_{max} for MB dye was found to be 665nm. With the use of catalyst absorption maxima were diminished gradually and started to disappear after 120min as shown in the Figures.

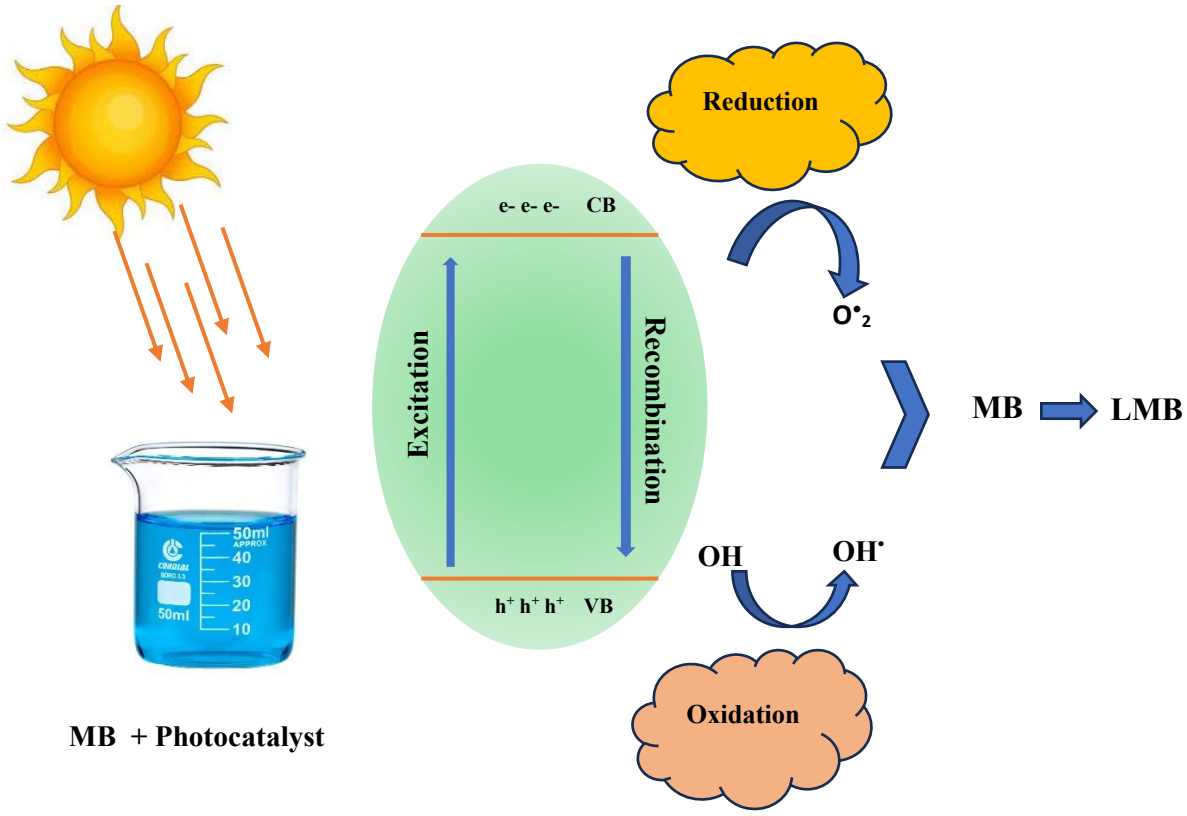

Figure 29 : Visual interpretation of MB dye degradation

Decoloration of Methylene Blue Dye with time:

Figure 30 : 0min

Figure 31 : 60min

Figure 32 : 120min

Figure 33 : 140min

Figure 34 :180min

4.7.1.1. Time dependent Absorbance of Methylene Blue in presence of sunlight

Fig shows change in absorbance of MB dye solution in absence of catalyst. MB dye show a very little color change showing the drgradation of 26.58% in 180minutes indicating that the dye is highly stable under sunlight. A suitable photocatalyst can degrade it effectively.

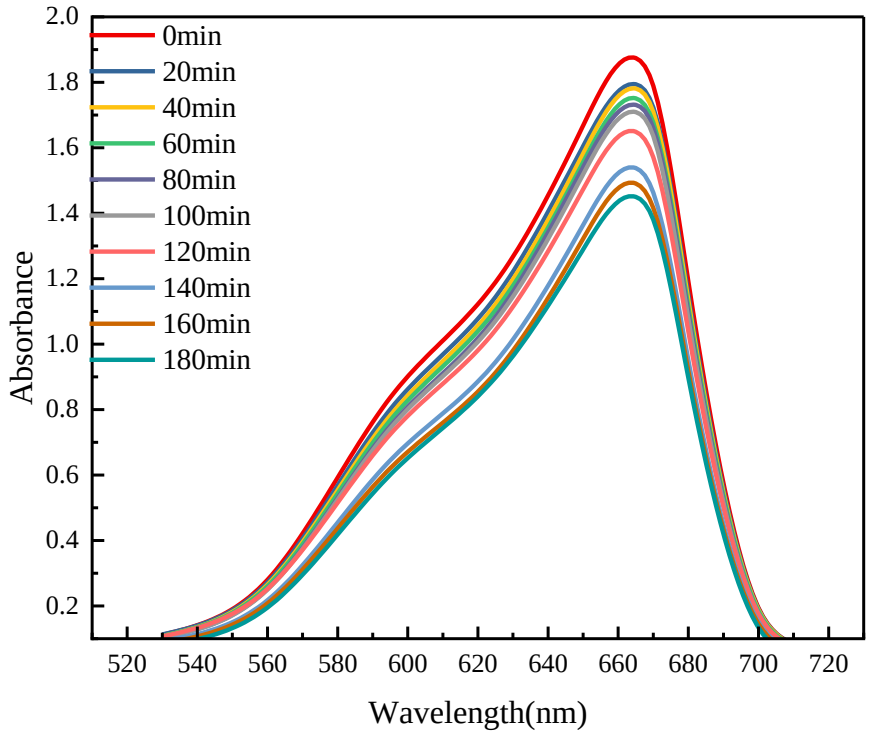

Figure 35 : Absorbance of MB dye without catalyst

4.7.1.2. Change in absorbance of Methylene Blue Dye after treating with ZnO/CuO in presence of sunlight

Fig. shows the decrease in absorbace of MB dye with the ZnO/CuO nanocomposite. The concentration of the dye solution was 5ppm and 5mg of nanocomposite was dissolved in 100ml of dye solution. At first absorbance of the MB dye solution at 665 nm was 1.604 which decreases to

0.035 after 180nm which is in good agreement with the literature [48]

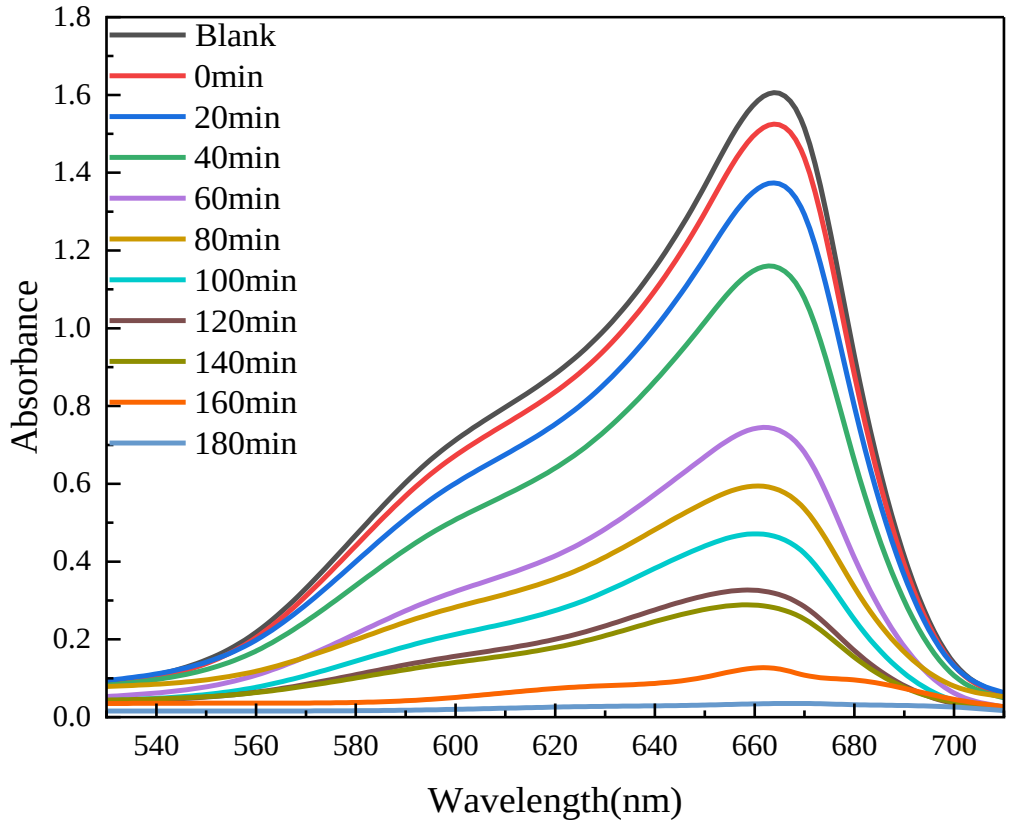

Figure 36 : Photocatalytic degradation of Methylene Blue Dye (Catalyst: 5mg/100ml ZnO/CuO nanocomposite, t=180min, MB concentration: 5ppm)

4.6.1.2. Change in absorbance of Methylene Blue Dye after treating with ZnO/Co_3O_4 in presence of sunlight

The organic dyes released by textile industries are considered as one of the major water pollutants because of their high resistance to chemical ,biological and photochemical degradation. The degradation efficiency of ZnO/Co_3O_4 nanocomposite was studied using MB dye under sunlight. A mixture of 100ml of 10ppm MB dye and 5mg of ZnO/Co3O4 nanocomposite photocatalyst was used.The change in absorbance value is observed which is in agreement with the literature[67]

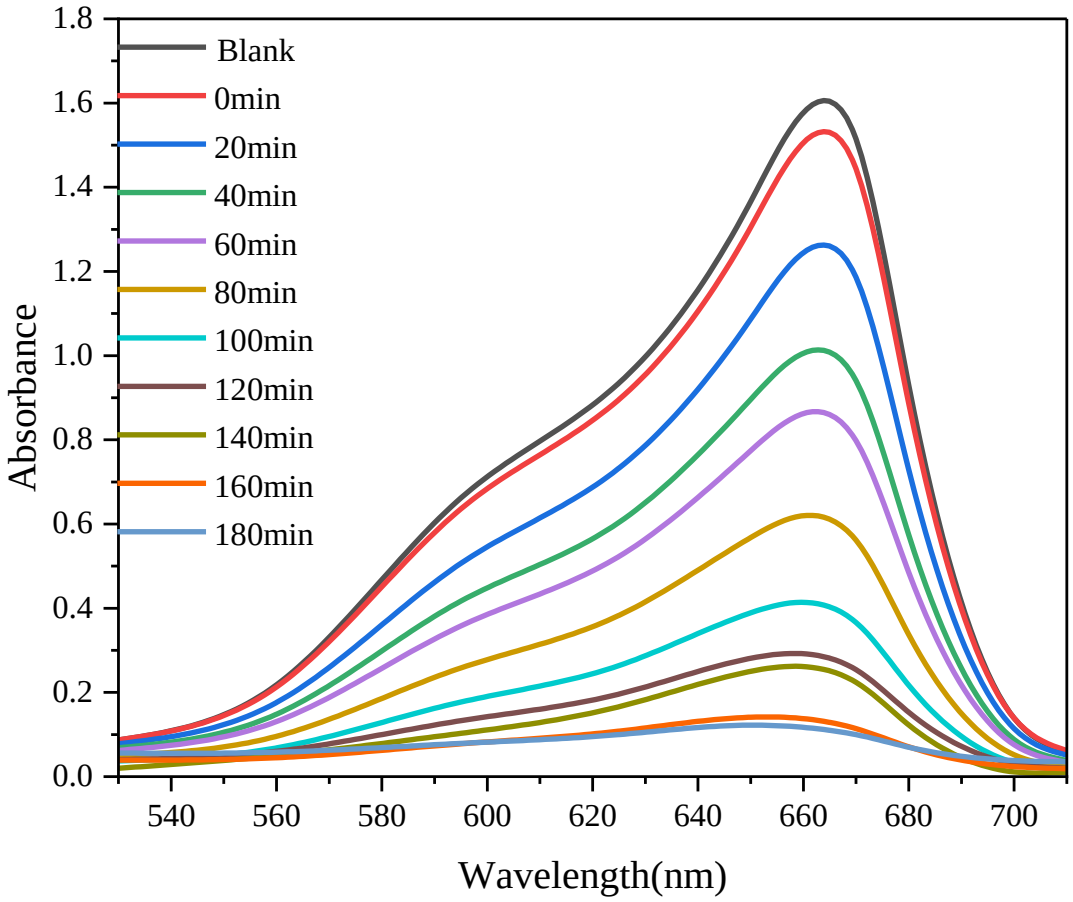

Figure 37 : Photocatalytic degradation of Methylene Blue Dye (Catalyst: 5mg/100ml ZnO/Co3O4 nanocomposite, t=180min, MB concentration: 5ppm,pH=8)

4.7.1.3. Change in absorbance of Methylene Blue Dye after treating with CuO/Co_3O_4 in presence of sunlight

The photocatalytic decomposition of Methylene Blue Dye by CuO/Co3O4 nanocomposite is demonstrtated in Fig. which displays the absorption spectra evaluated in the aqueous solution at various time interval under the influence of CuO/Co3O4 nanocomposite and sunlight. With the increase of absorption time the primary absorption peak at 665nm steadily lowererd showing the degradation of MB dye.

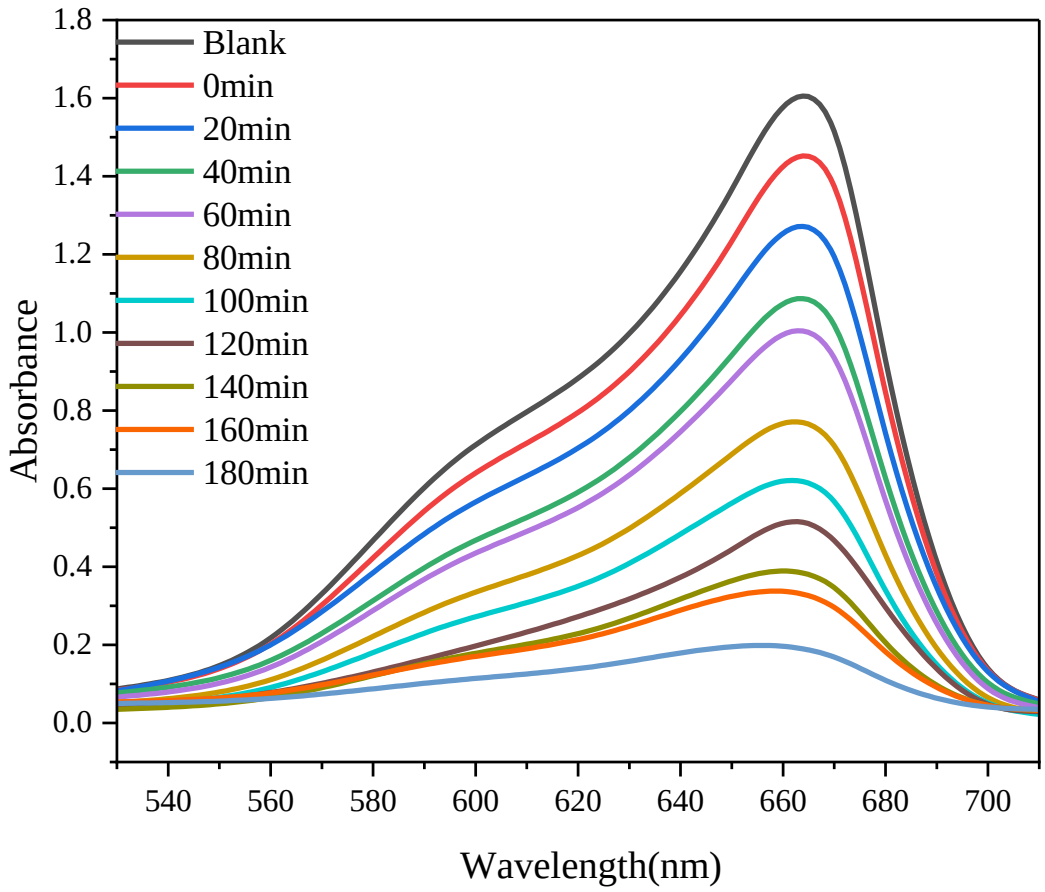

Figure 38 : Photocatalytic degradation of Methylene Blue Dye (Catalyst: 5mg/100ml CuO/Co3O4 nanocomposite, t=180min, MB concentration: 5ppm,pH=8)

4.7.1.4. Change in absorbance of Methylene Blue Dye after treating with ZnO/CuO/Co_3O_4 in presence of sunlight

The Ternary nanocomposite shows a different change in absorbance than the other three binary nanocomposite. Absorbance decreases very rapidly after 20min irradiation of ZnO/CuO/Co_3O_4 nanocomposite and MB dye mixture under sunlight. After 120min the ternary nanocomposite show 98.44% degradation efficiency.

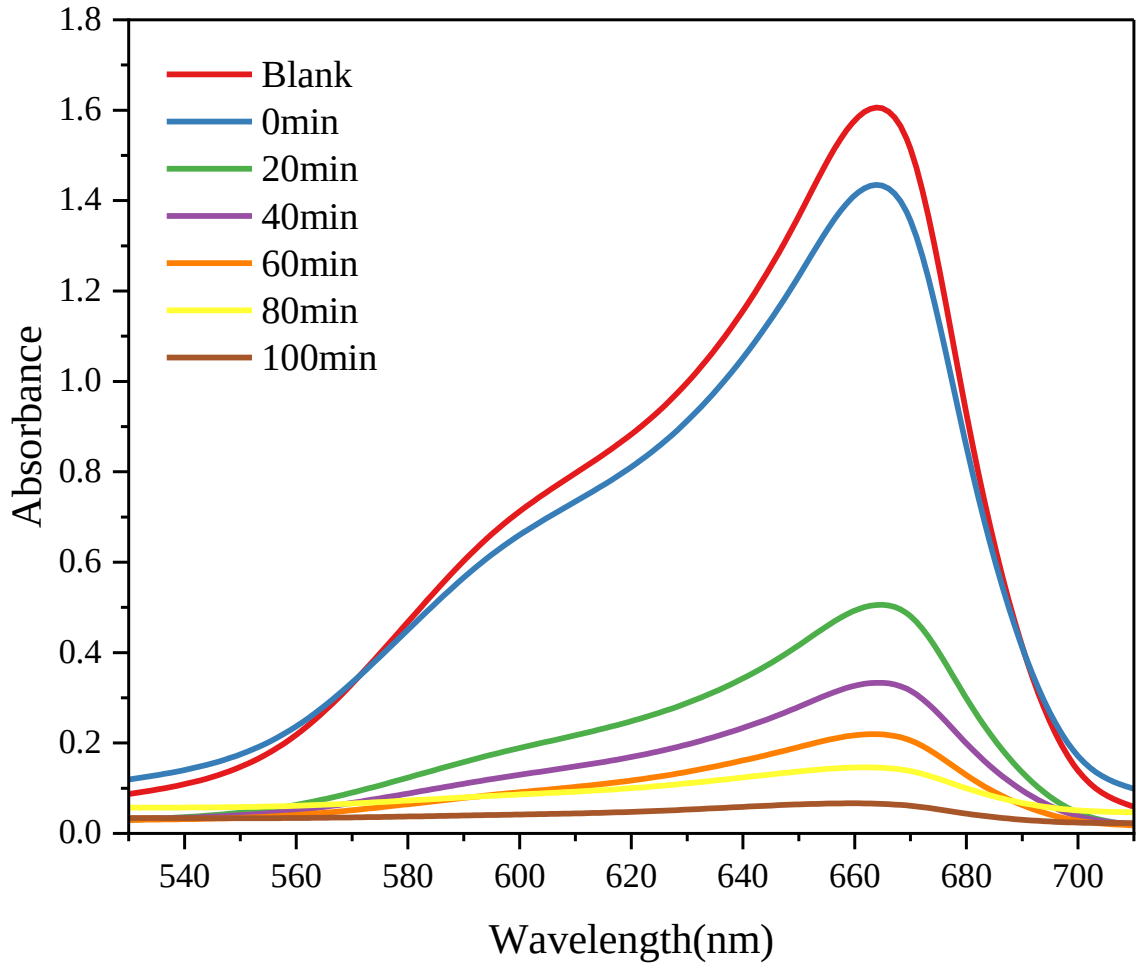

Figure 39 : Photocatalytic degradation of Methylene Blue Dye (Catalyst: 5mg/100ml $ZnO/CuO/Co_3O_4$ nanocomposite, t=180min, MB concentration: 5ppm,pH=8)

4.7.2. Effect of catalyst dosage on the photocatalytic degradation of MB dye

Effect of catalyst dosage on percent MB dye degradation on different amount was studied. The other parameters were kept constant. Concentration of MB dye dolution was 5ppm and the amount of the nanocomposite were 2mg, 4mg and 6mg per 20 ml of dye respectively. Irradiation time was 180min.

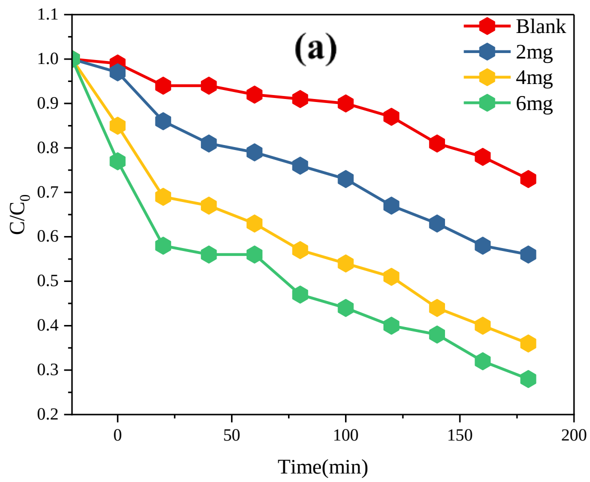

Figure 40 : MB dye degradation by ZnO/CuO nanocomposite (a)C/C0 vs Time

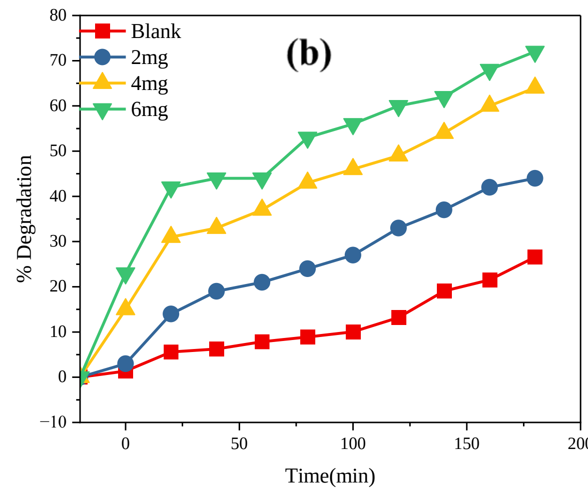

Figure 41 : MB dye degradation by ZnO/CuO nanocomposite (b) % Degradation vs Time

From the Fig. 40, Fig. 41, Fig. 42, Fig. 43 we can see with the increase of catalyst dosage the photodegradation increases. The number of photon absorbed and degraded dye molecules increases with the increase in catalyst concentration. This is due to the uniform dispersion of the catalyst and the availability of more active site on the catalyst [68]From our current study we can see higher the amount of ZnO/CuO nanocomposite percent of MB dye degradation increases. Here, MB dye solution with 2mg catalyst degraded at about 44% wheres the dye solution with 6mg shows 72% of degradation. % of Degradation was measured using the Beer-Lambert Law as shown in the equation

$$\%D = (1-C/C_0)\times 100 \ldots\ldots\ldots\ldots\ldots\ldots\ldots\ldots\ldots\ldots\ldots\ldots$$

Where, D = % of degradation

C_0 = initial dye concentration

C = concentration of dye after t time

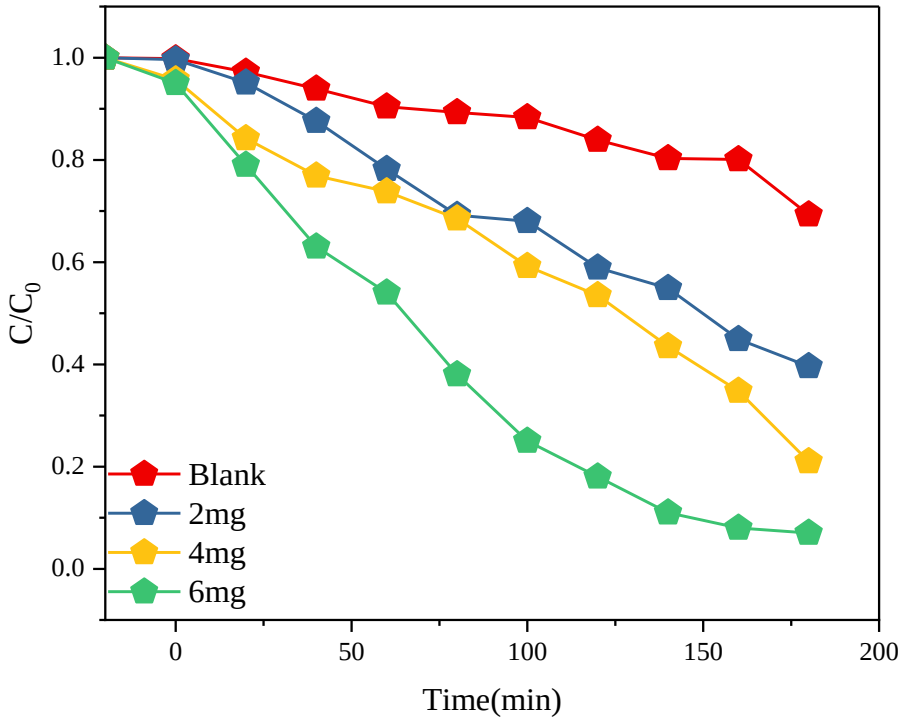

Figure 42 : MB dye degradation by ZnO/Co3O4 nanocomposite (a)C/C0 vs Time

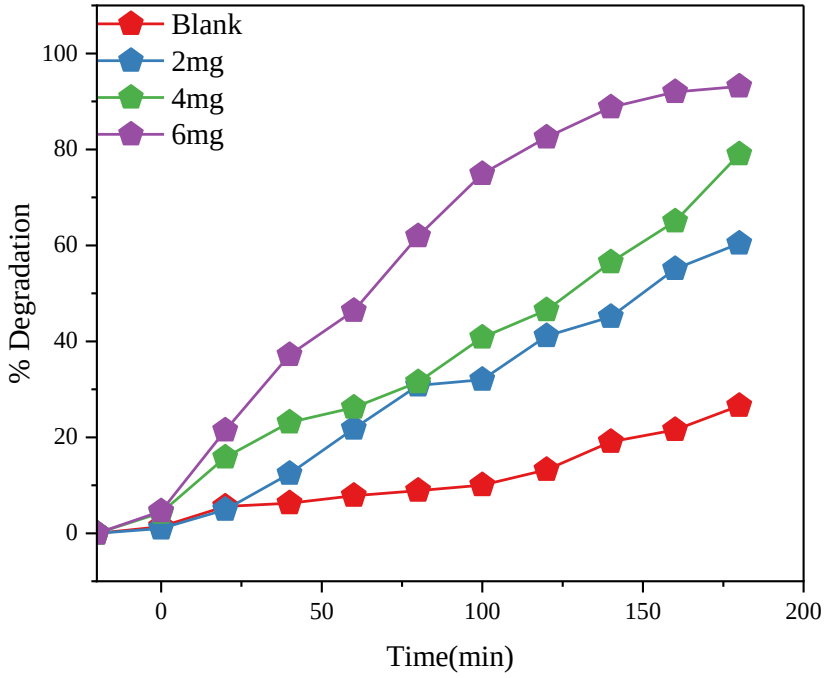

Figure 43 : MB dye degradation by ZnO/Co3O4 nanocomposite (b) % Degradation vs Tim

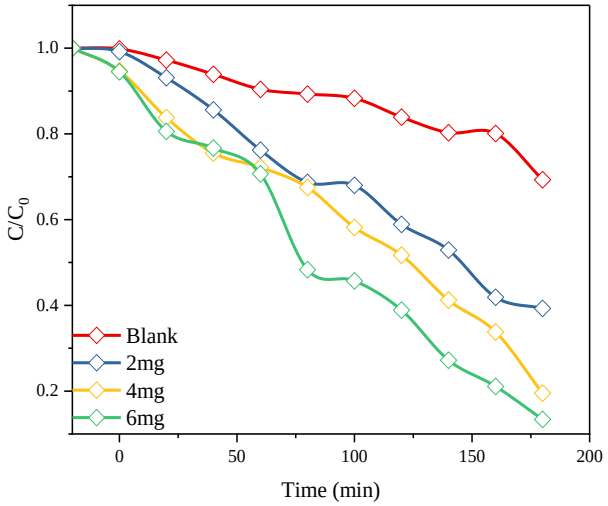

Figure 44 : MB dye degradayion using CuO/Co3O4 nanocomposite (a) C/C0 vs Time

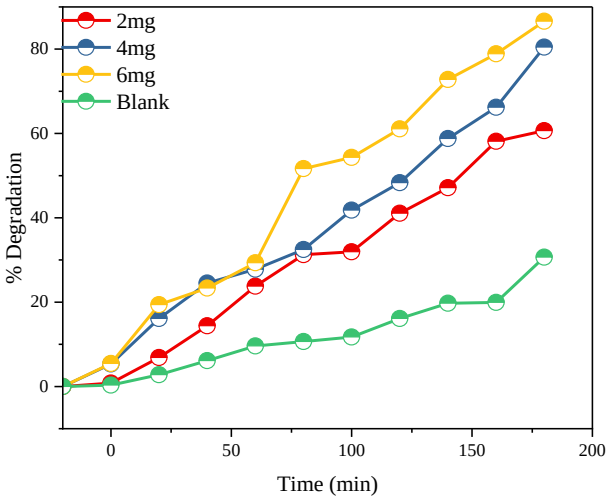

Figure 45 : MB dye degradayion using CuO/Co3O4 nanocomposite (b) % Degradation vs Time

In a similar way ZnO/Co_3O_4 nanocomposite show increase in degradation of MB with the increase of catalyst dosage. 2mg ZnO/Co_3O_4 nanocomposite shows degradation of 60.4% and 6mg of ZnO/Co_3O_4 nanocomposite shows 93.14% under an irradiation time of 180min in sunlight.

Both CuO and Co3O4 exhibit photocatalytic activity. Their composite CuO/Co_3O_4 also possesses a great dye drgradation efficiency. But compared to ZnO/CuO and ZnO/Co_3O_4 it has less degradation efficiency. Catalyst dosage effect was also be seen in case of CuO/Co_3O_4. Higher the amount of nanocomposite higher was the degradation efficiency and lower the C/C_0 with the increase of irradiation time.

4.7.3. Effect of time on the degradation of MB dye

The results obtained by UV-Visible spectroscopy confirmed that the prepared nanocomposites were active in the visible region. To achieve a best degradation result a suitable period of time is necessary. Because, reaction kinetics depends on the irradiation time [69] . The results obtained for the catalytic degradation of MB dye by the four nanocomposites show a continuous increase with increasing illumination time. Fig. shows percentage of degradation of Methylene Blue with the increase of exposure time. From the data shown in the table we can see that ternary nanocomposite shows higher degradation efficiency at less time than the binary nanocomposite. Among the three binary composites ZnO/Co_3O_4 shows lowest degradation efficiency and ZnO/CuO shows the highest degradation efficiency in 180min. Only MB dye solution degradation efficiency is much more lower without catalyst confirming that it is a stable dye. Among the synthesized nanocomposite the degradation rate of ZnO/CuO, ZnO/Co_3O_4, CuO/Co_3O_4 were 97.82%, 88.34%

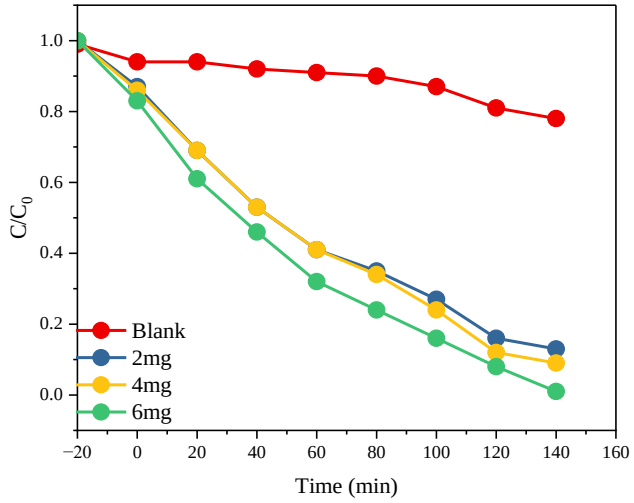

Figure 46 : MB dye degradation by ZnO/CuO/Co3O4 ternary nanocomposite (a) C/C0 vs Time

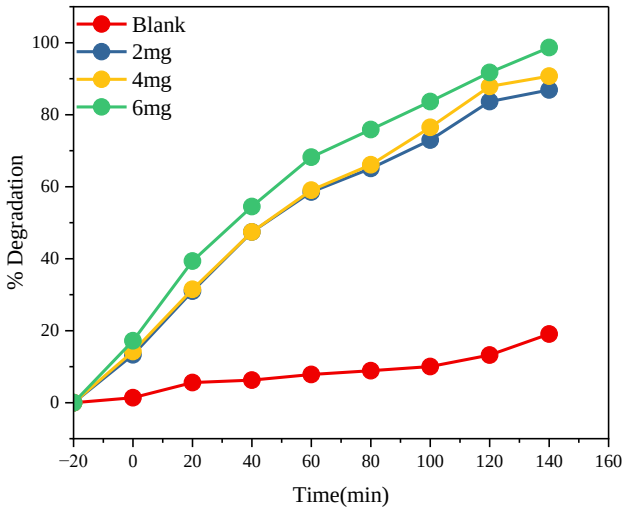

Figure 47 : MB dye degradation by ZnO/CuO/Co3O4 ternary nanocomposite (b) % Degradation vs Time

and 93.14% respectively in 180 minutes. The ternary nanocomposite shows an exceptional result in this aspect. The rate of degradation was 98.44% in 120 minutes for it which indicates higher photocatalytic activity of ZnO/CuO/Co_3O_4.

Table 12: Percentage of degradation of the synthesized nanocomposites

	MB	ZnO/CuO	ZnO/Co_3O_4	CuO/Co_3O_4	ZnO/CuO/Co_3O_4
Time(min)	%D	%D	%D	%D	%D
-20	0	0	0	0	0
0	1.36	5.05	9.54	4.61	10.66
20	5.58	14.53	20.89	21.44	68.45
40	6.26	28.05	32.42	37.16	79.24
60	7.84	54.05	37.66	46.38	86.35
80	8.89	63.65	52.31	61.91	90.96
100	10.05	71.26	61.72	74.88	95.95
120	13.21	80.36	68.2	82.48	98.44
140	19.05	82.67	76.31	88.78	
160	21.53	92.27	79.68	91.96	
180	26.58	97.82	88.34	93.14	

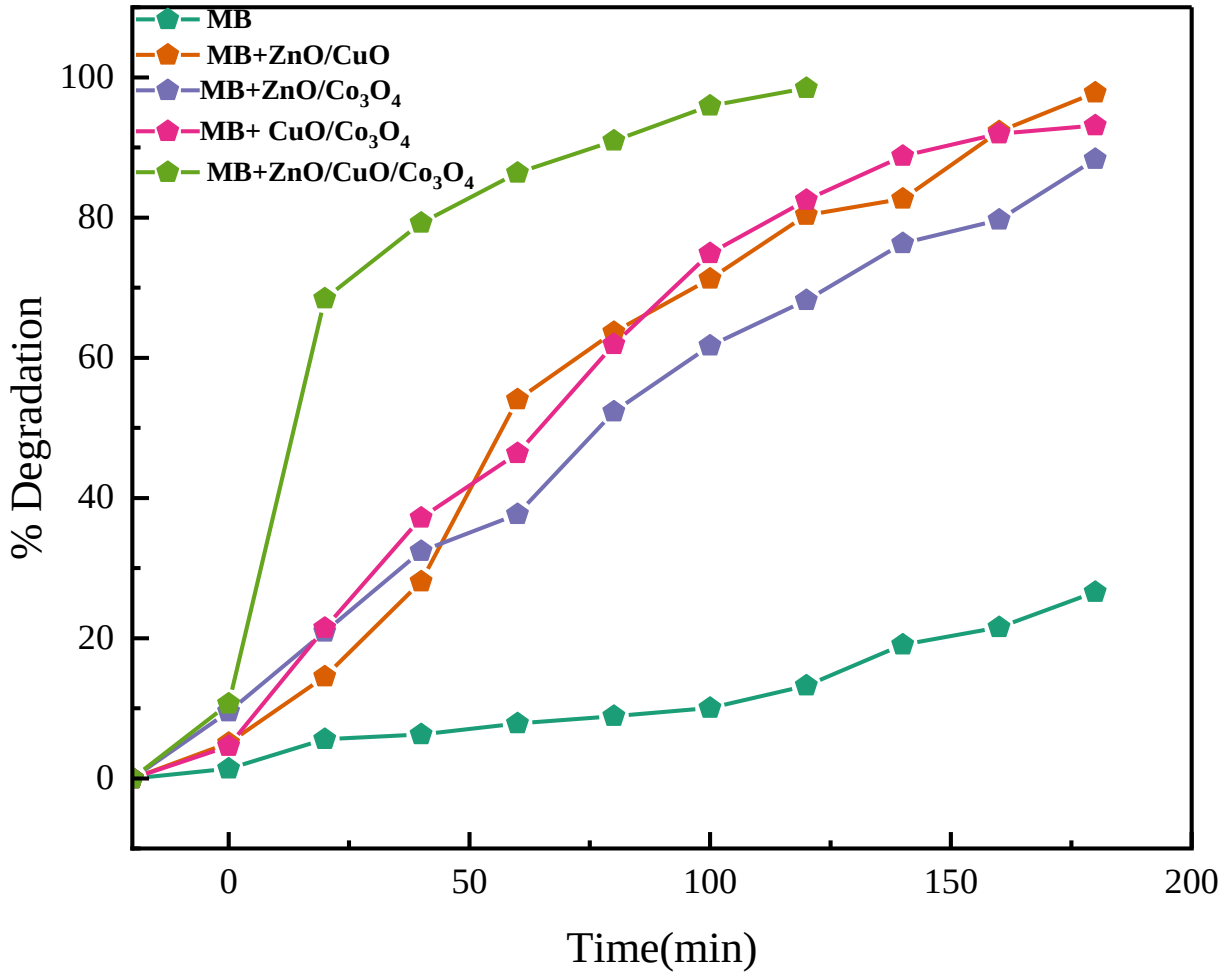

Figure 48 : Effect of reaction time on Degradation efficiency of the Nanocomposites

4.7.4.Effect of initial dye concentration :

The initial concentration of the dye had a significant impact on its photocatalytic activity. The amount of OH radicals produced on the nanocatalyst's surface and the quantity of collisions between active species and dye molecules determine the percentage of dye degradation. A significant portion of the irradiation light may also be absorbed by the dye molecules rather than the catalyst particles as a result of the dye molecules quenching the active sites of the photocatalyst and reducing the formation of OH radicals on the catalyst's surface.

[61].

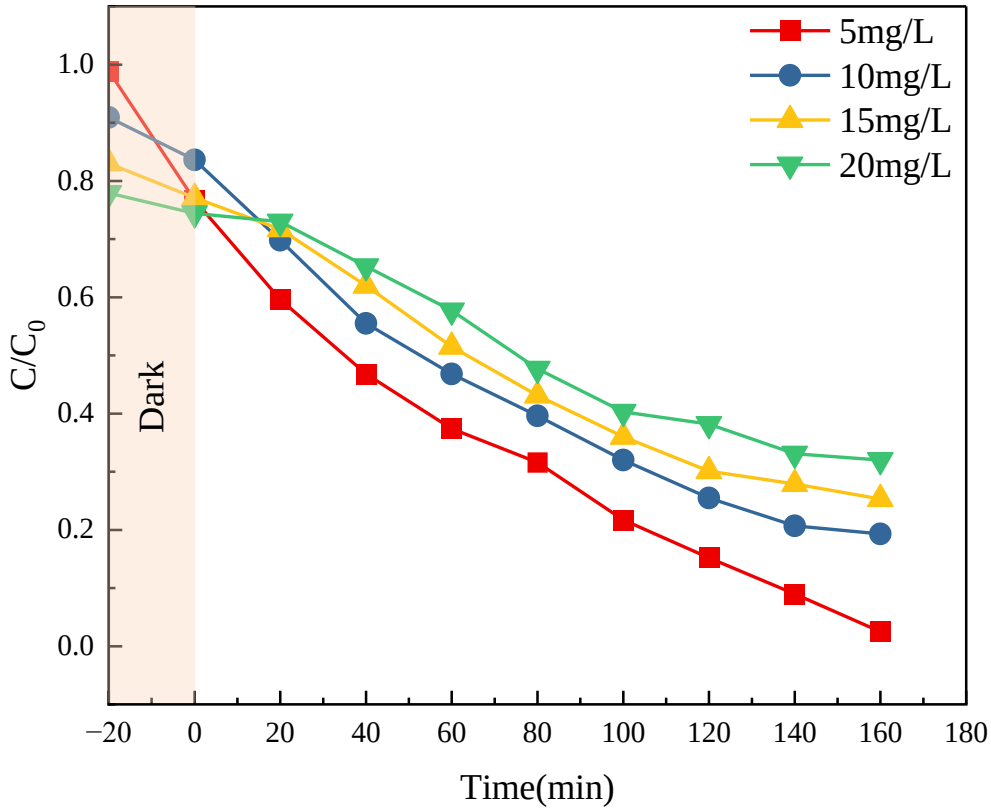

Figure 49 : Effect of initial dye concentration on MB dye degradation by ZnO/CuO (C/C_0) vs Time(min)

By increasing the dye concentration from 5 mg/L to 20 mg/L at an ideal pH and catalyst quantity, the impact of the starting dye concentration on the ability to degrade was investigated. To create an adsorption-desorption equilibrium, the catalyst and MB solution were combined and the mixture was left in the dark for 20 minutes. The impact of starting dye concentration on MB dye degradation by ZnO/CuO is depicted in Fig. 54. The maximum degradation efficiency of ZnO/CuO is 5 mg/L, whereas the lowest is 20 mg/L. After 180 minutes of solar light exposure, the percent of degradation for 5 mgL-1, 10 mgL-1, 15 mgL-1, and 20 mgL-1 was 97.47%, 78.77%, 69.52%, and 58.92%, respectively. This showed that the removal performance dropped as the dye concentration increased.

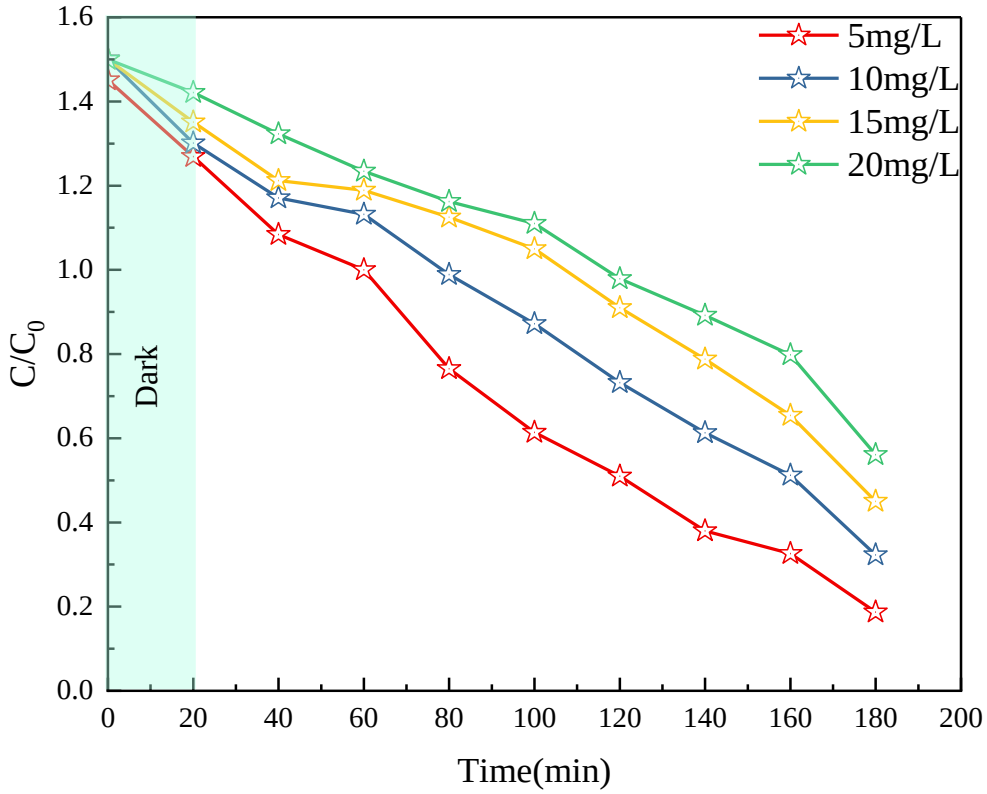

Figure 49 : Effect of initial dye concentration on MB dye degradation by ZnO/Co_3O_4

: (C/C_0) vs Time(min)

Fig.50 shows effect of initial dye concentration on the degradation of MB by ZnO/Co_3O_4 indicating a rapid decrease in degradation percentage with the increase of dye concentration. The effect was studied by using $5mgL^{-1}$, $10mgL^{-1}$,$15mgL^{-1}$ and $20mgL^{-1}$ dye solution showing 84.21%, 80.36%,70.91% and 65.87% of degradation respectively.

With the enhancement of dye concentration more dye moleculestended to quickly saturate the binding sites available on the surface area of photocatalyst. Consequently, with less absorption sites , the degradation rate would be slowed [21] . Fig. shows effect of concentration of synthesized ternary nanocomposite on the MB dye degradation. The result revealed that percent of drgradation is concentration dependent.

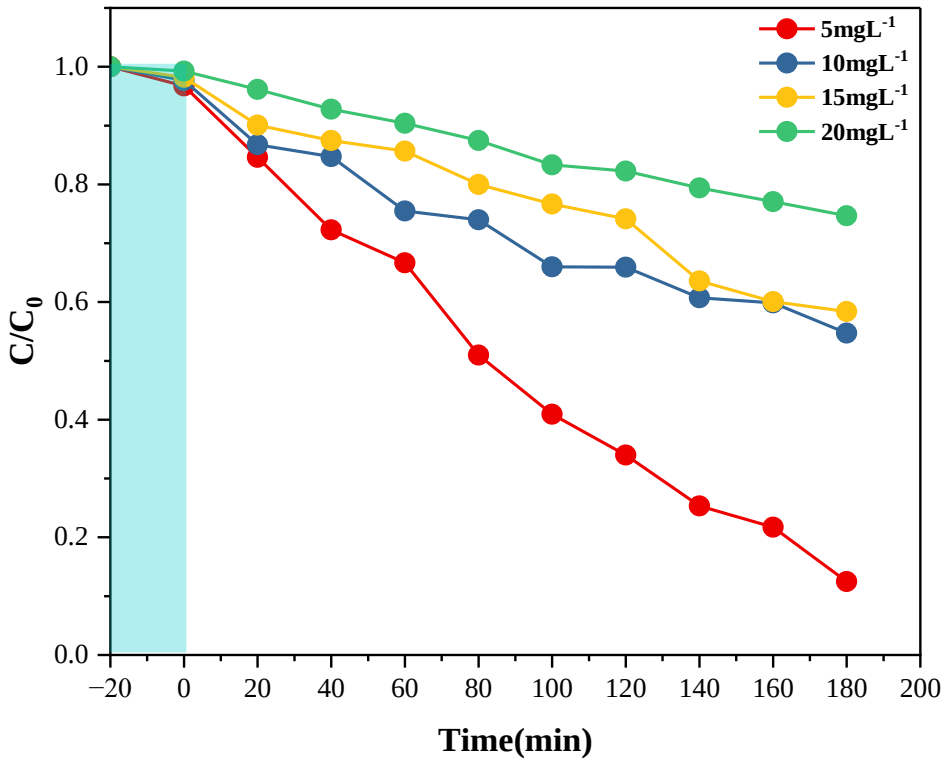

Figure 50 : Effect of initial dye concentration on MB dye degradation by ZnO/Co_3O_4 (C/C_0 vs Time

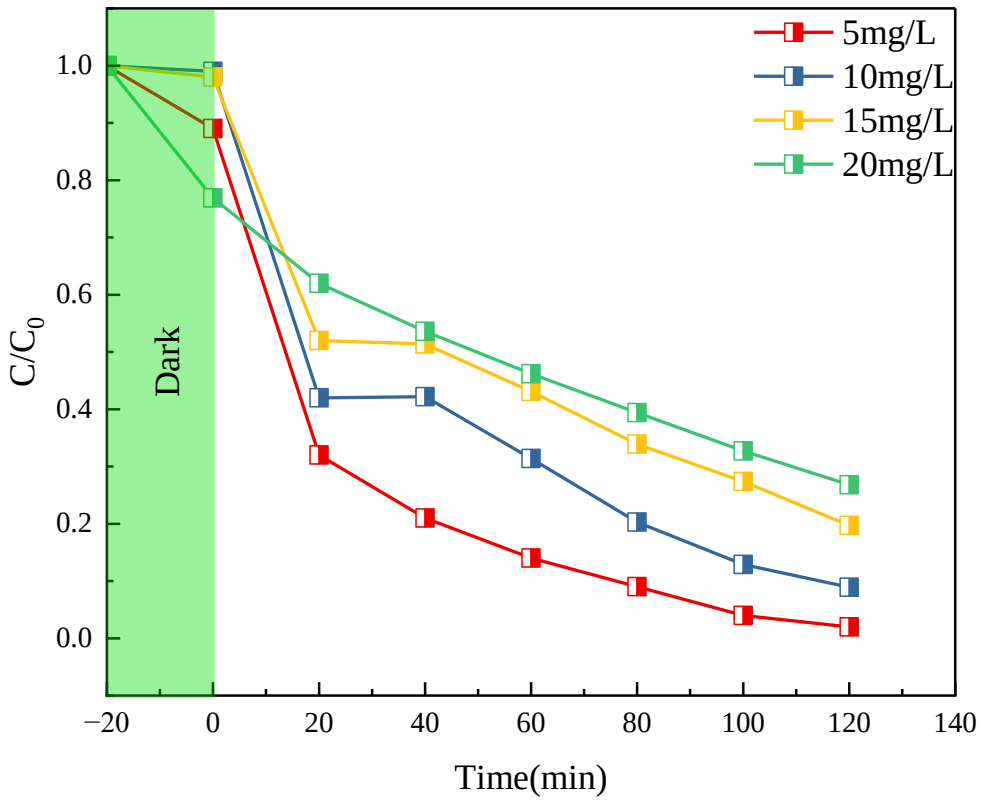

Figure 51 : Effect of initial dye concentration on MB dye degradation by CuO/Co_3O_4 : (C/C_0) vs Time(min)

4.8. Kinetic study:

With the aim of obtaining better comparison results of the photocatalytic degradation efficiencies of the prepared photocatalysts a kinetic model analysis was performed.

The Langmuir-Hinshelwood kinetic model can be applied to the following formula:

$$ln(C/C0) = -kt$$

The kinetics of photocatalytic degradation of Methylene Blue using ZnO/CuO, ZnO/Co_3O_4, CuO/Co_3O_4 and $ZnO/CuO/Co_3O_4$ nanocomposite were calculated under optimized conditions :

0.6g photocatalyst dosage, 5mgL^{-1} methylene blue dye concentration and 180minute for the first

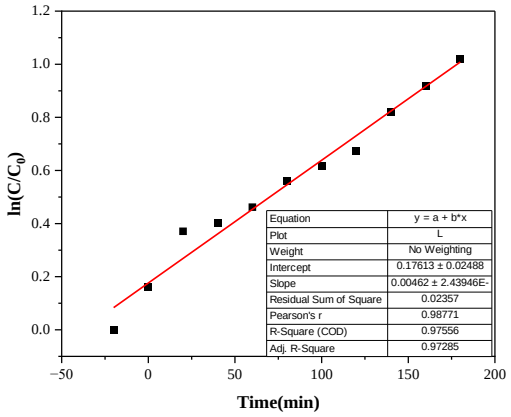

Figure 53 : ln(C/C$_0$) vs Time(min) : ZnO/CuO

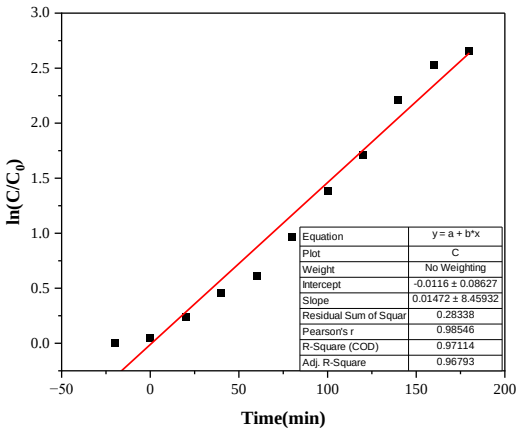

Figure 54 : ln(C/C$_0$) vs Time(min) : ZnO/Co$_3$O$_4$

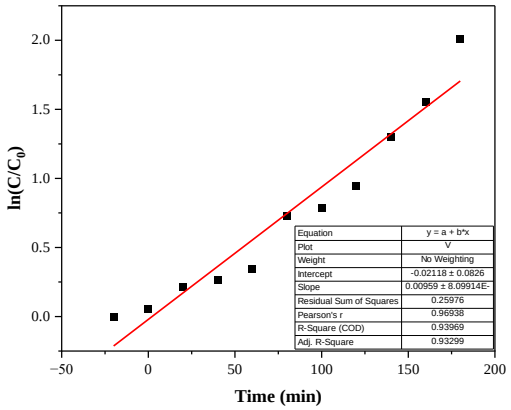

Figure 55 : ln(C/C0) vs Time(min) : CuO/Co$_3$O$_4$

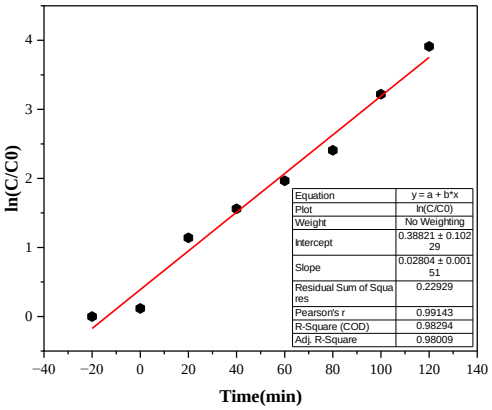

Figure 56 : ln(C/C0) vs Time(min) : ZnO/CuO/Co$_3$O$_4$

three binary composite , 120minute for the ternary composite. The graphs of ln(C/C$_0$) against time (minute) were drawn and presented in the figure 58, 59, 60, 61. The graph in Figure 58. illustrates a straight line with positive slope and the rate constant of the reaction is 0.00707min^{-1} . Rate of reaction for rest of the three composites are 0.01477min^{-1}, 0.01117min^{-1} and0.02105min^{-1}

respectively. From the graph the correlation co-efficient (R^2) were also calculated. The R^2 values for ZnO/CuO, ZnO/Co_3O_4 , CuO/Co_3O_4 and ZnO/CuO/Co_3O_4 0.97285, 0.96793, 0.93299, 0.98009 respectively. Higher value of R^2 of ZnO/CuO/Co_3O_4 indicates faster rate of degradation.

Table 13: Photocatalytic degradation of MB dye using ZnO/CuO nanocomposite

Catalytic reaction condition	**Varied parameters**	**K_{obs}(min^{-1})**	**R^2**	**Degradation %**
[MB]=5mgL-1 Catalyst dosage= 0.06mg	**pH** 8 9 10 11			
[MB] = 5mgL^{-1} pH=11	**Catalyst dosage** 2mg 4mg 6mg	 0.00322 0.00568 0.00707	 0.98443 0.97285 0.94494	 44.58 65.24 72.85
Catalyst dosage= 0.06mg pH=11	**Dye concentration** 5mgL^{-1} 10mgL^{-1} 15mgL^{-1} 20mgL^{-1}	 0.0205 0.0091 0.0086 0.0063	 0.84862 0.99345 0.99345 0.96723	 97.5 78.8 69.5 58.9

Table 14: Photocatalytic degradation of MB dye using ZnO/Co3O4 nanocomposite

Catalytic reaction condition	Varied parameters	$K_{obs}(min^{-1})$	R^2	% Degradation
	Catalyst dosage			
[MB] = $5mgL^{-1}$	2mg	0.00515	0.96187	60.4
pH=11	4mg	0.00867	0.87818	79
	6mg	0.01477	0.96793	93.14
	Dye Concentration			
Catalyst dosage =	$5mgL^{-1}$	0.01108	0.97527	86.4
0.6mg/100ml	$10mgL^{-1}$	0.00917	0.97729	80.8
pH=11	$15mgL^{-1}$	0.00736	0.96897	73.4
	$20mgL^{-1}$	0.95776	0.95776	64.9

Table 15 : Photocatalytic degradation of MB dye using CuO/Co_3O_4 nanocmposite

Catalytic reaction condition	Varied parameters	$K_{obs}(min^{-1})$	R^2	Degradation %
[MB]=5mgL-1 Catalyst dosage=0.06g	**pH** 8 9 10 11			
	Catalyst dosage			
[MB] = $5mgL^{-1}$	2mg	0.00519	0.95968	60.67
pH=11	4mg	0.00908	0.87736	80.47
	6mg	0.01117	0.93299	86.6
	Dye Concentration			
Catalyst dosage	$5mgL^{-1}$	0.01157	0.96117	87.53
= 0.6mg	$10mgL^{-1}$	0.00335	0.97266	45.27
pH=11	$15mgL^{-1}$	0.00299	0.9612	41.6

	$20mgL^{-1}$	0.00162	0.99636	25.33

Table 16 : Photocatalytic degradation of MB dye using ZnO/CuO/Co_3O_4 nanocomposite

Catalytic reaction condition	**Varied parameters**	**$K_{obs}(min^{-1})$**	**R^2**	**Degradation %**
[MB]=5mgL-1 Catalyst dosage=0.06mg	**pH** 8 9 10 11			
[MB] = $5mgL^{-1}$ pH=11	**Catalytic Dosage** 2mg 4mg 6mg	 0.01527 0.01767 0.02105	 0.97918 0.95396 0.81696	 86.88 90.92 98.67
Catalyst dosage = 0.6mg/100ml pH=11	**Dye Concentration** 5mgL-1 10mgL-1 15mgL-1 20mgL-1	 0.02016 0.01354 0.01354 0.01097	 0.9621 0.95301 0.98483 0.99196	 91.1 80.3 80.3 73.2

4.9. Catalytic reusability

The cost effectiveness of the degradation process is related to the catalytic reusability of the synthesized photocatalysts. It gives significant opportunities for scale up and laboratory applications. The most economical way to remove MB dye from wastewater is photocatalysis as it is safe, easy and reusable. This reduce the total cost of the MB dye degradation through deterioration at the inner and outer active sites of the catalyst photocatalytic surface which may result in reduction of active site availability. Therefore, the objectives of the study is to effectively analyze the best ways to use the synthesized nanocomposites as catalysts for their long term use. MB dye The efficiency of the photocatalytic degradation of MB dye using ZnO/CuO and

ZnO/Co_3O_4 in the first cycle reached about 95.29% and 86.54%, respectively. After 5^{th} cycle, degradation efficiency of ZnO/CuO decreased to 90.2%. ZnO/Co_3O_4 shows degradation efficiency of 76.78% in 4 cycles. At first cycle, the degradation efficiency of CuO/Co_3O_4 nanocomposite reached at about 91.56% which decreased to 56.34% at 4^{th} cycle. The ternary nanocomposite $ZnO/CuO/Co_3O_4$ nanocomposite degradation efficiency become 96.15% in 6^{th} cycle which indicates its better stability than the binary composites.

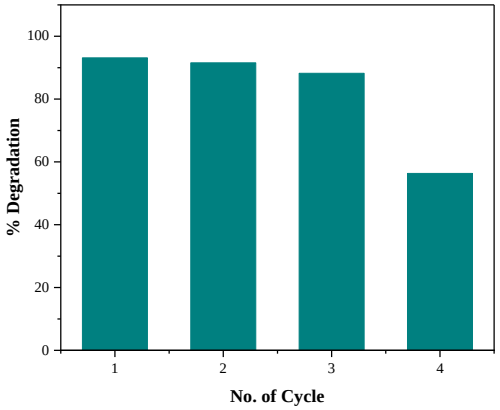

Figure 52 : Reusability of CuO/Co_3O_4 nanocomposite

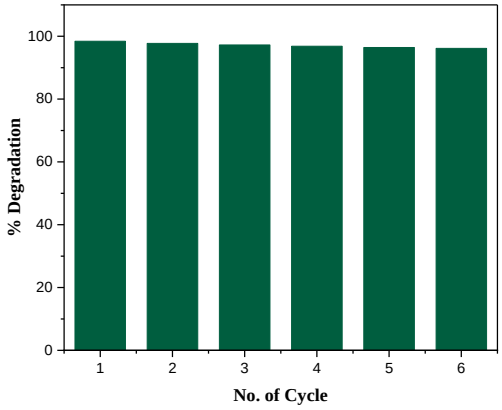

Figure 53 : Reusability of $ZnO/CuO/Co_3O_4$ nanocomposite

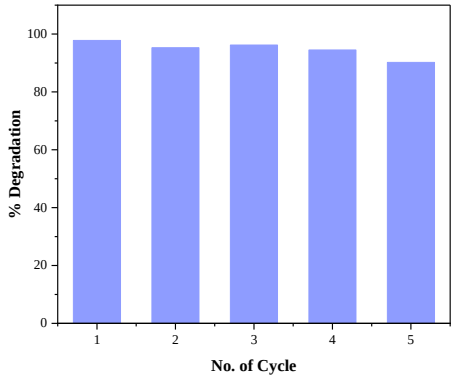

Figure 54 : Reusability of ZnO/CuO nanocomposite

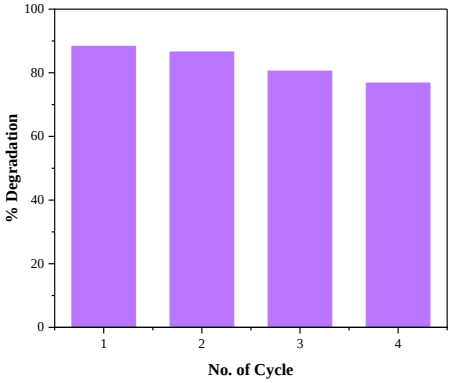

Figure 55 : Reusabiliy of ZnO/Co3O4 nanocomposite

4.10. Comparison with other works

Table 17 : Comparision of the degradation efficiencies obtained in this work with other previous works

Catalyst	Pollutant	Light source	Degradation(%)	Time	References
ZnO	MB	Sunlight	68.6	135	[57], [71]
CuO	MB	Visible light	31	120	[72]
Co_3O_4	RBO 3R	UV light	78.45	50	[73]
ZnO/CuO	MB	Sunlight	46	180	[11]
ZnO/CuO	MO	Visible light	27.7	120	[74]
ZnO NWs	MB	Sunlight	100	4320	[75]
ZnO/Mn_3O_4	MB	Sunlight	67	180	[11]
ZnO/Co_3O_4	MO	Visible light	79	-	[76]
ZnO/Co_3O_4	RhB	UV light	89	400	[77]
ZnO/CuO	MB	Sunlight	97.82	180	This work
ZnO/Co_3O_4	MB	Sunlight	88.34	180	This work
CuO/Co_3O_4	MB	Sunlight	93.14	180	This work
$ZnO/CuO/Co_3O_4$	MB	Sunlight	98.44	120	This work

Chapter Five : Conclusion

In this study , an attempt has been made to synthesize ZnO/CuO, ZnO/Co_3O_4, CuO/Co_3O_4 binary nanocomposites and ZnO/CuO/Co_3O_4 nanocompossite through chemical co-precipitation method

for their good photocatalytic activity.The products were characterized by UV-Vis, FTIR, XRD, FESEM and EDX. The morphological and compositional features of the composites were cgaracterized by FE-SEM and EDX which revealed that ZnO/CuO composite has flowerlike microstructure and leaflike nanopatches in between them, ZnO/Co_3O_4 nanocomposite has spherical shaped particles superimposed in the porous structure, CuO/Co_3O_4 nanocomposites are nanospheres in an agglomerated manner. The ternary nanocomposite also consisted of uniformly distributed spherical-shaped particles in aggregated and non-aggregated form. The crystallite size of the composites determined by from XRD using Scherrer equation are 23.14nm, 6.37nm, 18.15nm and 23.57nm for ZnO/CuO, ZnO/Co_3O_4, CuO/Co_3O_4 and $ZnO/CuO/Co_3O_4$ respectively. The band gap energy obtained from the Tauc plot are 2.37eV, 2.34 eV, 3.78 ev and 3.14eV. The FTIR data discloses the presence of Metal-Oxide bonds. MB dye solution mixed with the photocatalysts changes color from deep blue to light blue and then colourless in progress of irradiation time. Among the four nanocomposites $ZnO/CuO/Co_3O_4$ exhibits highest percent of degradation at lowest time. Effect of catalyst dosage, irradiation time and initial dye concentration was studied. With the increase of dye concentration the degradation efficiency decrease and dosage showed the reverse change . With the increase of catalyst dosage the percent of degradation increases. After 180min , ZnO/CuO , ZnO/Co_3O_4 and CuO/Co_3O_4 the ternary nanocomposite showed 97.82%, 88.34% and 93.14% of degradation respectively wheres $ZnO/CuO/Co_3O_4$ showed 98.44% of degradation at 120min. So, the order of degradation efficiency can be in this order ZnO/Co_3O_4 ‹ CuO/Co_3O_4 ‹ ZnO/CuO ‹ $ZnO/CuO/Co_3O_4$.

Chapter six : References

[1] E. S. Al-Farraj and E. A. Abdelrahman, “Efficient Photocatalytic Degradation of Congo Red Dye Using Facilely Synthesized and Characterized MgAl2O4 Nanoparticles,” *ACS Omega*, vol. 9, no. 4, pp. 4870–4880, Jan. 2024, doi: 10.1021/acsomega.3c08485.

[2] M. Althamthami, E. Guettaf Temam, H. Ben Temam, R. Saad, and G. G. Hasan, “Improved photocatalytic activity under the sunlight of high transparent hydrophilic Bi-doped TiO2 thin-films,” *J Photochem Photobiol A Chem*, vol. 443, Sep. 2023, doi: 10.1016/j.jphotochem.2023.114818.

[3] K. Kemp, J. Griffiths, S. Campbell, and K. Lovell, “An exploration of the follow-up up needs of patients with inflammatory bowel disease,” *J Crohns Colitis*, vol. 7, no. 9, Oct. 2013, doi: 10.1016/j.crohns.2013.03.001.

[4] F. Zhan *et al.*, “Facile preparation and highly efficient catalytic performances of pd-cu bimetallic catalyst synthesized via seed-mediated method,” *Nanomaterials*, vol. 10, no. 1, Jan. 2020, doi: 10.3390/nano10010006.

[5] P. C. Nagajyothi, S. V. Prabhakar Vattikuti, K. C. Devarayapalli, K. Yoo, J. Shim, and T. V. M. Sreekanth, “Green synthesis: Photocatalytic degradation of textile dyes using metal and metal oxide nanoparticles-latest trends and advancements,” *Crit Rev Environ Sci Technol*, vol. 50, no. 24, pp. 2617–2723, Dec. 2020, doi: 10.1080/10643389.2019.1705103.

[6] S. S. Hashmi *et al.*, “Potentials of phyto-fabricated nanoparticles as ecofriendly agents for photocatalytic degradation of toxic dyes and waste water treatment, risk assessment and probable mechanism,” Apr. 01, 2021, *Elsevier B.V.* doi: 10.1016/j.jics.2021.100019.

[7] A. A. Bentley and J. C. Adams, “The evolution of thrombospondins and their ligand-binding activities,” *Mol Biol Evol*, vol. 27, no. 9, pp. 2187–2197, Sep. 2010, doi: 10.1093/molbev/msq107.

[8] J. Kavil, A. Alshahrie, and P. Periyat, “CdS sensitized TiO2 nano heterostructures as sunlight driven photocatalyst,” *Nano-Structures and Nano-Objects*, vol. 16, pp. 24–30, Oct. 2018, doi: 10.1016/j.nanoso.2018.03.011.

[9] H. N. Jayasimha, K. G. Chandrappa, P. F. Sanaulla, and V. G. Dileepkumar, “Green synthesis of CuO nanoparticles: A promising material for photocatalysis and electrochemical sensor,” *Sensors International*, vol. 5, Jan. 2024, doi: 10.1016/j.sintl.2023.100254.

[10] D. Tahir and S. Tougaard, “Electronic and optical properties of Cu, CuO and Cu 2O studied by electron spectroscopy,” *Journal of Physics Condensed Matter*, vol. 24, no. 17, May 2012, doi: 10.1088/0953-8984/24/17/175002.

[11] B. Ben Salem *et al.*, “Synthesis and comparative study of the structural and optical properties of binary ZnO-based composites for environmental applications,” *RSC Adv*, vol. 13, no. 9, pp. 6287–6303, Feb. 2023, doi: 10.1039/d2ra07837f.

[12] M. Ma *et al.*, “Engineering the photoelectrochemical behaviors of ZnO for efficient solar water splitting,” *J. Semicond*, vol. 2020, no. 9, p. 91702, doi: 10.1088/1674.

[13] A. Das, N. S.K., and R. G. Nair, “Influence of surface morphology on photocatalytic performance of zinc oxide: A review,” Jul. 01, 2019, *Elsevier B.V.* doi: 10.1016/j.nanoso.2019.100353.

[14] J. Chang and E. R. Waclawik, “Facet-controlled self-assembly of ZnO nanocrystals by non-hydrolytic aminolysis and their photodegradation activities,” *CrystEngComm*, vol. 14, no. 11, pp. 4041–4048, Jun. 2012, doi: 10.1039/c2ce25154j.

[15] D. Letsholathebe *et al.*, “Optical and structural stability of Co3O4nanoparticles for photocatalytic applications,” in *Materials Today: Proceedings*, Elsevier Ltd, 2019, pp. 499–503. doi: 10.1016/j.matpr.2020.05.205.

[16] J. A. Rodriguez, X. Wang, J. C. Hanson, G. Liu, A. Iglesias-Juez, and M. Fernández-García, “The behavior of mixed-metal oxides: Structural and electronic properties of Ce1-xCaxO2 and Ce1-xCa xO2-x,” *Journal of Chemical Physics*, vol. 119, no. 11, pp. 5659–5669, Sep. 2003, doi: 10.1063/1.1601595.

[17] A. Hamrouni, N. Moussa, A. Di Paola, F. Parrino, A. Houas, and L. Palmisano, “Characterization and photoactivity of coupled ZnO-ZnWO4 catalysts prepared by a sol-gel method,” *Appl Catal B*, vol. 154–155, pp. 379–385, 2014, doi: 10.1016/j.apcatb.2014.02.042.

[18] K. Yuan *et al.*, “Synthesis of WO3@ZnWO4@ZnO-ZnO hierarchical nanocactus arrays for efficient photoelectrochemical water splitting,” *Nano Energy*, vol. 41, pp. 543–551, Nov. 2017, doi: 10.1016/j.nanoen.2017.09.053.

[19] S. A. Ansari, M. M. Khan, M. O. Ansari, and M. H. Cho, “Nitrogen-doped titanium dioxide (N-doped TiO2) for visible light photocatalysis,” Apr. 01, 2016, *Royal Society of Chemistry*. doi: 10.1039/c5nj03478g.

[20] V. Kumari, S. Yadav, J. Jindal, S. Sharma, K. Kumari, and N. Kumar, “Synthesis and characterization of heterogeneous ZnO/CuO hierarchical nanostructures for photocatalytic degradation of organic pollutant,” *Advanced Powder Technology*, vol. 31, no. 7, pp. 2658–2668, Jul. 2020, doi: 10.1016/j.apt.2020.04.033.

[21] V. U. Siddiqui *et al.*, “Optimization of facile synthesized zno/cuo nanophotocatalyst for organic dye degradation by visible light irradiation using response surface methodology,” *Catalysts*, vol. 11, no. 12, Dec. 2021, doi: 10.3390/catal11121509.

[22] P. Sable, N. Thabet, J. Yaseen, and G. Dharne, “Effects on Structural Morphological and Optical Properties Pure and CuO/ZnO Nanocomposite,” *Trends in Sciences*, vol. 19, no. 24, Dec. 2022, doi: 10.48048/tis.2022.3092.

[23] M. Nami, S. Sheibani, and F. Rashchi, “Photocatalytic performance of coupled semiconductor ZnO–CuO nanocomposite coating prepared by a facile brass anodization process,” *Mater Sci Semicond Process*, vol. 135, Nov. 2021, doi: 10.1016/j.mssp.2021.106083.

[24] J. Shokraiyan, M. Asadi, and M. Rabbani, “A comparison of photocatalytic activity of CuO, ZnO, and ZnO/CuO Nanocomposites for degrading water pollutants under LED light,” Aug. 01, 2021, *Elsevier B.V.* doi: 10.1016/j.cdc.2021.100747.

[25] N. Jalali, A. Rakhsha, M. Nami, F. Rashchi, and V. R. Mastelaro, “Photocatalytic activity and pH-induced morphological changes of ZnO/CuO nanocomposites prepared by chemical bath precipitation,” *Energy Advances*, vol. 2, no. 7, pp. 1051–1063, Jun. 2023, doi: 10.1039/d3ya00160a.

[26] S. Das and V. C. Srivastava, “Synthesis and characterization of ZnO/CuO nanocomposite by electrochemical method,” *Mater Sci Semicond Process*, vol. 57, pp. 173–177, Jan. 2017, doi: 10.1016/j.mssp.2016.10.031.

[27] N. Kumaresan, M. M. A. Sinthiya, K. Ramamurthi, R. Ramesh Babu, and K. Sethuraman, “Visible light driven photocatalytic activity of ZnO/CuO nanocomposites coupled with rGO

heterostructures synthesized by solid-state method for RhB dye degradation," *Arabian Journal of Chemistry*, vol. 13, no. 2, pp. 3910–3928, Feb. 2020, doi: 10.1016/j.arabjc.2019.03.002.

[28] A. G. Bekru, L. T. Tufa, O. A. Zelekew, M. Goddati, J. Lee, and F. K. Sabir, "Green Synthesis of a CuO-ZnO Nanocomposite for Efficient Photodegradation of Methylene Blue and Reduction of 4-Nitrophenol," *ACS Omega*, vol. 7, no. 35, pp. 30908–30919, Sep. 2022, doi: 10.1021/acsomega.2c02687.

[29] A. Ashar *et al.*, "Enhanced solar photocatalytic reduction of cr(Vi) using a (zno/cuo) nanocomposite grafted onto a polyester membrane for wastewater treatment," *Polymers (Basel)*, vol. 13, no. 22, Nov. 2021, doi: 10.3390/polym13224047.

[30] I. Shaheen, K. S. Ahmad, C. Zequine, R. K. Gupta, A. G. Thomas, and M. A. Malik, "Green synthesis of ZnO-Co3O4nanocomposite using facile foliar fuel and investigation of its electrochemical behaviour for supercapacitors," *New Journal of Chemistry*, vol. 44, no. 42, pp. 18281–18292, Nov. 2020, doi: 10.1039/d0nj03430d.

[31] H. T. Mohammed *et al.*, "ZnO/Co3 O4 Nanocomposites: Novel Preparation, Characterization, and Their Performance toward Removal of Antibiotics from Wastewater," *Journal of Nanostructures*, vol. 12, no. 3, pp. 503–509, Jun. 2022, doi: 10.22052/JNS.2022.03.003.

[32] Y. Liu, G. Zhu, J. Chen, H. Xu, X. Shen, and A. Yuan, "Co 3 O 4 /ZnO nanocomposites for gas-sensing applications," *Appl Surf Sci*, vol. 265, pp. 379–384, Jan. 2013, doi: 10.1016/j.apsusc.2012.11.016.

[33] E. M. Abebe and M. Ujihara, "Influence of Temperature on ZnO/Co3O4Nanocomposites for High Energy Storage Supercapacitors," *ACS Omega*, vol. 6, no. 37, pp. 23750–23763, Sep. 2021, doi: 10.1021/acsomega.1c02059.

[34] D. Bekermann *et al.*, "Co 3O 4/ZnO nanocomposites: From plasma synthesis to gas sensing applications," *ACS Appl Mater Interfaces*, vol. 4, no. 2, pp. 928–934, Feb. 2012, doi: 10.1021/am201591w.

[35] R. Kumar, A. Umar, R. Kumar, M. S. Chauhan, G. Kumar, and S. Chauhan, "Spindle-like Co3O4-ZnO Nanocomposites Scaffold for Hydrazine Sensing and Photocatalytic Degradation of Rhodamine B Dye," *Engineered Science*, vol. 16, pp. 288–300, 2021, doi: 10.30919/es8d548.

[36] I. Shaheen, K. S. Ahmad, C. Zequine, R. K. Gupta, A. G. Thomas, and M. A. Malik, "Green synthesis of ZnO-Co3O4nanocomposite using facile foliar fuel and investigation of its electrochemical behaviour for supercapacitors," *New Journal of Chemistry*, vol. 44, no. 42, pp. 18281–18292, Nov. 2020, doi: 10.1039/d0nj03430d.

[37] B. A. Hussein, A. A. Tsegaye, G. Shifera, and A. M. Taddesse, "A sensitive non-enzymatic electrochemical glucose sensor based on a ZnO/Co3O4/reduced graphene oxide nanocomposite," *Sensors and Diagnostics*, vol. 2, no. 2, pp. 347–360, Mar. 2023, doi: 10.1039/d2sd00183g.

[38] M. Rashad, S. A. Amin, A. M. Ali, and A. A. Hendi, "Fabrication of p-p type nanocomposite of NiO/Co3O4 and CuO/Co3O4 with different contents," *Mater Res Express*, vol. 6, no. 9, Aug. 2019, doi: 10.1088/2053-1591/ab2dd8.

[39] D. T. Tefera and T. Desalegn Zeleke, “Green synthesis, characterization, and evaluation of antimicrobial and antioxidant activities of CuO, Co 3 O 4 , and CuO-Co 3 O 4 Nano system using Moringa stenopetala plant leaf extracts,” 2024.

[40] K. A. M. A. R. A. J. MAHENDRAPRABHU and P. E. R. U. M. A. L. ELUMALAI, “Effect of citric acid on formation of oxides of Cu and Zn in modified sol-gel process: A comparative study,” *Journal of Chemical Sciences*, vol. 128, no. 5, pp. 831–837, May 2016, doi: 10.1007/s12039-016-1079-z.

[41] S. B. Dhage *et al.*, “ZnO-CuO Nanocomposite Synthesized by Co-precipitation: Characterization and Antibacterial Properties,” 2024, doi: 10.33263/BRIAC143.059.

[42] D. Saravanakkumar *et al.*, “Synthesis and characterization of ZnO-CuO nanocomposites powder by modified perfume spray pyrolysis method and its antimicrobial investigation,” *Journal of Semiconductors*, vol. 39, no. 3, Mar. 2018, doi: 10.1088/1674-4926/39/3/033001.

[43] D. Abdrabou, M. K. Ahmed, S. A. Khairy, and T. M. El-Sherbini, “Gd2O3/CdS Nanocomposites were Synthesized for Photocatalytic Elimination of Methyl Blue (MB) Dye Under Visible Light Irradiation,” *Int J Environ Res*, vol. 18, no. 2, Apr. 2024, doi: 10.1007/s41742-023-00563-5.

[44] A. Sáenz-Trevizo, P. Amézaga-Madrid, P. Pizá-Ruiz, W. Antúnez-Flores, and M. Miki-Yoshida, “Optical band gap estimation of ZnO nanorods,” in *Materials Research*, Universidade Federal de Sao Carlos, Dec. 2016, pp. 33–38. doi: 10.1590/1980-5373-MR-2015-0612.

[45] M. Izaki, S. Abe, K. Nakakita, and P. L. Khoo, “Photoelctrochemically Fabricated and Heated Cu2O/CuO Bilayers with Enhanced Photovoltaic Characteristics,” *ACS Omega*, vol. 6, no. 41, pp. 27587–27597, Oct. 2021, doi: 10.1021/acsomega.1c05163.

[46] Y. F. Lim, J. J. Choi, and T. Hanrath, “Facile synthesis of colloidal CuO nanocrystals for light-harvesting applications,” *J Nanomater*, vol. 2012, 2012, doi: 10.1155/2012/393160.

[47] R. Yoo, S. Yoo, D. Lee, J. Kim, S. Cho, and W. Lee, “Highly selective detection of dimethyl methylphosphonate (DMMP) using CuO nanoparticles /ZnO flowers heterojunction,” *Sens Actuators B Chem*, vol. 240, pp. 1099–1105, Mar. 2017, doi: 10.1016/j.snb.2016.09.028.

[48] V. U. Siddiqui *et al.*, “Optimization of facile synthesized zno/cuo nanophotocatalyst for organic dye degradation by visible light irradiation using response surface methodology,” *Catalysts*, vol. 11, no. 12, Dec. 2021, doi: 10.3390/catal11121509.

[49] B. A. Hussein, A. A. Tsegaye, G. Shifera, and A. M. Taddesse, “A sensitive non-enzymatic electrochemical glucose sensor based on a ZnO/Co3O4/reduced graphene oxide nanocomposite,” *Sensors and Diagnostics*, vol. 2, no. 2, pp. 347–360, Mar. 2023, doi: 10.1039/d2sd00183g.

[50] D. T. Tefera and T. Desalegn Zeleke, “Green synthesis, characterization, and evaluation of antimicrobial and antioxidant activities of CuO, Co 3 O 4 , and CuO-Co 3 O 4 Nano system using Moringa stenopetala plant leaf extracts,” 2024.

[51] H. R. Naika *et al.*, “Green synthesis of CuO nanoparticles using Gloriosa superba L. extract and their antibacterial activity,” *Journal of Taibah University for Science*, vol. 9, no. 1, pp. 7–12, 2015, doi: 10.1016/j.jtusci.2014.04.006.

[52] A. E. Kandjani *et al.*, “Optical and magnetic properties of Co3O4/ZnO Core/Shells Optical and magnetic properties of Co 3 O 4 /ZnO Core/Shell nanoparticles,” 2010. [Online]. Available: https://www.researchgate.net/publication/210071708

[53] M. Y. Nassar, “Size-controlled synthesis of CoCO3 and Co3O 4 nanoparticles by free-surfactant hydrothermal method,” *Mater Lett*, vol. 94, pp. 112–115, 2013, doi: 10.1016/j.matlet.2012.12.039.

[54] S. Meghdadi, M. Amirnasr, M. Zhiani, F. Jallili, M. Jari, and M. Kiani, “Facile Synthesis of Cobalt Oxide Nanoparticles by Thermal Decomposition of Cobalt(II) Carboxamide Complexes: Application as Oxygen Evolution Reaction Electrocatalyst in Alkaline Water Electrolysis,” *Electrocatalysis*, vol. 8, no. 2, pp. 122–131, Mar. 2017, doi: 10.1007/s12678-016-0345-7.

[55] A. A. Radhakrishnan and B. Baskaran Beena, “Structural and Optical Absorption Analysis of CuO Nanoparticles.” [Online]. Available: www.ijacskros.com

[56] V. Gandhi, R. Ganesan, H. H. Abdulrahman Syedahamed, and M. Thaiyan, “Effect of cobalt doping on structural, optical, and magnetic properties of ZnO nanoparticles synthesized by coprecipitation method,” *Journal of Physical Chemistry C*, vol. 118, no. 18, pp. 9717–9725, May 2014, doi: 10.1021/jp411848t.

[57] L. Rohmawati, L. R. Lailia, N. P. Putri, M. Nasir, and D. Darminto, “Characterization of ZnO Nanoparticles Pineapple Skin Extract (Ananas comosus L.) as Photocatalytic Activity,” *Journal of Water and Environmental Nanotechnology*, vol. 9, no. 1, pp. 112–123, Feb. 2024, doi: 10.22090/jwent.2024.01.08.

[58] A. Diallo, A. C. Beye, T. B. Doyle, E. Park, and M. Maaza, “Green synthesis of Co3O4 nanoparticles via Aspalathus linearis: Physical properties,” Oct. 02, 2015, *Taylor and Francis Ltd.* doi: 10.1080/17518253.2015.1082646.

[59] A. B. Vennela, D. Mangalaraj, N. Muthukumarasamy, S. Agilan, and K. V. Hemalatha, “Structural and optical properties of Co 3 O 4 nanoparticles prepared by sol-gel technique for photocatalytic application,” *Int J Electrochem Sci*, vol. 14, no. 4, pp. 3535–3552, Apr. 2019, doi: 10.20964/2019.04.40.

[60] S. B. Endeshaw *et al.*, “Croton macrostachyus Leaf Extract-Mediated Green Synthesis of ZnO Nanoparticles and ZnO/CuO Nanocomposites for the Enhanced Photodegradation of Methylene Blue Dye with the COMSOL Simulation Model,” *ACS Omega*, vol. 9, no. 1, pp. 559–572, Jan. 2024, doi: 10.1021/acsomega.3c06155.

[61] B. A. Hussein, A. A. Tsegaye, G. Shifera, and A. M. Taddesse, “A sensitive non-enzymatic electrochemical glucose sensor based on a ZnO/Co3O4/reduced graphene oxide nanocomposite,” *Sensors and Diagnostics*, vol. 2, no. 2, pp. 347–360, Mar. 2023, doi: 10.1039/d2sd00183g.

[62] V. Kumari, S. Yadav, J. Jindal, S. Sharma, K. Kumari, and N. Kumar, “Synthesis and characterization of heterogeneous ZnO/CuO hierarchical nanostructures for photocatalytic degradation of organic pollutant,” *Advanced Powder Technology*, vol. 31, no. 7, pp. 2658–2668, Jul. 2020, doi: 10.1016/j.apt.2020.04.033.

[63] S. Prabhu, S. Sohila, D. Navaneethan, S. Harish, M. Navaneethan, and R. Ramesh, “Three dimensional flower-like CuO/Co3O4/r-GO heterostructure for high-performance asymmetric supercapacitors,” *J Alloys Compd*, vol. 846, Dec. 2020, doi: 10.1016/j.jallcom.2020.156439.

[64] M. Jayanetti, C. Thambiliyagodage, H. Liyanaarachchi, G. Ekanayake, A. Mendis, and L. Usgodaarachchi, “In vitro influence of PEG functionalized ZnO–CuO nanocomposites on bacterial growth,” *Sci Rep*, vol. 14, no. 1, Dec. 2024, doi: 10.1038/s41598-024-52014-6.

[65] D. T. Tefera and T. Desalegn Zeleke, “Green synthesis, characterization, and evaluation of antimicrobial and antioxidant activities of CuO, Co 3 O 4 , and CuO-Co 3 O 4 Nano system using Moringa stenopetala plant leaf extracts,” 2024.

[66] A. M. Sudapalli and N. G. Shimpi, “Tetragonal SnO2 Nanoparticles: An Efficient Photocatalyst for the Degradation of Hazardous Ionic Dyes,” *ChemistrySelect*, vol. 8, no. 1, Jan. 2023, doi: 10.1002/slct.202203310.

[67] R. Kumar, A. Umar, R. Kumar, M. S. Chauhan, G. Kumar, and S. Chauhan, “Spindle-like Co3O4-ZnO Nanocomposites Scaffold for Hydrazine Sensing and Photocatalytic Degradation of Rhodamine B Dye,” *Engineered Science*, vol. 16, pp. 288–300, 2021, doi: 10.30919/es8d548.

[68] S. G. Firisa, G. G. Muleta, and A. A. Yimer, “Synthesis of Nickel Oxide Nanoparticles and Copper-Doped Nickel Oxide Nanocomposites Using Phytolacca dodecandra L’Herit Leaf Extract and Evaluation of Its Antioxidant and Photocatalytic Activities,” *ACS Omega*, vol. 7, no. 49, pp. 44720–44732, Dec. 2022, doi: 10.1021/acsomega.2c04042.

[69] B. Hameeda, A. Mushtaq, M. Saeed, A. Munir, U. Jabeen, and A. Waseem, “Development of Cu-doped NiO nanoscale material as efficient photocatalyst for visible light dye degradation,” *Toxin Rev*, vol. 40, no. 4, pp. 1396–1406, 2021, doi: 10.1080/15569543.2020.1725578.

[70] D. A. Kader, S. O. Rashid, and K. M. Omer, “Green nanocomposite: fabrication, characterization, and photocatalytic application of vitamin C adduct-conjugated ZnO nanoparticles,” *RSC Adv*, vol. 13, no. 15, pp. 9963–9977, Mar. 2023, doi: 10.1039/d2ra06575d.

[71] A. Khatri and P. S. Rana, “Visible Light Assisted Enhanced Photocatalytic Performance of ZnO/NiO Nanocomposites Prepared by Chemical Co-Precipitation Method,” *J Nanosci Nanotechnol*, vol. 19, no. 8, pp. 5233–5240, Mar. 2019, doi: 10.1166/jnn.2019.16835.

[72] L. Vimala Devi *et al.*, “Synthesis, defect characterization and photocatalytic degradation efficiency of Tb doped CuO nanoparticles,” *Advanced Powder Technology*, vol. 28, no. 11, pp. 3026–3038, Nov. 2017, doi: 10.1016/j.apt.2017.09.013.

[73] I. Bibi *et al.*, “Green and eco-friendly synthesis of cobalt-oxide nanoparticle: Characterization and photo-catalytic activity,” *Advanced Powder Technology*, vol. 28, no. 9, pp. 2035–2043, Sep. 2017, doi: 10.1016/j.apt.2017.05.008.

[74] R. Saravanan, S. Karthikeyan, V. K. Gupta, G. Sekaran, V. Narayanan, and A. Stephen, “Enhanced photocatalytic activity of ZnO/CuO nanocomposite for the degradation of textile dye on visible light illumination,” *Materials Science and Engineering C*, vol. 33, no. 1, pp. 91–98, Jan. 2013, doi: 10.1016/j.msec.2012.08.011.

[75] A. Mahana, O. I. Guliy, S. C. Momin, R. Lalmuanzeli, and S. K. Mehta, “Sunlight-driven photocatalytic degradation of methylene blue using ZnO nanowires prepared through ultrasonication-assisted biological process using aqueous extract of Anabaena doliolum,” *Opt Mater (Amst)*, vol. 108, Oct. 2020, doi: 10.1016/j.optmat.2020.110205.

[76] M. J. Enayat, “Facile synthesis of ZnO/Co3O4 nanocomposites as an effective photocatalyst for degradation and removal of organic contaminant,” *Journal of Materials Science: Materials in Electronics*, vol. 29, no. 2, pp. 1510–1516, Jan. 2018, doi: 10.1007/s10854-017-8060-6.

[77] R. Kumar, A. Umar, R. Kumar, M. S. Chauhan, G. Kumar, and S. Chauhan, “Spindle-like Co3O4-ZnO Nanocomposites Scaffold for Hydrazine Sensing and Photocatalytic Degradation of Rhodamine B Dye,” *Engineered Science*, vol. 16, pp. 288–300, 2021, doi: 10.30919/es8d548.